



I.R.Iran

ISSN:2423-5547

e-ISSN:2423-7469



Journal of Renewable Energy and Environment

Volume 7, Number 2, Spring 2020



Materials and Energy
Research Center



Iranian Association of
Chemical Engineers

CONTENTS

Mehdi Zare Barat Ghobadian Seyed Reza Hassan-Beygi Gholamhasan Najafi	Evaporation Characteristics of Diesel and Biodiesel Fuel Droplets on Hot Surfaces	1-7
Mahdieh Rezagholizadeh Majid Aghaei Omid Dehghan	Foreign Direct Investment, Stock Market Development, and Renewable Energy Consumption: Case Study of Iran	8-18
Mohammad Hossein Jahangir Mahnaz Abolghasemi Seyedeh Mahsa Mousavi Reineh	Application of Artificial Neural Networks to the Simulation of Climate Elements, Drought Forecast by Two Indicators of SPI and PNPI, and Mapping of Drought Intensity; Case Study of Khorasan Razavi	19-26
Fatemeh Boshagh Khosrow Rostami	A Review of Application of Experimental Design Techniques Related to Dark Fermentative Hydrogen Production	27-42
Saeed Hosseinpour Seyed Alireza Haji Seyed Mirza Hosseini Ramin Mehdipour Amir Hooman Hemmasi Hassan Ali Ozgoli	Energy Modeling and Techno-Economic Analysis of a Biomass Gasification-CHAT-ST Power Cycle for Sustainable Approaches in Modern Electricity Grids	43-51
Arash Abedi Behrooz Rezaie Alireza Khosravi Majid Shahabi	A Novel Local Control Technique for Converter-Based Renewable Energy Resources in the Stand-Alone DC Micro-Grids	52-63

AIMS AND SCOPE

Journal of Renewable Energy and Environment publishes original papers, review articles, short communications and technical notes in the field of science and technology of renewable energies and environmental-related issues including:

- Generation
- Storage
- Conversion
- Distribution
- Management (economics, policies and planning)
- Environmental Sustainability

INSTRUCTIONS FOR AUTHORS

Submission of manuscript represents that it had neither been published nor submitted for publication elsewhere and is result of research carried out by author(s). Only the extended and upgraded articles presented in a conference and/or appeared in a symposium proceedings could be evaluated for publication.

Authors are required to include a list describing all the symbols and abbreviations in the paper. Use of the international system of measurement units is mandatory.

- On-line submission of manuscripts results in faster publication process and is recommended. Instructions are given in the JREE web sites: www.jree.ir
- References should be numbered in brackets and appear in sequence through the text. List of references should be given at the end of the paper. All journal articles listed in the References section must follow with article doi.
- Figure captions are to be indicated under the illustrations. They should sufficiently explain the figures.
- Illustrations should appear in their appropriate places in the text.
- Tables and diagrams should be submitted in a form suitable for reproduction.
- Photographs should be of high quality saved as jpg files.
- Tables' illustrations, figures and diagrams will be normally printed in single column width (8 cm). Exceptionally large ones may be printed across two columns (17 cm).



Evaporation Characteristics of Diesel and Biodiesel Fuel Droplets on Hot Surfaces

 Mehdi Zare^a, Barat Ghobadian^{a*}, Seyed Reza Hassan-Beygi^b, Gholamhasan Najafi^a
^a Department of Biosystems Engineering, Tarbiat Modares University (TMU), Tehran, Iran.

^b Department of Agrotechnology, College of Abouraihan, University of Tehran, Tehran, Iran.

PAPER INFO

Paper history:

Received 15 October 2019

Accepted in revised form 03 March 2020

Keywords:

Critical Surface Temperature

Evaporation Time

ANOVA

CI Engine

Transesterification

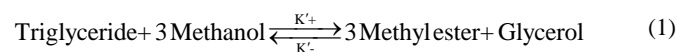
ABSTRACT

In CI engines, the evaporation rate of fuel on various hot surfaces, including the combustion chamber, has a significant effect on deposit formation and accumulation, the exhaust emissions of PM and NO_x, and their efficiency. Therefore, the evaporation of liquid fuel droplets impinging on hot surfaces has become an important subject of interest to engine designers, manufacturers, and researchers. The aim of this study is to investigate the evaporation characteristics based on droplet lifetime and critical surface temperature (the maximum heat transfer rate) of diesel and biodiesel fuel droplets on hot surfaces. In order to determine the effects of diesel fuel, canola oil biodiesel, and castor oil biodiesel, the droplets impinging on the hot surfaces of aluminum alloy (7075) and steel alloy (1.5920) and the evaporation lifetime of diesel and biodiesel fuels were measured. Statistical analysis (ANOVA and Duncan's multiple-range test) was carried out using SAS software. The results showed the maximum critical surface temperature of 450 °C for the castor oil biodiesel on steel 1.5920 surface and the minimum one for diesel fuel (350 °C). In this case, both surfaces had the same droplet lifetimes of approximately 2 s. The results of ANOVA showed the significant effect of the surface material and fuel type on the evaporation lifetime of fuel droplet at 1 % probability.

1. INTRODUCTION

The reduction of fuel resources and the environmental problems caused by the excessive use of fossil fuels have led to many environmental repercussions. In order to overcome these environmental problems and provide sustainable energy, various approaches have been developed, the most notable of which include increasing the fuel conversion efficiency and its replacement with renewable resources.

One of the renewable fuel types, which can be used as an alternative to fossil fuels in diesel engines, is biodiesel derived from vegetable oils and animal fats. It is worth mentioning that the invented engine by Rudolf Diesel was ignited using peanut oil for the first time [1]. Direct use of vegetable oils and animal fats has many disadvantages due to their high viscosity [2,3]. Therefore, many studies conducted so far have aimed to reduce the viscosity level of such renewable resources and optimize them to be applied as fuels for diesel engines. The methods used to reduce the viscosity include microemulsions, pyrolysis, and transesterification [3–5]. The most commonly used method, which is substantially significant in terms of both research and commerce, is transesterification. As represented in Equation 1, a mole of triglyceride with three moles of alcohol in the presence of a catalyst was converted to one mole of glycerol as a valuable byproduct and biodiesel, which is defined as the mono-alkyl esters of vegetable oils or animal fats [6].



The methyl ester produced through the transesterification reaction ought to meet the fuel standard requirements such as ASTM D6751 and EN14214 so as to be accepted as standard

biodiesel fuel. In addition to the aforementioned standards, there are other important characteristics, too. For instance, an important parameter is the fuel evaporation. The evaporation of liquid fuel droplets impinging on hot surfaces is the subject of interest to engine designers, manufacturers, and researchers. In compression ignition engines, the evaporation rate of fuel on various hot surfaces, including the combustion chamber, has an important effect on exhaust emissions, such as PM and NO_x, and their efficiency.

The literature review revealed a number of studies on the evaporation behavior of fuel droplets on hot surfaces. Mizomoto et al. (1978) investigated the evaporation process of n-cetane and n-heptane droplets with a diameter of 2 mm on a stainless steel hot surface. They found that the evaporation process could be divided into different regions. With an increase in the hot surface temperature (in the range of 300 °C to 600 °C), the modes of droplet evaporation including the film evaporation region, the boiling evaporation region, the transition region, and the spheroidal evaporation region will change [7]. Abu-Zaid (1994) studied the evaporation time durations of gasoline and diesel droplets impinging on different surfaces made of different materials (aluminum, stainless-steel, carbon-steel, ceramic MgO, and kaolin). He reported that, at the same surface temperature, the time required for the droplets to evaporate on the porous materials (MgO and Kaolin) was shorter than that on the metallic materials (aluminum, stainless-steel, and carbon-steel) [8]. In a research study, Fardad and Ladommatos (1999) studied the evaporation of various single- and multi-component hydrocarbon compounds on hot surfaces. The results revealed that the minimum amount of time required for droplet evaporation for gasoline, diesel fuel, and a hexane–octane mixture was the same (about 1 s). In addition, it was observed that increasing the surface roughness enhanced the evaporation rate [9]. Arifin et al. (2008) and Arifin and Arai

*Corresponding Author's Email: ghobadib@modares.ac.ir (B. Ghobadian)

(2009) studied the state of fuel evaporation on a hot surface made of aluminum alloy (JIS 2017S). In this study, the evaporation characteristics of dodecane, diesel, and palm oil methyl ester were investigated by defining the maximum evaporation rate point (equal to critical temperature point in this study), which is equal to the minimum lifetime of the droplet. The investigation of evaporation features close to the maximum evaporation rate point and beyond the maximum evaporation rate point showed no obvious differences between the diesel and palm oil ester features. However, some notable differences were observed in the features of dodecane, which could be attributed to multi- and mono-component structures of these fuels. Furthermore, in this study, the diesel fuel (DF), Philippines national standard diesel fuel (contains 1 % of coconut oil methyl ester) (DFP), palm oil methyl ester (B100P), and coconut oil methyl ester (B100C) were investigated in terms of evaporation characteristics. The obtained results revealed that DF and DFP showed a similar behavior in terms of the droplet lifetime profile before reaching the maximum evaporation rate point. Yet, DFP reached a slightly lower point than the maximum evaporation rate point and obtained a longer droplet lifetime at this point. Taking the behavior of B100C into consideration, one could notice a shorter droplet lifetime before the maximum evaporation rate point, compared to that of the B100P. Meanwhile, the maximum evaporation rate point for B100C was far lower than that for B100P, DF, and DFP [10,11].

The synthesized biodiesel's Physiochemical properties (viscosity, surface tension, and so on) are affected by the feedstocks used in the production process. These properties are significant in terms of the evaporation characteristics of the biofuel. To date, the examination of renewable fuels derived from different oils in terms of evaporation on hot surfaces has received scant attention. In addition, almost no such study has statistically analyzed the matter so far.

In the present study, the evaporation behavior of two renewable fuels (castor oil methyl ester and canola oil methyl ester) on aluminum alloy 7075 and steel 1.5920 surfaces is evaluated. The reason for choosing the methyl esters of these two vegetable oils is the significant difference in their viscosity, which can affect their behaviors. Aluminum alloy 7075 and steel 1.5920 were chosen due to their application in components related to the combustion chamber of internal combustion engines, especially in diesel engines.

2. MATERIALS AND METHODS

2.1. Materials

The oils used to produce biodiesel in the current study include canola oil and castor oil, which were purchased from the market. The fatty acid profiles of these oils were determined using Metcalfe method [12,13]. The alcohol required for producing biodiesel was the methanol made by Merck Company with 99.9 % purity. Moreover, the catalyst used was the hydroxide potassium produced by Merck Company with 99.99 % purity. The diesel fuel used was diesel No. 2, which was obtained from a gas station. Table 1 gives some of the important properties of the diesel fuel used in this research work.

2.2. The test equipments

The used experimental apparatus for droplet evaporation is shown in Figure 1. The hot surfaces were flat plates with a

raised edge to avoid jumping out of the droplet. The surfaces are made of aluminum alloy 7075 and steel 1.5920. The surface roughness of each plate was measured by MarSurf M300+RD 18, Mahr Co, Germany. The arithmetic average surface roughness (R_a) rates of the surfaces made of aluminum alloy 7075 and steel 1.5920 are 0.6 μm and 0.2 μm , respectively.

Table 1. Important properties of the test diesel fuel (measured).

Item	Unit	Amount
Density	kg/m ³ at 15 °C	830
Kinematic viscosity	mm ² /s at 40 °C	2.88
Flash point	°C	77
Final boiling point	°C	350

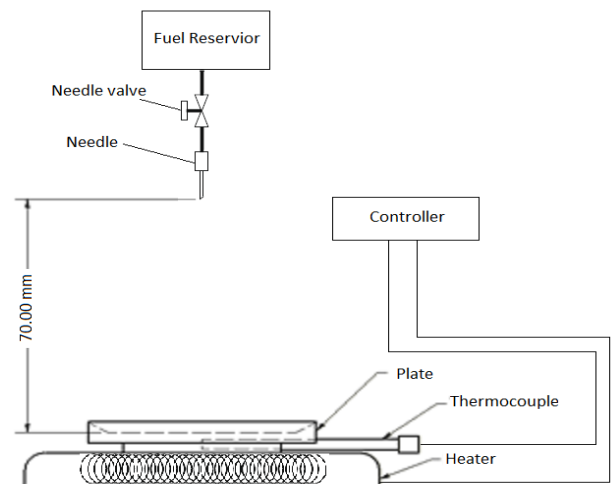


Figure 1. Schematic of an experimental apparatus used in this study.

A radius hole was considered for each surface for the temperature measurement by a thermocouple (J type, ± 2.5 °C accuracy, JUMO, Germany). The hole was placed because the tip of the thermocouple must be 2 mm below the surface. Using the thermocouple, a controller (TZ4ST, ± 0.3 % F.S. accuracy, Autonics, South Korea), and an electric heater, the plate temperature was set to the desired temperature.

A stainless steel needle (G20- 1,1/4") and a needle valve were used as droplet generators. The distance between surface of plate and needle tip was set at 70 mm (trial and error) to avoid the splash loss of impinged droplet and minimize preheating. The average mass of a droplet for diesel fuel, biodiesel of canola, and castor is calculated from the weighing of 100 droplets. The measured values were 5.77 gr, 6.12 gr, and 6.8 gr respectively.

2.3. The tests procedure

To run the experiments, the surface temperature was set to the desired value. To maintain a uniform surface temperature and prevent temperature fluctuations occurred by the surrounding air, a portable transparent insulation chamber was used around the heater and plate in all experiments. Moreover, before starting each experiment, enough time (around 5 min) was given to experimental setup in order to improve the uniformity of the surface temperature. A droplet of the fuel impinged on the center of surface. The lifetime of evaporation droplet is defined either as the duration of droplet hitting the total evaporation (specifically for the mono-component

hydrocarbons) or the case in which no other evaporation occurs. Since the studied fuels in this research were of the multi-component type, the lifetime of droplet for these fuels was considered as the duration of droplet hitting the hot surface until no other evaporation occurred. The lifetime of the droplet was measured using two stopwatches, and the average values were recorded. After conducting each experiment, the surface was cleaned and prepared for further experiments. The temperature ranged from 300 °C to 500 °C at an interval of 25 °C.

2.4. Statistical analysis

All the experiments were repeated three times. The data was statistically analyzed using three completely randomized factors designed to determine the effects of hot surface materials, fuel types, and temperature of surfaces (independent parameters) on the droplet lifetime as the dependent parameter. Moreover, Duncan's multiple range tests were used to compare whether the mean values of the droplet lifetime varied significantly or not when the hot surface materials and fuel types changed. Common letters were used to show no significant difference at a probability level of 5 % between the mean values. Spreadsheet software of Microsoft EXCEL 2007 and SAS 9.2 software were used to analyze the data.

3. RESULTS AND DISCUSSION

3.1. Characteristics of produced biodiesel

The fatty profile of biodiesel base oils is given in Table 2. Moreover, some of the physical characteristics of the biodiesel produced from these oils are given in Table 3.

Table 2. Fatty acid composition (wt %) of the used oils.

Fatty acid	Canola oil	Castor oil
Palmitic acid	6.1	1.1
Stearic acid	2.2	0.9
Oleic acid	60.5	3.2
Linoleic acid	19.5	4.6
Linolenic acid	9.1	-
Ricinoleic acid	-	88.2
Others	2.6	2

Table 3. Some properties of synthesized Canola and Castor biodiesel fuels.

Item	Unit	Accuracy	Amount	
			Canola oil biodiesel	Castor oil biodiesel
Methyl ester content	% mass		97.2	96.6
Density	kg/m ³ at 15 °C	1 kg/m ³	867	909.6
Kinematic viscosity	mm ² /s at 40 °C	±0.1 mm ² /s	4.63	14.9
Flash point	°C	±1 °C	175	196

The properties of the vegetable oils and their biodiesels, given in tables 2 and 3, were measured at Renewable Energy Research Institute of Tarbiat Modares University laboratories. The data of fatty acids given in Table 2 were measured by a

Perkin-Elmer Clarus 580 gas chromatograph (GC) instrument, operating under conditions of the EN 14103 standard. The methyl ester content of biodiesels given in Table 3 was also measured by the GC under conditions of the EN 14103 standard. The density and kinematic viscosity were measured by an Anton Paar-SVM 3000 viscometer. The flash point was measured by an MINIFLASH FLP/H/L Grabner Instrument according to the methods described in ASTM D 93.

3.2. The effects of temperature on the droplet lifetime

Figure 2 illustrates the trend of evaporation related to diesel fuel droplets on hot surfaces. As shown in this figure, an increase in surface temperature results in a sudden reduction in droplet lifetime; therefore, an increase in the temperature from 300 °C to 350 °C leads to a reduction in droplet lifetime by about 5 times (i.e., reducing 9.8 seconds to 1.81 seconds). The 350 °C temperature is called the "critical temperature point", because it is at this point where the minimum droplet lifetime occurs. By increasing the temperature at this point, the evaporation rate decreases and the droplet lifetime increases to some degrees. This occurs as a result of the evaporation regime change from nucleate boiling to transition regime [14,15].

According to this figure, for both aluminum and steel surfaces, the diesel fuel evaporation is similar. At a temperature of 350 °C, the critical temperature points (equal to the droplet's minimum lifetime or the maximum evaporation point) for diesel fuel on aluminum and steel surfaces were 1.81 s and 1.97 s, respectively. As expected, since the critical temperature points on both surfaces were equal, it could be concluded that the critical temperature point was independent of the surface material.

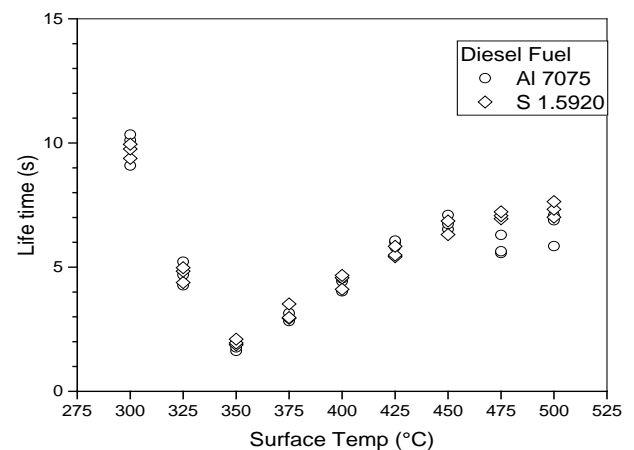


Figure 2. Droplet evaporation lifetime for diesel fuel.

Arifin and Aray (2010) examined the diesel fuel evaporation on the aluminum surface (JIS 2017S). They found that the vapor bubble and splash droplets occurred at temperatures lower than the critical temperature point, and the vigorous boiling occurred at temperatures close to the critical temperature point. In addition, the evaporation was identified to be of vapor layer type at temperatures greater than the critical temperature point. Accordingly, the formation of a thin layer of vapor between the hot surface and the evaporating liquid phase resulted in a relative increase in droplet lifetime [16]. The results reported by Fardad and Ladomatou (1999) and Revankar (2017) indicated a similar evaporation trend for diesel fuel on the surfaces of aluminum and stainless steel materials [9, 15]. Moreover, Abu-zaid (2004) reported the

critical temperature point of diesel fuel on the aluminum surface at 345 °C [17]. The findings of the present study are in accordance with those reported by the aforementioned studies.

Figure 3 shows the evaporation characteristics of the canola oil biodiesel fuel. At temperatures ranging from 300 °C to 350 °C, the evaporation of canola oil biodiesel fuel on the steel surface occurred at a level greater than that of the aluminum surface. Additionally, by increasing the temperature from 300 °C to 325 °C, the fuel droplet lifetime on the aluminum and steel surfaces reduced 3 times (reduction from 20.1 s to 6.74 s) and 1.7 times (from 26.58 s to 15.6 s), respectively. When the temperature increased up to 375 °C, the evaporation of canola oil biodiesel fuel droplets occurred on both surfaces nearly to the same degree. The critical temperature points observed on the aluminum and steel surfaces are 2.25 s and 1.14 s, respectively, at 400 °C.

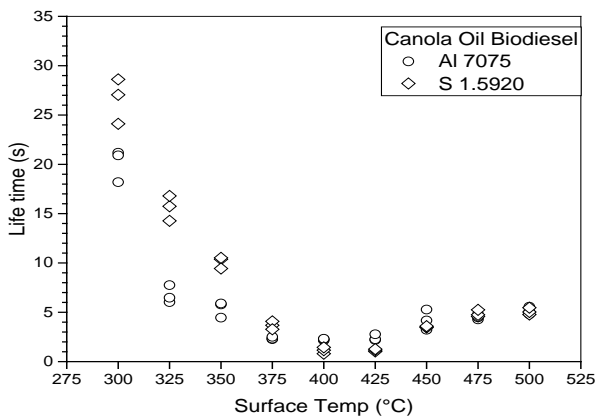


Figure 3. Droplet evaporation lifetime for canola oil biodiesel.

The comparison of evaporation trends of diesel fuel and the canola oil biodiesel fuel reveals that the droplet evaporation of these two fuels on both aluminum and steel surfaces follows a similar trend. The only difference is that the critical temperature point for the canola biodiesel fuel is about 50 °C greater than that of the diesel fuel.

In the present study, as reported by Arifin and Aray (2009), the evaporation trend of canola oil biodiesel on steel surfaces was similar to that of the coconut biodiesel fuel on aluminum surfaces.

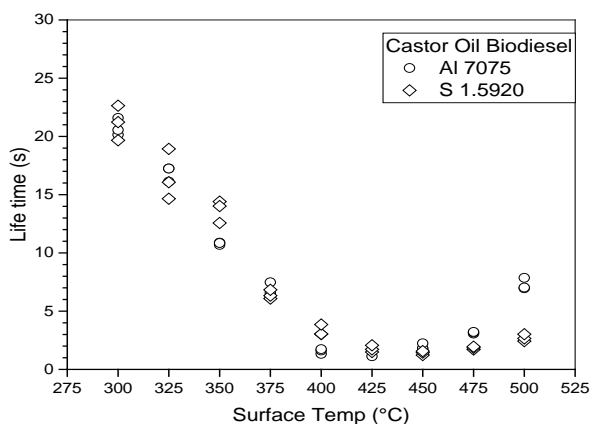


Figure 4. Droplet evaporation lifetime for the castor oil biodiesel.

The evaporation characteristics of the castor oil biodiesel fuel are represented in Figure 4. Although the critical temperature point was reached at the same temperature on both surfaces for the two previously mentioned fuels, the critical temperature point for the castor oil biodiesel fuel was

reached at 425 °C and 450 °C on aluminum and steel surfaces, respectively. As depicted in this figure, the evaporation of castor oil biodiesel fuel occurred at temperatures greater than those of the canola biodiesel fuel, which could be attributed to the greater boiling point of fatty acid methyl ester as castor oil biodiesel (ricinoleate ca. 412 °C at 760.00 mm Hg) than that of the fatty acid methyl ester as canola biodiesel (methyl oleate ca. 352 °C at 760.00 mm Hg).

To gain a better understanding, the values of the critical temperature point for the fuels used on different surfaces are given in Table 4. According to the table, the critical temperature point of biodiesel fuels, compared with diesel fuel, is reached at higher temperatures. In an engine using diesel fuel blended with biodiesel fuel, there might be wall wetting. To prevent this undesirable effect, engine designers should take this issue into consideration.

Table 4. The critical temperature point of diesel and biodiesel fuels on the hot surfaces.

Fuel Type	Surface material	
	Al 7075	Steel 1.5920
Diesel	350 °C	350 °C
Canola oil biodiesel	400 °C	400 °C
Castor oil biodiesel	425 °C	450 °C

3.3. Results of the statistical analysis

The results of the analysis of variance (ANOVA) with respect to the type of surface material, fuel type, and surface temperature (independent parameters) on the evaporation time (dependent parameter) are given in Table 5. As shown in the table, the simple effects of the independent parameters and their interaction on the evaporation time are significant.

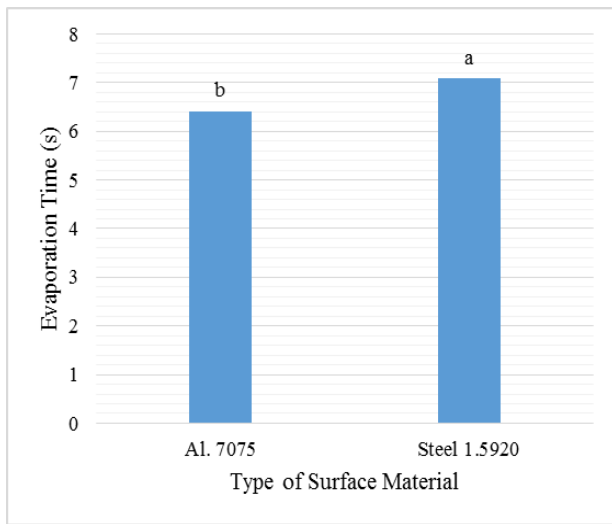
Table 5. Analysis of variance (ANOVA) of parameters effective in the time of evaporation.

Source	Degree of freedom	Mean sum of squares
Type of surface material	1	19.15**
Fuel type	2	67.86**
Temperature of surface	8	433.7**
Type of surface material × Fuel type	2	19.67**
Type of surface material × Temperature of surface	8	10.10**
Fuel type × Temperature of surface	16	95.5**
Type of surface material × Fuel type × Temperature of surface	16	8.65**
Error	106	

**stands for significant at 1 % probability level.

Figure 5 indicates the results of Duncan's multiple range test to compare the mean values of the evaporation time with the type of surface material. As illustrated in this figure, the type of the surface material had a significant effect (at a 5 % probability level) on the fuel evaporation time. The evaporation time on the steel surface has a greater mean than that on the aluminum surface, indicating that the evaporation of fuels from the aluminum surface occurs faster. Abu Zeid (1994) stated that the droplet evaporation from a hot surface

was strongly dependent upon thermal diffusivity of surface material. He also proposed that, with an increase in the thermal diffusivity of the material, the evaporation time decreased, or vice versa.

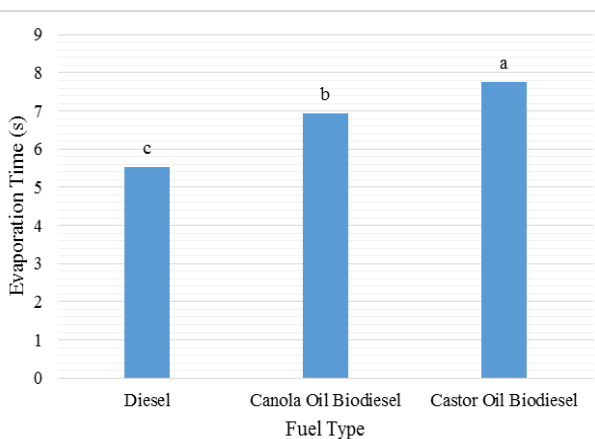


Un-common letters imply that there are significant differences between means at a 5 % probability level.

Figure 5. The effects of type of surface material on the evaporation time.

In the present study, the thermal diffusivities of aluminum and steel are 4.83×10^{-5} and 4.53×10^{-6} m²/s, respectively; therefore, it could be concluded that this is the main reason for the higher evaporation rate on aluminum surface than that on steel surface.

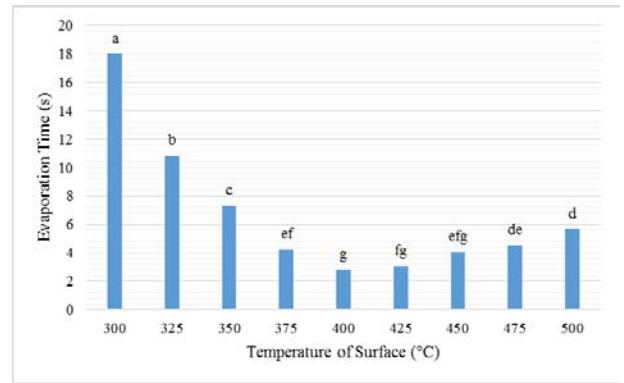
The results of comparing the means through Duncan's method for different fuels are depicted in Figure 6. According to the findings, the fuel type has a significant effect (at a 5 % probability level) on the fuel evaporation on the hot surface. The maximum and minimum evaporation time durations were measured for the castor oil biodiesel fuel and diesel fuel, respectively. The evaporation time of canola oil biodiesel fuel has a mean ranging between two categories of the tested fuels.



Un-common letters mean that there are significant differences between means at a 5 % probability level.

Figure 6. The effects of fuels type on the evaporation time.

The results of Duncan's multiple range tests to compare the mean values of the evaporation time versus surface temperature are given in Figure 7.



Un-common letters mean that there are significant differences between means at a 5% probability level.

Figure 7. The effects of the surface temperature on the evaporation time.

According to the results, increasing the surface temperature in the range of 300 °C to 400 °C significantly decreases the evaporation time ($P < 0.05$) from 18 s to 5.7 s. However, the evaporation time increases significantly if the surface temperature increases.

The interaction effects of the surface type by fuel type on the evaporation time are given in Table 6. Although canola oil biodiesel on the steel surface experienced the maximum evaporation time (7.97 s), it can be observed that the evaporation time for castor oil biodiesel on both surfaces was not insignificantly different through this treatment. On the other hand, the evaporation time of diesel fuel on the aluminum surface was the minimum one (5.43 s). Additionally, the evaporation time for the steel diesel fuel and canola oil biodiesel on the aluminum surface was not significantly different.

Table 6. Interaction effects of fuel type × surface type on the evaporation time of fuel droplets.

Type of surface material	Fuel type		
	Diesel	Canola biodiesel	Castor biodiesel
Al. 7075	5.43 ^b	5.91 ^b	7.84 ^a
St. 1.5920	5.63 ^b	7.97 ^a	7.65 ^a

Un-common letters mean that there are significant differences between means at a 5 % probability level.

Table 7 shows the interaction effects of the surface temperature by surface material type on the evaporation time. The maximum evaporation time (19.15 s) was related to the surface temperature of 300 °C on the steel surface, and the minimum evaporation time (2.72 s) was observed at a surface temperature of 400 °C on the surface with aluminum material. Increasing the surface temperature from 300 °C to 350 °C on the aluminum surface and increasing the surface temperature from 300 °C to 375 °C on the steel surface caused a significant decrease in the evaporation time.

As given in Table 7, in the temperature range of 300 °C to 350 °C, the evaporation time of steel surface was significantly ($P < 0.05$) longer than that of the aluminum surface at each temperature level; in other words, the droplet lifetime varies on the surface materials at low surface temperatures. The difference of droplet lifetime on different surface materials at lower temperatures could be attributed to some physical

phenomena such as spreading and so on. In the temperature range of 375 °C to 500 °C, there were no significant differences between the evaporation times of aluminum and steel surfaces at each level of temperature; in other words, at high surface temperatures, the lifetime is independent of surface materials. At high temperatures, the wettability of the fuel droplet on the hot surfaces decreased.

Table 7. Interaction effect of surface temperature × surface type on the evaporation time of fuel droplets.

Surface temperature (°C)	Type of surface material	
	Al. 7075	St. 1.5920
300	16.9 ^b	19.15 ^a
325	9.45 ^d	12.29 ^c
350	5.99 ^{ef}	8.58 ^d
375	4.04 ^{fgh}	4.41 ^{efgh}
400	2.72 ^h	2.97 ^h
425	3.28 ^{gh}	2.83 ^h
450	4.32 ^{fgh}	3.87 ^{gh}
475	4.51 ^{efgh}	4.59 ^{efgh}
500	6.35 ^e	5.04 ^{efg}

Un-common letters mean that there are significant differences between means at a 5 % probability level.

The interaction effects of the surface temperature by fuel types on the evaporation time are given in Table 8.

Table 8. Interaction effects of surface temperature × fuel type on the evaporation time of fuel.

Surface temperature (°C)	Fuel type		
	Diesel	Canola biodiesel	Castor biodiesel
300	9.77 ^{cd}	23.34 ^a	20.97 ^a
325	4.73 ^{fghi}	11.18 ^c	16.71 ^b
350	1.89 ^{jk}	7.74 ^{de}	12.24 ^c
375	3.06 ^{hijk}	3.03 ^{hijk}	6.58 ^{ef}
400	4.39 ^{fghij}	1.69 ^k	2.44 ^{ijk}
425	5.78 ^{efg}	1.79 ^{jk}	1.61 ^k
450	6.73 ^{ef}	3.88 ^{ghijk}	1.68 ^k
475	6.46 ^{efg}	4.69 ^{fghi}	2.49 ^{ijk}
500	6.97 ^{ef}	5.13 ^{efgh}	4.99 ^{fghi}

Un-common letters mean that there are significant differences between means at a 5 % probability level.

For the castor biodiesel, by increasing the surface temperature from 300 °C to 400 °C, the evaporation time decreased significantly ($P < 0.05$). The further increment of the surface temperature to 500 °C caused an insignificant increase in the evaporation time. For the canola oil biodiesel, the increment of the surface temperature in the range of 300

°C to 375 °C reduced the evaporation time significantly ($P < 0.05$). For diesel fuel, increasing the surface temperature from 300 °C to 350 °C caused a significant ($P < 0.05$) decrease in the evaporation time, while the evaporation time increased significantly due to the further increment of the surface temperature.

4. CONCLUSIONS

The conclusions drawn from this research work are as follows:

1. The simple effects of surface material, fuel type, and surface temperature parameters and their interaction effects were significant on the evaporation lifetime of fuel droplets.
2. For the steel surface, the evaporation time of biodiesel fuels was significantly greater than that of the diesel fuel, while, on the aluminum surface, the evaporation time of castor oil biodiesel was significantly greater than that of the canola biodiesel and diesel fuels.
3. The droplet lifetime at high temperatures was not dependent on the surface materials.
4. The value of the critical temperature point for the diesel fuel on both surfaces was 350 °C. In this temperature, the fuel droplet lifetime was about 2 s.
5. The canola oil biodiesel fuel droplet lifetimes on the aluminum and steel surfaces at a temperature of 400 °C were 2.25 s and 1.14 s, respectively.
6. The critical temperature point for the castor oil biodiesel on the steel surface (450 °C) was higher than that on the aluminum surface (425 °C).

5. ACKNOWLEDGEMENT

This research was supported by the Renewable Energy Institute of Tarbiat Modares University. The authors would like to thank Dr. Fayyazi for his useful and constructive recommendations for this research.

REFERENCES

1. Diesel, R., The diesel oil engine, (1897). (<https://doi.org/10.1111/j.1559-3584.1912.tb03562.x>).
2. Ma, F. and Hanna, M.A., "Biodiesel production: A review", *Bioresource Technology*, Vol. 70, No. 1, (1999), 1-15. (doi:10.1016/S0960-8524(99)00025-5).
3. Abbaszaadeh, A., Ghobadian, B., Omidkhan, M.R. and Najafi, G., "Current biodiesel production technologies: A comparative review", *Energy Conversion Management*, Vol. 63, (2012), 138-148. (doi:10.1016/j.enconman.2012.02.027).
4. Knothe, G., Krahl, J. and Van Gerpen, J., editors, 4-Biodiesel Production, Biodiesel Handbook (Second ed.), AOCS Press, (2010), 31-96. (<https://doi.org/10.1016/B978-1-893997-62-2.50009-7>).
5. Schwab, A.W., Bagby, M.O. and Freedman, B., "Preparation and properties of diesel fuels from vegetable oils", *Fuel*, Vol. 66, (1987), 1372-1378. (doi:[https://doi.org/10.1016/0016-2361\(87\)90184-0](https://doi.org/10.1016/0016-2361(87)90184-0)).
6. Fayyazi, E., Ghobadian, B., Mousavi, S.M. and Najafi, G., "Intensification of continuous biodiesel production process using a simultaneous mixer-separator reactor", *Energy Sources, Part A: Recover Utilization and Environmental Effects*, (2018), 1125-1136. (<https://doi.org/10.1080/15567036.2018.1474293>).
7. Mizomoto, M., Hayano, H. and Ikai, S., "Evaporation and ignition of a fuel droplet on a hot surface: Part 1, Evaporation", *Bulletin of JSME*, Vol. 21, (1978), 1765-1771. (doi:10.1299/jsme1958.21.1765).
8. Abu-Zaid, M., "An experimental study of the evaporation of gasoline and diesel droplets on hot surfaces", *International Communications in*

- Heat and Mass Transfer*, Vol. 21, (1994), 315-322. (doi:10.1016/0735-1933(94)90029-9).
9. Fardad, D. and Ladommatos, N., "Evaporation of hydrocarbon compounds, including gasoline and diesel fuel, on heated metal surfaces", *Proceedings of The Institution of Mechanical Engineers, Part D, Journal of Automobile Engineering*, Vol. 213, (1999), 625-445. (doi:10.1243/0954407991527152).
 10. Arifin, Y.M. and Arai, M., "Deposition characteristics of diesel and biodiesel fuels", *Fuel*, Vol. 88, (2009), 2163-2170. (doi:10.1016/j.fuel.2009.01.021).
 11. Arifin, Y.M., Furuhashi, T., Saito, M. and Arai, M., "Diesel and biodiesel fuel deposits on a hot surface", *Fuel*, Vol. 87, (2008), 1601-1609. (doi:10.1016/j.fuel.2007.07.030).
 12. Metcalfe, L.D. and Schmitz, A.A., "The rapid preparation of fatty acid esters for gas chromatographic analysis", *Analytical Chemistry*, Vol. 33, (1961), 363-364. (doi:10.1021/ac60171a016).
 13. Moosavi, S.A., Aghaalkhani, M., Ghobadian, B. and Fayyazi, E., "Okra: A potential future bioenergy crop in Iran", *Renewable and Sustainable Energy Reviews*, Vol. 93, (2018), 517-524. (doi:10.1016/j.rser.2018.04.057).
 14. Xiong, T.Y. and Yuen, M.C., "Evaporation of a liquid droplet on a hot plate", *International Journal of Heat and Mass Transfer*, Vol. 34, (1991), 1881-1894. (doi:10.1016/0017-9310(91)90162-8).
 15. Tamura, Z. and Tanasawa, Y., "Evaporation and combustion of a drop contacting with a hot surface", *Symposium on Combustion*, Vol. 7, No. 1, (1958), 509-522. (doi:10.1016/S0082-0784(58)80086-7).
 16. Arifin, Y.M. and Arai, M., "The effect of hot surface temperature on diesel fuel deposit formation", *Fuel*, Vol. 89, (2010), 934-942. (doi:10.1016/j.fuel.2009.07.014).
 17. Abu-Zaid, M., "An experimental study of the evaporation characteristics of emulsified liquid droplets", *Heat and Mass Transfer*, Vol. 40, (2004), 737-741. (doi: 10.1007/s00231-003-0473-5).



Foreign Direct Investment, Stock Market Development, and Renewable Energy Consumption: Case Study of Iran

 Mahdiah Rezagholizadeh^{a*}, Majid Aghaei^a, Omid Dehghan^b
^a Department of Economics and Administrative Sciences, University of Mazandaran, Babolsar, Iran.

^b Department of Energy Economics, Petroleum University of Technology, Tehran, Iran.

PAPER INFO

Paper history:

Received 28 November 2019

Accepted in revised form 11 April 2020

Keywords:

 Foreign Direct Investment
 Stock Market
 Renewable Energy
 GDP
 ARDL Test

ABSTRACT

Concerning environmental pollution issues derived from fossil energy consumption, the application of renewable energies plays an important role in countries, especially in their energy sector policymaking. Since determining the relationship between different variables and renewable energy not only has significant policy applications in energy sector but also is necessary in achieving sustainable development goals, this study assesses the impact of effective factors on the development of renewable energy consumption in Iran with emphasis on the role of foreign direct investment (FDI) and financial sector development (especially stock market development). This study applies Auto-Regressive Distributed Lag (ARDL) bounding test method over the period of 1978-2016. The research findings show that there is a causal relationship between foreign direct investment and the stock market and renewable energy consumption in Iran such that the increase of foreign direct investment and stock market development will increase the consumption of renewable energies in Iran. On the other hand, a growth in renewable energies consumption will significantly reduce CO₂ emission in the long run. Besides, increasing FDI and stock market development will raise the economic growth of a country and, in return, increase CO₂ emission.

1. INTRODUCTION

In recent years, numerous studies have estimated the relationship between energy consumption and economic growth in Iran. Most of them have indicated that energy use has an important role in increasing economic activities. Apart from energy security, environmental issues and climate changes arising from massive conventional energy consumption (like fossil fuel) represent another challenge for the Iranian economy. Therefore, the focus of energy economists and policy-makers has moved towards the use of renewable energies in the production process and consumption rather than the use of nonrenewable energy sources, e.g., fossil fuels. Because renewable energies can meet the increasing demand for energy, they can significantly reduce CO₂ emissions.

Since renewable energies are harmless in environmental pollution by decreasing the emission of CO₂ and other greenhouse gasses, their consumption is not limited and, finally, the ever-increasing energy demand for and the development and expansion of renewable energies are necessary for the sustainable development of developing countries as important factors. To reduce CO₂ emission, the consumption of renewable energies has become an important topic of interest among energy economists, environmental scientists, and policy-makers in developing countries, primarily due to increasing economic activities.

Therefore, policymakers have made an attempt to develop the use of these energies through different policies in Iran. Despite the governments' backbreaking efforts in the development of renewable energies, the ratio of the

consumption share of renewable energies to total energy in Iran is still very low. One of the most important obstacles to the expansion of renewable energies includes a high initial investment and the lack of appropriate finance in this sector. The deployment of the renewable energy sector is one of the capital-intensive sectors in each country because renewable energy projects need a high amount of investment before production. Investing in the production of these energies is the same as infrastructure projects such as highways, airports, ports, and railways. For Youngho (2016), renewable energy projects are more dependent on high initial investment than other conventional energies. They also have low rates of return and long payback period of capital; therefore, investment in these projects that demand abundant financial resources would be risky. Some of the economic research studies (e.g., Jeayoon and Kwangwoo (2016); Paramati et al. (2016); Li (2013); Li and Wang (2011); Brunnschweiler (2010)) seek to answer whether there is a significant relationship between the financing of renewable energy projects (like foreign direct investment inflow or Stock market development) and the deployment of these energies and also reduction of environmental pollution in other countries. On the one hand, stock market development and the entrance of capital flow provide investment opportunities in a commercial and competitive environment in a country; moreover, by increasing the country's economic activities, energy demand will increase. On the other hand, some economic theories state that foreign direct investment in the host country and its stock market development through international finance can reduce the consumption of fossil fuels and affect the environment by financing renewable energy projects.

Therefore, this study argues that increasing both stock market developments and FDI inflows in Iranian market

*Corresponding Author's Email: m.gholizadeh@umz.ac.ir (M. Rezagholizadeh)

economies can lead this economy to enhance the use of advanced technologies in clean energy production and energy efficiency, leading to the significant reduction of CO₂ emissions. Regarding the importance of this issue, the relationship between foreign direct investment and country financial development (stock market in particular) with renewable energy consumption is analyzed from 1978 to 2016 in the Iranian economy by using economic theories and an econometric model in this study. To do so, time series data and ARDL bounding test will be used.

The rest of the paper is organized as follows. Following the presentation of the theoretical foundation and literature review, an appropriate empirical model will be discussed. Then, after data introduction and research methodology, the regression model will be estimated and the results will be analyzed.

2. LITERATURE REVIEW

Regarding the research goal, the literature review is divided into three parts. In the first group of studies, the relationship between foreign direct investment flow and energy consumption level and CO₂ emission is considered. This group aims to answer whether foreign direct investment can be an important factor in changing energy consumption. It should be noted that, generally, in most of these studies, the positive relationship among FDI, economic growth, and energy consumption has been concluded. The second group of studies investigates the effect of financial development (stock market growth in particular) on energy consumption seeking the reaction of energy consumption against the development of the financial sector. The third group of studies investigates the effect of FDI and financial development on energy consumption. Some of the most important studies related to each group are shown in Table 1 in Appendix. The main goal of this research is to investigate the effective factors in renewable energy consumption in Iran through Foreign Direct Investment and stock market development as a financial development index from 1978 to 2016. More specifically, to our knowledge, no study so far has empirically investigated the impact of both FDI inflows and stock market development on renewable energy use and CO₂ emissions in Iran.

Energy consumption trend in developed countries shows that despite an increase in energy consumption, fossil fuel consumption has decreased due to the emission of greenhouse gasses in recent years. According to the EIA report, the use of renewable energy resources is not available for all countries due to their high initial cost; however, developed countries invest in renewable energies through foreign direct investment and, as a result, energy production through renewable resources is increasing rapidly. Also, these countries attempt to increase their renewable energy resources and replace fossil fuels with them by attracting foreign investments, direct and indirect stock market development, energy security, and reducing greenhouse gasses emission (Constantini and Martini (2010); Inglesi-Lotz (2013)). According to that, it can be concluded that energy consumption – renewable energies in particular- can be affected by Foreign Direct Investment and stock market growth.

Renewable energy project developers need a combination of debt (loan) and stock investment (ownership) for a project building cost. A Loan is available through public markets (bonds) or private sector (bank loans or organization loans), and the stock is available by internal resources and foreign

investors in public or private markets. Loans are less expensive than stocks. Therefore, developers prefer loans to finance the projects. Regarding technological issues, the financial period of renewable energies is important due to being capital intensive; therefore, it needs loan and stocks more than other plants. Some problematic factors that hinder alluring financial resources into renewable energies are as follows:

- 1) Project risks: most of the financial institutes do not have enough experience in risk assessment of renewable resources. Renewable projects failure leads to a more difficult and expensive increase in capital.
- 2) Industry size and investor attraction: the renewable industry is smaller than other energy sectors and investors are reluctant to invest in this sector.
- 3) Unpredictable policies: most of the renewable projects are dependent on government policies (tax credits, subsidies, etc.). These policies are almost unpredictable and have a negative effect on the investment in renewable energies.

Ryan and Steven (1997) and Brunnchweiler (2010) also divided the problem of renewable projects finance into two groups: first, availability of long-run loans for renewable companies, related to the development of the banking system. Second, limited financial resources are available for renewable companies because they are newer and more expensive than fossil fuel projects. According to the aforementioned reasons, the development of internal financial sectors is a very important factor in estimating the energy demand growth in less developed economies.

In developed economies, finance is mostly done through debt. However, in emergent economies, this study needs a greater stock market investment due to the disability in debt presentation (Thiam and Jacqueline (2016)). Therefore, foreign finance is available to a greater degree in countries with the advanced financial market and renewable sectors, which are highly dependent on foreign finance. The main reason for developing financial markets is to facilitate the process of less expensive finance in projects, which are compatible with the environment (Jiun and Kuangwoo (2016)).

Financial development is also considered as a significant factor in environmental performance such that higher financial development provides more financial resources for environmental projects with low financial costs. In a developed financial system, technological changes have significant effects on energy supply and CO₂ emission reduction. The capital market as an inseparable part of a financial system will react to the release of environmental performance information. Financial development in a country leads to foreign direct investment, research, and development that can increase economic growth level and also the dynamism of environmental performance (Abul and Mete (2011)). In most of the rural areas of developing countries, there is not appropriate infrastructure for renewable energy systems on a small scale. This lack of financial sources is one of the main obstacles to the application of renewable energies for final consumer and small entrepreneurs.

Commercial financial infrastructure is located mostly in large urban areas, and lending loan criteria to rural areas are limited to the needs and credits repayment opportunities. Finance should be cost effective for both lender and borrower in an appropriate time frame. Finance is not the only factor in

projects' success. Product quality, repair, and maintenance to increase trust and trained personnel for repair and maintenance are also needed in project success (Derrick (1998)).

In this part of the research, we will theoretically investigate the role and importance of financial development in the growth and development of renewable energies. Theoretical foundations of the relationship between financial development and renewable technologies development analyze how the development of financial markets overcomes adverse selection and moral hazard, resulting in the reduction of foreign finance cost in the renewable energy sector. Regarding the objective of this research, theoretical foundations of the relationship between stock market development and energy consumption (in particular renewable energies) will be presented, and the role of the stock market in the easy availability of foreign finance for renewable energies sector and their development will be investigated.

Generally, financial market development will have an effect on energy consumption directly and indirectly:

(A) Direct effect:

In developed stock markets, information will be presented based on rational expectation with respect to the balanced stock price. Therefore, investors recognize undesirable and incompatible information through balanced prices (Grossman 1976)). Besides, a quick balance of stock prices will provide valuable periodic information from enterprise investment opportunities (Hsu et al.) and gain investors' trust through the lack of information balance between investors and enterprises. Finally, developed stock markets with valuable balanced prices reduce the problem of incorrect choice. On the other hand, liquidity and other risks in developed stock markets will be reduced. In undeveloped stock markets, the investor refuses to invest in some of the projects due to a high risk of liquidity; however, in the developed stock market, liquidity risk is decreased by the facilitation of exchanges (Levin (1997)). As a result, investors will tend to invest more in projects when they are able to sell their stocks easily. Regarding risk management in developed stock markets, there is the possibility of reducing other risks in this market, too. Developed stock markets encourage investors to invest in high-risk projects by providing risk covers and various tools of diversification (Levin (2005)). Therefore, in terms of direct effect, developing the stock market by making a healthy competitive environment for factories and investors has a significant effect on energy consumption. Therefore, by listing factories' stock, it provides available and excess investments in the stock market. This will offer opportunities to internal and external investors that increase the economic activities of a country and lead to an increase in energy demand (Parmati et al. (2016)). Therefore, financing renewable energies projects, which need lots of funds, are more possible in developed financial markets. Developed financial markets with low liquidity risk, various tools of diversification, and risk cover will minimize side effects derived from undesirable choices.

The development of financial markets can also have an effect on energy demand by increasing the household budget. Based on microeconomics theories, lower limitations in the household budget will lead to an increase in their goods and services consumption. Financial markets lower the household budget limitation by providing loans with lower interest rates. This is how the demand for energy devices such as

automobile, housing, electrical devices, etc. increases, which consequently affects the energy consumption directly and gives it a rise (Sadorsky (2012)).

Finally, it can be said that stock market development can lead to the development of advanced projects and superior technologies like renewable energy projects. Due to the fact that stockholders share stock financing in case of high returns, there are no collateral requirements in the stock market and, therefore, extra stock supply will not lead to chaos and financial indiscipline (Brown et al. (2009)). In return, financing high technology enterprises, which are sensitive to financial indiscipline, is useful.

(B) Indirect effect:

In terms of indirect effect, stock market development can increase investment and economic activities through quantity and efficiency effect and increase the demand. Stock market development and more investment together with more trade and consumption can create a wealth effect that stimulates consumption and leads to an increase in applying advanced technologies in clean energy products and, finally, reducing CO₂ emission significantly (Parmati et al. (2016)).

On the other hand, the financial market development can lead to an increase in energy consumption through an increase in investment and in economic growth. More developed financial markets provide enterprises with easier and less expensive financial resources. Enterprises expand their production units by hiring new staff and purchasing equipment and machinery. Therefore, by developing the financial market and reducing the cost of borrowing, investment activities along with the employment opportunities for skilled and unskilled workers will increase. This will lead to an increase in production and national income and, also, energy consumption (Kakar et al. (2011)).

Existing views revolve around the relationship between stock market development and the development of renewable energies technology. Under a common economic mechanism, in financial sectors that overcome undesirable choice and moral dangers, foreign financial costs decrease and developed stock markets make finance easier through stocks. Finally, it can be said that the greater development of financial markets can lead to the development of renewable technologies, which need lots of funds. Beck and Levine (2002) investigated the effect of financial system development (comprised of the stock market and credit market) on the growth and development of production industries, which are dependent on foreign finance. According to their study results, the development of the entire financial system will decrease the finance cost of production industries.

Despite the fact that capital is considered as the engine of growth and economic development, developing countries usually encounter with lack of investment and try to compensate it through foreign borrowing. However, foreign direct investment is now considered as an alternative to foreign borrowing due to the crisis derived from its repayment and is an instrument to achieve economic growth. Foreign direct investment booms economic growth by providing foreign investment and, as a result, affects energy consumption. Borensztein et al. (1998) stated that, generally, the addition of foreign direct investment in a healthy competitive environment of a country would result in economic growth and an increase in economic activities and energy consumption.

In every country, the consumption of renewable and non-renewable energies is highly dependent on the level of economic activities and that country's growth (Salim et al. (2014)) such that high economic rates will increase energy consumption by creating new demand. According to this fact, income, wealth, and households demand luxurious energy-intensive goods increase via an increase in economic growth. Energy consumption is also increased through consumption increase in the household and transportation sector, resulting from the income raise in the household's income (Barghi et al. (2013)).

In addition, an increase in economic growth will raise energy consumption through the booming service sector, transportation, and commerce, which are energy consumers (Medlock and Soligo (2001)). On the other hand, with economic growth, countries seek to improve and increase the efficiency of energy consumption. They will reduce the final cost of energy through increased effectiveness and efficiency of energy and, finally, lead to an increase in energy consumption. This is known as Rebound effect (Brookes (2000); Manzur et al. (2012); Medlock and Soligo (2001)).

On the other hand, based on Porter Theory, Foreign direct investment, which accelerates the host country's economic growth as a production factor, will provide the host country with efficient technology in protecting the environment. The availability of clean and environmentally friendly technologies improves the quality of the environment and, therefore, it can be said that foreign direct investment facilitates the replacement of clean and environmentally friendly technology (Energy saver) with destructive and polluting technologies (Asghari and Rafsanjani pour (2014)).

3. DATA AND METHODOLOGY

Because of the economic dependence on energy consumption and with respect to the lack of energy, particularly fossil fuels, determining the effective factors in renewable energies consumption has been always one of the most important issues between economists and politicians. Based on the considered theoretical foundations in the previous sector, i.e., the effect of foreign direct investment and stock market growth on energy consumption through various ways, with respect to previous studies (such as Sbia et al. (2014); Chang (2015)) and economic texts, the related model for determining the reaction of renewable energies consumption against foreign direct investment, stock price index, total energy consumption, CO₂ emission per capita, and gross domestic production per capita is given as follows:

$$CEC_t = f(ST_t, FDI_t, TEC_t, CO_t, GDPPC_t) \quad (1)$$

CEC: is renewable energy consumption, which is equal to renewable energy consumption ratio (total renewable energy

$$\Delta \ln CEC_t - \beta_1 + \beta_{CEC} \ln CEC_{t-1} + \beta_{FDI} \ln FDI_{t-1} + \beta_{ST} \ln ST_{t-1} + \beta_{TEC} \ln TEC_t + \beta_{CO} \ln CC_{t-1} + \beta_{GDPPC} \ln GDPPC_{t-1} + \sum_{i=1}^p \beta_i \Delta \ln CEC_{t-i} + \sum_{j=0}^q \beta_j \Delta FDI_{t-j} + \sum_{k=0}^r \beta_k \Delta \ln ST_{t-k} + \sum_{l=0}^u \beta_l \Delta TEC_{t-1} + \sum_{m=0}^s \beta_m \Delta \ln CO_{t-m} + \sum_{n=0}^z \beta_n \Delta \ln GDPPC_{t-n} + \mu_t \quad (3)$$

$$\Delta \ln CO_t = \gamma_1 + \gamma_{ECE} \ln CEC_{t-1} + \gamma_{FDI} \ln FDI_{t-1} + \gamma_{ST} \ln ST_{t-1} + \gamma_{TEC} \ln TEC_{t-1} + \gamma_{CO} \ln CO_{t-1} + \gamma_{GDPPC} \ln GDPPC_{t-1} + \sum_{i=1}^p \gamma_i \Delta \ln CEC_{t-i} + \sum_{j=0}^q \gamma_j \Delta FDI_{t-j} + \sum_{k=0}^r \gamma_k \Delta \ln ST_{t-k} + \sum_{l=0}^u \gamma_l \ln TEC_{t-1} + \sum_{m=0}^s \gamma_m \Delta \ln CO_{t-m} + \sum_{n=0}^z \gamma_n \Delta \ln GDPPC_{t-n} + \mu_t \quad (4)$$

$$\Delta \ln GDPPC_t = \phi_1 + \phi_{CEC} \ln CEC_{t-1} + \phi_{FDI} \ln FDI_{t-1} + \phi_{ST} \ln ST_{t-1} + \phi_{TEC} \ln TEC_{t-1} + \phi_{CO} \ln CO_{t-1} + \phi_{GDPPC} \ln GDPPC_{t-1} + \sum_{i=1}^p \phi_i \Delta \ln CEC_{t-i} + \sum_{j=0}^q \phi_j \Delta FDI_{t-j} + \sum_{k=0}^r \phi_k \Delta \ln ST_{t-k} + \sum_{l=0}^u \phi_l \Delta TEC_{t-1} + \sum_{m=0}^s \phi_m \Delta \ln CO_{t-m} + \sum_{n=0}^z \phi_n \Delta \ln GDPPC_{t-n} + \mu_t \quad (5)$$

In these equations, Δ is the difference operator and μ_t is the Error Correction component at t (time). In order to test the existence of Co-integration relationship between variables,

to total energy consumption). ST: is the stock market development price. With respect to previous studies such as (Levine and Zervos (1998); Beck & Levine (2002); Hso et al. (2014); Jion and Kongvo (2016)), stock market investment GDP ratio and stock market transactions GDP ratio represent stock market development. According to Beck and Levin (2002) and Coban and Topcu (2013), by applying Principle Component Analysis (PCA), stock market development index, which is one of the sub-indices of Stock Market Capitalization and Stock Market Traded Value, is given as follows:

$$Equity_{i,t} = 1^{st} \text{ principal component of } \frac{\text{market}_{i,t}}{GDP_{i,t}} \times 100 \text{ and } \frac{\text{market}_{i,t}}{GDP_{i,t}} \times 100 \quad (2)$$

where Marketcap: the stock market value equals the stock market value of the entire companies in Iran stock exchange market. Market trade: the total value of exchanged stocks over a specific period. Stock market value is the stock market size and exchanged stock value variable is the liquidity amount of market. Investment in the stock market represents the total size, and transaction value represents stock market liquidity. Stock market development index is calculated based on the first main component of these two variables regarding the covariance matrix. FDI: Foreign Direct Investment, GDPPC: is gross domestic product per capita, which is calculated by dividing GDP into country's population. This variable has been used as a substitution for economic growth in various studies (e.g., Tou et al. (2013); Omri and Chaibi (2014); Fotros et al. (2013)). Installing renewable energy technology is dependent on not only environmental finance but also the economic level of each country. Economic growth has a positive relationship with the development of renewable energies. CO: is Carbon dioxide emission per capita, which has been calculated by dividing total CO₂ into the country's population as Kilogram per each person. TEC: Total Energy Consumption (based on Million Barrels of Crude Oil Equivalent).

Required Data for modeling has been collected from Central Bank Statistical sources, World Bank, Securities, Exchange Organization, and Energy Balance sheet in this research.

In order to analyze the long-run and short-run dynamic relationship among Foreign Direct Investment variables, stock price index, total energy consumption, CO₂ Emission per capita, Gross Domestic Production per capita, and renewable energy consumption in Iran, Autoregressive Distributed Lag Bounding test method by Pesaran, Shin and Smith (2001) is used as the Time Series model. This method is the most appropriate co-integration estimation method in small samples (Haug (2002)). Unrestricted Error Correction Model that has been used in this research to investigate the long-run and short-run dynamic relationship between variables is as follows:

each equation is estimated based on the significance of common F statistics of lagged variables coefficients in the model. With respect to the fact that the considered sample is

small, in order to distinguish co-integration, Narayan critical amounts will be used in this study (Narayan and Narayan (2005)).

After investigating the existence of the co-integration relationship between effective factors in renewable energy consumption, the causal relationship between model variables

$$\Delta \ln CEC_t = \alpha_{01} + \sum_{i=1}^l \alpha_{11} \Delta \ln CEC_{t-i} + \sum_{j=1}^m \alpha_{22} \Delta FDI_{t-j} + \sum_{k=1}^n \alpha_{33} \Delta \ln ST_{t-k} + \sum_{l=1}^o \alpha_{44} \Delta TEC_{t-1} + \sum_{m=1}^p \alpha_{55} \Delta \ln CO_{t-k} + \sum_{n=1}^q \alpha_{66} \Delta GDPPC_{t-1} + \eta_1 ECT_{t-1} + \mu_t \quad (6)$$

where Δ is the difference operator and μ_{it} is the model's residual component with normal and independence distribution.

4. RESULTS AND DISCUSSION

4.1. Stationary test of variables

This study starts the investigation by checking the order of integration for variables included in the model. This step is necessary because the tabulated critical value bounds in bounds testing can be only applicable to I (0) and I (1) variables. To determine the order of integration, this study

should be analyzed. Based on Granger (1969) study, in the co-integrated variables that are of first order, Vector Error Correction Method (VECM) is the best method to recognize the causal relationship between variables (Narayan and Narayan (2004)). VECM model of variables to investigate the long-run relationship is as follows:

applies Dickey-Fuller Generalised Least Square tests and unit root test with structural breaks including Ng-Perron Unit Root Test and reports the test results for the intercept-and-trend case in Table 1.

Based on the results of Unit Root Tests, all variables are stationary considering intercept and time trend at the level or by one difference. Therefore, there would not be any concerns about the unreliability of Pesaran F statistics, and the research models can be estimated and analyzed through the ARDL Bounding Test.

Table 1. Unit root test results.

Variable	Ng-Perron test						DF-GLS test		
	Optimum lag	MZa	MZt	MSB	MPT	Integration degree	DF-GLS statistic	Optimum lag	Integration degree
Renewable Energy Consumption (CEC)	0	-1.3653	-0.477	0.34992	10.5398*	I(0)	-6.4413*	1	I(1)
Foreign Direct Investment (FDI)	0	-0.4415	-0.412	0.93372	162.142*	I(0)	-5.7158*	1	I(1)
Stock Index (ST)	0	0.1289	0.8921	6.91937	243.03	I(0)	-2.164780*	0	I(0)
Total Energy Consumption (TEC)	0	-3.314	-0.977	0.29504	7.15026*	I(0)	-1.797973*	0	I(0)
CO ₂ Emission (CO)	0	0.8276	0.6171	0.74561	40.3379*	I(0)	-3.547831*	0	I(0)
Gross Domestic Production Per Capita (GDPPC)	0	-0.781	-0.480	0.61441	21.2916*	I(0)	-2.325043**	0	I(0)

Source: Author's calculations. The * and ** denote rejection of the null at 1 % and 5 % levels, respectively.

4.2. Determining optimum lags, co-integration test result and other diagnostic statistics

After conducting stationary test and making sure that all of our selected variables are integrated at either I(0) or I(1), in this section, in order to assure the stability of each model, this study begins with identifying optimal lag structure and choosing Co-integration test between variables and other diagnostic tests. The results of co-integration test, which is presented in the third column, are based on the long-run relationship between renewable energy consumption and Foreign Direct Investment, Stock market growth, total energy consumption, CO₂ Emission, and Gross domestic production, and indicate that the co-integration relationship between variables is confirmed based on various equations and is significant at a 1 % level based on Pesaran Bounding test. Other tables' columns represent model diagnostic statistics in order to investigate the classic assumptions and validity of estimated models. The diagnostic tests indicate that all Equations are correctly specified, and all Gaussian errors are normally distributed, homoscedastic, and not serially correlated.

4.3. Estimation of long-run and short-run coefficients

Table 3 shows the short-run and long-run causal relationship from foreign direct investment, stock market development index, total energy consumption, carbon dioxide emission, and gross domestic production to renewable energy consumption in Iran. As can be observed from the table, the coefficient of foreign direct investment in the short run is 0.024 and statistically significant. According to this estimation, a one percent increase in FDI leads to a 0.02 % increase in the consumption of renewable energies. The estimation of long-run coefficients in this equation indicates that FDI has a positive and significant impact on renewable energy consumption in the long run in Iran so it can be inferred that an increase in FDI in Iran will result in energy consumption increase in both short-run and long-run terms. Increasing FDI through clean and environmentally friendly technology replacement with destructive and pollutant technology can lead to an increase in clean energy consumption.

The Coefficient of stock market development is positive and equal to 0.019, which is statistically insignificant in the short run, but as it can be observed, lagged stock market development variable has a positive and significant effect on

renewable energy consumption. On the other hand, the estimation of long-run coefficients in this equation represents that stock market growth has had a positive and significant effect on energy consumption in this country over the research period. Financial market development increases investment

activities and expands employment opportunities for skilled and unskilled workers by decreasing the cost of borrowing, resulting in an increase in production and national income and high energy consumption.

Table 2. Results of ARDL co-integration test and other diagnostic tests.

Estimated model	Optimum lag length	Pesaran F statistic	Normality test	ARCH test statistic	LM test	Reset test	DW-statistic	F-stat	Adjusted R-squared
$F_{CEC}(L_{CEC}/FDI, L_{ST}, L_{TEC}, L_{CO}, L_{GDPPC})$	(2,4,1,4,4,1)	21.56*	0.09 (0.9517)	0.48 (0.9314)	2.59 (0.1196)	7.22 (0.0797)	2.61	2895.46*	0.99
$F_{GDPPC}(L_{GDPPC}/L_{CEC}, FDI, L_{ST}, L_{TEC}, L_{CO})$	(3,3,2,2,0,1)	7.65*	1.09 (0.5772)	0.64 (0.8061)	2.32 (0.1280)	0.75 (0.3959)	2.22	425.428*	0.99
$F_{CO}(L_{CO}/L_{CEC}, FDI, L_{ST}, L_{TEC}, L_{GDPPC})$	(4,3,4,4,2,3)	5.52*	1.39 (0.4980)	0.63 (0.8222)	1.14 (0.3706)	6.33 (0.1360)	2.55	716.154*	0.99

The optimal lag structure of the ARDL model is determined by AIC. The asterisks * and ** denote significance at 1 % and 5 % levels, respectively. The Normality, LM, ARCH, and RESET tests represent the normality test, the Breusch-Godfrey Lagrange multiplier test, the autoregressive conditional heteroscedastic Lagrange multiplier test, and the Ramsey specification test, respectively. F-stat indicates Fisher F test to determine the significance of all variables in the model. The figures in parenthesis represent the probability of diagnostic tests.

Table 3. The ARDL long-run and short-run estimates.

Dependent variable: log of renewable energy consumption (Causality from stock market growth, foreign direct investment, CO ₂ emission, total energy consumption and gross domestic production to renewable energy consumption).				
Short-run coefficient estimates				
Variables	Coefficient	Standard error deviation	T statistic	Probability
D(LCEC(-1))	0/7423	0/0818	9/0671	0/0000
D(LST)	0.0199	0.0097	0.0561	0.0284
D(LST (-1))	0.2160	0.0180	11.9727	0.0000
D(LST (-2))	0.1452	0.0166	8.7000	0.0000
D(LST (-3))	0.1032	0.0124	8.2997	0.0000
D(FDI)	0.0245	0.0059	4.1388	0.0012
D(LCO)	0.2817	0.1804	1.5612	0.0839
D(LCO(-1))	0.0093	0.0677	0.1376	0.8927
D(LCO(-2))	0.1361	0.0726	1.8740	0.0836
D(LCO(-3))	-0.6987	0.0612	-11.4145	0.0000
D(LTEC)	0.04922	0.01456	3.3786	0.0036
D(LTEC(-1))	-1.4805	0.1402	-10.5582	0.0000
D(LTEC(-2))	-0.6524	0.0974	-6.6925	0.0000
D(LTEC(-3))	-0.1714	0.1092	-1.5699	0.1404
D(LGDP)	0.0036	0.0214	0.1709	0.8669
CointEq(-1)	-0.4421	0.0903	-4.8939	0.0020
Cointeq = LCEC - (-0.1913*LST1 + 0.0079*LFDI2 - 0.1924*LCO + 0.0237*LTEC + 0.0568*LGDP - 1.5696)				
Long-run coefficient estimates				
Variables	Coefficient	Standard error deviation	T statistic	probability
LST	-0.1912	0.0530	-3.6031	0.0032
FDI	0.0079	0.0040	1.9550	0.0724
LCO	0.1924	0.0879	-2.1878	0.0259
LTEC	0.0236	0.0088	2.6697	0.0203
LGDP	0.0568	0.0202	2.8118	0.0180
constant	-1.5695	0.4442	-3.5331	0.0034

According to the results, the coefficient of Co emission in the short run is 0.281, which is statistically insignificant. On the other hand, this coefficient in the long run is equal to -0.192, which is statistically significant and indicates that a one percent decrease in CO₂ emission in the long run will lead to a 0.192 % increase in renewable energy consumption, which shows the relatively high impact of this variable on energy consumption in the country. In other words, the coefficient of this variable indicates that by decreasing the emission of greenhouse gasses, renewable energy sources will increase and gradually become the alternative to fossil fuels and non-renewable energies.

According to the results, the coefficients of total energy consumption in the short and long run are 0.049 and 0.023, respectively, which are statistically at a high level of significance. The positive coefficients indicate that total energy consumption in the country has a positive and significant effect on renewable energy consumption. As can be seen from the table, economic growth has positive, but insignificant, effect on renewable energy consumption in the short run, while the coefficient of this variable in the long run is 0.056 and statistically significant. It is implied that renewable energy consumption is dependent on the level of economic activities and its growth in the country such that

high economic growth rates will increase energy consumption and clean energy consumption by creating new demands.

ECT coefficient is -0.442 and significant at all conventional levels, corroborating the established cointegration relationship between underlying variables. It is also implied that a 44.2 % change in renewable energy consumption is corrected by deviations in the short run towards the long-run equilibrium path.

The causal relationship from renewable energy consumption, total energy consumption, foreign direct investment, stock market development index, and CO₂ emission to the log of gross domestic product per capita (as an index for economic growth) is presented in Table 4. The

results of the long-run elasticity of gross domestic products in the table indicate that renewable energy consumption, total energy consumption, foreign direct investment, and stock market index growth have a positive and significant effect on GDP and lead to more economic growth in Iran, while CO emission has a negative and significant effect on GDP. According to these results, a one percent increase in renewable energy consumption, total energy consumption, FDI, and stock market development will lead to increasing GDP for 0.337, 0.231, 0.17, and 0.417 percents, respectively, and a one percent decrease in CO₂ emission will lead to a 0.428 percent increase in GDP.

Table 4. The ARDL long-run and short-run estimates.

Dependent variable: log of gross domestic production (causality from stock market growth, foreign direct investment, CO emission, total energy consumption, and renewable energy consumption to gross domestic production).				
Short-run coefficient estimates				
Variables	Coefficient	Standard error deviation	T statistic	Probability
D(LGDP(-1))	0/3942	0/0921	4/2788	0/0004
D(LGDP(-2))	-0.1765	0.0960	-1.8378	0.0818
D(LST)	0.3323	0.0461	7.1998	0.0000
D(LST (-1))	0.4630	0.0812	5.7019	0.0000
D(LST (-2))	0.1340	0.0601	2.2264	0.0383
D(FDI)	0.1104	0.0353	3.1301	0.0055
D(FDI (-1))	0.1820	0.0384	4.7384	0.0001
D(LCEC)	0.3697	0.2785	1.3275	0.2001
D(LCEC(-1))	0.7031	0.3469	2.0267	0.0001
D(LTEC)	0.0828	0.5846	0.1416	0.0796
D(LCO)	-0.7599	0.2869	-2.6483	0.0000
CointEq(-1)	-0.6546	0.0774	-8.4553	0.0000
Cointeq = LGDP - (0.4177*LST1 + 0.1701*LFDI2 + 0.3373*LCEC + 0.2312*LTEC - 0.4288*LCO - 5.5286)				
Long-run coefficient estimates				
Variables	Coefficient	Standard error deviation	T statistic	Probability
LST	0.4176	0.1747	2.3896	0.0000
FDI	0.1700	0.0557	3.0516	0.0066
LCEC	0.3373	0.1449	2.3264	0.0018
LTEC	0.2312	0.1137	2.0325	0.0498
LCO	-0.4287	0.1201	-3.5675	0.0000
constant	-5.5285	2.3242	-2.3786	0.0000

Table 5 shows the result of a causal relationship of renewable energy consumption, total energy consumption, foreign direct investment, stock market index, and economic growth and CO emission. The results indicate that an increase in clean energy consumption in the long run significantly reduces Carbon emission, because an increasing share of this energy in total energy consumption has a negative effect on greenhouse gasses emission and will result in a considerable reduction in CO₂ emission. On the other hand, the results show that an increase in economic growth, foreign direct investment, and stock market development has a positive and significant relationship with CO₂ emission because, by increasing these variables, economic activities will increase and, finally, CO₂ emission will be increased. The results also indicate that the effect of total energy consumption on CO₂ emission is positive in the long run and is statistically significant.

5. CONCLUSIONS

With respect to the importance of investigating the relationship between financing renewable energy projects (such as foreign direct investments inflow or stock market development) and deployment of renewable and clean energy

use, the current study analyzed the relationship between foreign direct investment and financial development (particularly stock market) with renewable energy consumption based on existing economic theories and an econometric model from 1978-2016 in Iran.

In order to analyze that, this study used time series data and ARDL Bounding test method. The results showed that there was a causal relationship of foreign direct investment and stock market and renewable energy consumption in Iran, such that an increase in foreign investment and stock market development led to an increase in the consumption of these kinds of energies in the country. On the other hand, an increase in them in the long run significantly decreases CO₂ emission, increases foreign direct investment, stock market development, and economic growth of the country and, in return, it will increase CO₂ emission. FDI inflows and stock market developments substantially increased the economic activities and, therefore, led to the increasing demand for energy on the one hand and emittance of more CO₂ into the atmosphere on the other hand. As a result, to reduce CO₂ emissions and maintain the level of economic activities, the only possible way is increasing the share of clean and renewable energy in total energy consumption and the adaptation of modern (green) technologies.

Table 5. The ARDL long-run and short-run estimates.

Dependent variable: log of CO ₂ emission (Causality from renewable energy consumption, stock market growth, foreign direct investment, total energy consumption, and gross domestic production to carbon emission).				
Short-run coefficient estimates				
Variables	Coefficient	Standard error deviation	T statistic	Probability
D(LCO(-1))	0.2019	0.0963	2.0961	0.0285
D(LCO(-2))	-0.1415	0.1074	-1.3171	0.2203
D(LCO(-3))	0.5381	0.0968	5.5559	0.0004
D(LST)	0.0935	0.0119	7.8122	0.0000
D(LST (-1))	0.1528	0.0238	6.4179	0.0001
D(LST (-2))	0.0555	0.0183	3.0296	0.0143
D(FDI)	0.0172	0.0121	1.4219	0.1887
D(FDI (-1))	0.0572	0.0196	2.9105	0.0202
D(FDI (-2))	0.0057	0.0112	2.5074	0.6240
D(LFDI2(-3))	0.0423	0.0118	3.5710	0.0114
D(LCEC)	-0.4457	0.1107	-4.0251	0.0050
D(LCEC(-1))	-0.9415	0.1432	-6.5707	0.0001
D(LCEC(-2))	-0.1616	0.1149	-1.4065	0.1931
D(LCEC(-3))	-0.2609	0.0795	-3.2810	0.0095
D(LTEC)	0.4967	0.1766	2.8119	0.0213
D(LTEC(-1))	0.9270	0.1735	5.3422	0.0005
D(LGDP)	0.1521	0.0250	6.0801	0.0002
D(LGDP(-1))	0.1214	0.0271	4.4772	0.0015
D(LGDP(-2))	0.1104	0.0232	4.7540	0.0010
CointEq(-1)	-0.6576	0.0819	-8.0261	0.0000
Cointeq = LCO - (0.0424*LST1 + 0.0601*LFDI2 -0.0299*LCEC+0.1042*LTEC + 0.2899*LGDP + 18.4379)				
Long-run coefficient estimates				
Variables	Coefficient	Standard error deviation	T statistic	Probability
LST	0.0424	0.0197	2.1484	0.0260
LFDI	0.0600	0.0277	2.1679	0.0268
LCEC	-0.0299	0.0093	-3.2002	0.0184
LTEC	0.1041	0.0385	0.6991	0.0247
LGDP	0.2898	0.0451	6.4196	0.0001
constant	18.4379	2.9914	6.1635	0.0002

Regarding the research findings, more foreign direct investments inflow and stock market development in Iran can lead to an increase in clean energy consumption and a decrease in the emission of pollutant gases through the replacement of clean and environmentally friendly technologies with pollutant technologies; therefore, there should be regular policy makings regarding investment in renewable energies. On the other hand, findings show that increasing foreign direct investment and stock market development will increase economic activities and, finally, result in an increase in CO₂ emission. It also should be noted that a country's policymakers should orient investments and

the benefits derived from stock market development toward financing renewable projects; furthermore, they should place the priorities of financial institutions on these projects and, finally, encourage the private sector to invest in this sector.

6. ACKNOWLEDGEMENT

The authors would like to thank all organizations that provided data for this research.

APPENDICES

Table 1. Summary of previous studies.

The first group of empirical studies: the relationship between foreign direct investment flow with energy consumption and CO ₂ Emission.			
Author/Authors	Country and time period	Methodology	Research findings
Ben Jebli, M. et al. (2019)	USA 1995-2010	Granger causality test	Short-run Granger causality tests illustrate positive relationship between variables. In the long run, bidirectional causality between renewable energy, tourism, FDI, trade, and CO ₂ emissions should be considered.
Khandker, L.L. et al. (2018)	Bangladesh 1980-2015	Johansen's cointegration and Granger causality test	Johansen's cointegration test confirms that variables are cointegrated in the long run and Granger causality test reveals that there is a bidirectional causality between variables of interest. Through Vector Error Correction Model (VECM) found no causality between the variables in the short run.

Ghazouani, T. (2018)	MENA 1990-2015	ARDL	The long run analysis found the evidence of cointegration for all of the MENA countries Variables. The short-run Granger-causality reveals varied nature of direction of causality between Foreign direct investment, Renewable energy consumption, and economic growth and that is different among countries.
Chor, F.T. and Bee, W.T. (2015)	Vietnam 1976–2009	Granger causality test	There is a long-run balance between energy consumption, income, foreign direct investment, and CO ₂ emission.
Sbia, R. et al. (2014)	UAE 1975-2011	Autoregressive distributed lag model (ARDL) and Vector Error correction model (VECM)	There is a Mutual Causality relationship between foreign direct investment and clean energy consumption in UAE economics. Also, clean energy and economic growth have a positive and significant effect on energy consumption.
Hsiago, T.P. and Chung, M.T. (2011)	Brazil, Russia, India and China 1980-2007	Panel cointegration test and Granger causality test	In long-run balance, CO ₂ emission is elastic with energy consumption and not elastic on FDI. There is a long-run and short-run mutual causality relationship between FDI and energy consumption, CO ₂ emission, and GDP.
Asadpour and Eskruchi (2016)	1977-2013	Vector Autoregressive (VAR) and Vector Error Correction (VEC)	There is a positive relationship between FDI, trade openness, CO ₂ emission, and economic growth with energy demand.
Sadeghi et al. (2013)	Iran 1981-2008	Toda – Yamamoto test	The causality relationship between CO ₂ emission and GDP is not confirmed.
Barghi et al. (2013)	D8 countries 1990-2010	Generalized method of moments	Variables have a positive and significant relationship between CO ₂ emission and other variables except for FDI.
The second group of empirical studies: the effect of financial development (stock market in particular) on energy consumption.			
Researcher name	Country and time period	Research method	Research findings
Shujing, Sh. et al. (2019)	21 transitional countries 2006-2015	Panel data	Stock markets development led to decreased energy consumption in China and Poland. Financial openness development reduced energy use except in Georgia and the Kyrgyz Republic.
Gomez, M. and Rodriguez, C.J. (2019)	USA 1971-2015	Panel data	There is a positive relationship between GDP and EC, while there is a negative relationship among FD, CPI, URB, and TO and Energy Consumption.
Saini, S. and Nego, Y. (2018)	India 1978-2014	Granger causality test	There is no long-run causality between the variables, but there exists bi-directional short-run causality relationship between financial development and energy consumption in India.
Jeayoon and Kwangwoo (2016)	30 countries 2000-2013	Tobin panel model	With respect to the results, renewable energy sectors need foreign finance and developed financial market strongly. In countries with developed financial markets, renewable energies have been more developed.
Suh, C.C. (2015)	53 countries (countries with low and high income) 1999-2008	Threshold panel regression	Stock market development- as a financial development factor- in emergent economics with high income leads to an increase in energy consumption.
Serap, C. and Mert, T. (2013)	27 of European Union countries 1990-2011	GMM model	Financial development leads to an increase in energy consumption in these countries regardless of its source whether it derives from bank sector or stock market.
Sadorsky (2011)	9 European countries 1996-2006	Dynamic panel Demand	Only stock market turnover has a positive and significant effect on energy consumption.
Zhang, Y.J. et al. (2011)	1992- 2009	Granger causality test	There is a unilateral causality relationship between stock market development and energy consumption.
Farazmand et al. (2016)	Iran 1977-2010	Unbound Error correction model (UECM) and Toda-Yamamoto Granger causality test	Financial development indices such as allocated credit to private sector- GDP ratio, Cash, traded stocks to stock market total trades ratio and economic growth have a long-run relationship with energy consumption and also unilateral causality relationship from financial development and economic growth to energy consumption.
Oladi et al. (2013)	Iran 1981-2008	ARDL model	There is a positive and significant statistical relationship between financial development and energy demand.
Ebrahimi and Al morad Jabdarghi (2013)	D8 countries 1988-2008	Panel data pattern	Financial market development has a positive and significant effect on energy consumption.
The third group of empirical studies: investigation of simultaneous effect of FDI and stock market development on energy consumption.			

Researcher name	Country and time period	Research method	Research findings
Razmi, S.F. et al. (2020)	Iran 1990-2014	ARDL	Growth rate significantly affects total hydropower, wind, solar, and nuclear energies in both the short and long run, although it is only significant in the short run for combustible renewable and waste energies. Neither type of renewable energy consumption affects growth in either the short or long run.
Kutan, A.M. et al. (2018)	Brazil, China, India, and South Africa 1990-2012	panel	Renewable energy consumption helps to mitigate the growth of CO ₂ emissions and promotes economic development.
Paramati, R.S. et al. (2016)	20 emergent economics 1991- 2012	Heterogeneity test panel	Economic production, FDI, and stock market development have a positive and significant effect on clean energy consumption and, in the short run, there is a unilateral causality relationship between FDI and clean energy consumption.

REFERENCES

- Asadpour, A.A. and Eskruchi, E., "Investigation of the relationship between foreign direct investment, clean energy, trade openness, economic growth with energy demand in Iran", *Quarterly Journal of Government Management*, Vol. 4, No. 9-10, (2013), 16-22. (<http://noo.rs/vsZ0d>).
- Asghari, M. and Nazar Rafsanjani Pour, S., "The effect of foreign direct investment on environmental quality of selected countries", *Quarterly Journal of Economic Development Research*, No. 9, (2013), 1-30. (<http://noo.rs/KEvPp>).
- Barghi, O., Mohammad Mahdi, F.F. and Zhende Khatibi, S., "The effect of factory production and foreign direct investment on CO₂ emission in D8 countries", *Quarterly Journal of Economic Modelling*, Vol. 6, No. 4, (2012), 93-109. (magiran.com/p1131949).
- Beck, T. and Levine, R., "Industry growth and capital allocation: Does having a market-or bank-based system matter?", *Journal of Financial Economics*, Vol. 64, (2002), 147-180. ([https://doi.org/10.1016/S0304-405X\(02\)00074-0](https://doi.org/10.1016/S0304-405X(02)00074-0)).
- Ben, J.M., Youssef, S.B. and Apergis, P., "The dynamic linkage between renewable energy, tourism, CO₂ emissions, economic growth, foreign direct investment and trade", *Latin American Economic Review*, Vol. 28, No. 2, (2019), 2182-2195. (<https://doi.org/10.1186/s40503-019-0063-7>).
- Bornesstein, E., Gregorio, J. and De Lee, J.W., "How does foreign direct investment effect economic growth?", *Journal of International Economics*, Vol. 45, No. 1, (1998), 115-135. ([https://doi.org/10.1016/S0022-1996\(97\)00033-0](https://doi.org/10.1016/S0022-1996(97)00033-0)).
- Brookes, L.G., "Energy efficiency fallacies revisited", *Energy Policy*, Vol. 28, (2000), 355-366. ([https://doi.org/10.1016/S0301-4215\(00\)00030-6](https://doi.org/10.1016/S0301-4215(00)00030-6)).
- Brown, J.R., Fazzari, S.M. and Petersen, B.C., "Financing innovation and growth: Cash flow, external equity, and the 1990s R&D boom", *The Journal of Finance*, Vol. 64, No. 1, (2009), 151-185. (<https://doi.org/10.1111/j.1540-6261.2008.01431.x>).
- Brunnschweiler, C.N., "Finance for renewable energy: An empirical analysis of developing and transition economies", *Environment and Development Economics*, Vol. 15, (2010), 241-274. (<https://doi.org/10.1017/S1355770X1000001X>).
- Chang, S.C., "Effects of financial developments and income on energy consumption", *The International Review of Economics & Finance*, Vol. 35, (2015), 28-44. (<https://doi.org/10.1016/j.iref.2014.08.011>).
- Chor, F.T. and Bee, W.T., "The impact of energy consumption, income and foreign direct investment on carbon dioxide emissions in Vietnam", *Energy Economics*, Vol. 79, (2015), 447-454. (<https://doi.org/10.1016/j.energy.2014.11.033>).
- Coban, S. and Topcu, M., "The nexus between financial development and energy consumption in the EU: A dynamic panel data analysis", *Energy Economics*, Vol. 39, (2015), 81-88. (<https://doi.org/10.1016/j.eneco.2013.04.001>).
- Costantini, V. and Martini, C., "The causality between energy consumption and economic growth: A multi-sectoral analysis using nonstationary cointegrated panel data", *Energy Economics*, Vol. 32, (2010), 591-603. (<https://doi.org/10.1016/j.eneco.2009.09.013>).
- Derrick, A., "Financing mechanisms for renewable energy", *Renewable Energy*, Vol. 15, (1998), 211-214. ([https://doi.org/10.1016/S0960-1481\(98\)00159-1](https://doi.org/10.1016/S0960-1481(98)00159-1)).
- Ebrahimi, M. and Ebrahimi Al Morad, M., "Development of financial markets and energy consumption in D8 countries", *Quarterly Journal of Economic Policies*, Vol. 20, No. 61, (2019), 159-174. (<http://noo.rs/biO5Q>).
- International Energy Statistics, U.S. Energy Information Administration (EIA), (2015).
- Farazmand, H., KamranPour, S. and Ghorban Nezhad, M., "The relationship between financial development, economic growth and energy consumption in Iran, Toda-Yamamoto and Bond test", *Quarterly Journal of Economics (Former Economic Investigations)*, Vol. 10, No. 1, (2015), 33-58. (<http://noo.rs/PB0wi>).
- Fotros, M.H., Aghazadeh, A. and Jebraeli, S., "Investigation of the effect of renewable and non-renewable energies consumption on economic growth of selected developing countries (including Iran)", *Quarterly Journal of Energy Economics Studies*, Vol. 9, No. 32, (2012), 51-72. (<https://doi.org/10.22055/JQE.2013.12284>).
- Ghazouani, T., "Re-examining the foreign direct investment, renewable energy consumption and economic growth nexus: Evidence from a new bootstrap ARDL test for cointegration, MIPRA 89975", (2018), 1-27. (<https://mpira.ub.uni-muenchen.de/id/eprint/89975>).
- Gomez, M. and Jose, R.C., "Energy consumption and financial development in NAFTA countries, 1971-2015", *Economic and Business Research Institute*, Vol. 9, No. 2, (2019), 302-314. (<https://doi.org/10.3390/app9020302>).
- Grossman, S., "On the efficiency of competitive stock markets where trades have diverse", (1976). (<https://doi.org/10.1111/j.1540-6261.1976.tb01907.x>).
- Hsiao-Tien, P. and Chung-Ming, T., "Multivariate granger causality between CO₂ emission, energy consumption, FDI (foreign direct investment) and GDP (gross domestic product): Evidence from a panel of BRIC (Brazil, Russian Federation, India, and China)", *Countries Energy Policy*, Vol. 36, (2011), 685-693. (<https://doi.org/10.1016/j.energy.2010.09.041>).
- Hsu, P.H., Tian, X. and Xu, Y., "Financial development and innovation: Cross-country evidence", *Journal of Financial Economics*, Vol. 112, No. 1, (2014), 116-135. (<https://doi.org/10.1016/j.jfineco.2013.12.002>).
- Inglesi-Lotz, R., "The impact of renewable energy consumption to economic welfare: A panel data application", *Energy Economics*, Elsevier, Vol. 53, No. C, (2015), 58-63. (<https://doi.org/10.1016/j.eneco.2015.01.003>).
- Kakar, K., Khilji, B. and Khan, M., "Financial development and energy consumption: Empirical evidence from Pakistan", *International Journal of Trade, Economics and Finance*, (2011), 2-6. (<https://doi.org/10.1080/15567249.2011.603020>).
- Khandker, L., Sakib, B.A. and Khan, F., "Renewable energy consumption and foreign direct investment: Reports from Bangladesh", *Journal of Accounting, Finance and Economics*, Vol. 8, No. 3, (2018), 72-87. (<https://doi.org/10.1016/j.rser.2015.08.017>).
- Kim, J. and Park, K., "Financial development and deployment of renewable energy technologies", *Energy Economics*, Vol. 59, (2018), 238-250. (<https://doi.org/10.1016/j.eneco.2016.08.012>).

28. Kutan, M.A., Sudharshan, P.R., Mallesh, U. and Abdurashed, Z., "Financing renewable energy projects in major emerging market economies: Evidence in the perspective of sustainable economic development", *Energy Finance*, Vol. 54, No. 8, (2018), 1761-1777. (<https://econpapers.repec.org/RePEc:mes:emftr:v:54:y:2018:i:8:p:1761-1777>).
29. Lee, J.W., "The contribution of foreign direct investment to clean energy use, carbon emissions and economic growth", *Energy Policy*, Vol. 55, (2013), 483-489. (<https://doi.org/10.1016/j.enpol.2012.12.039>).
30. Levine, R., "Financial development and economic growth: Views and agenda", *Journal of Economic Literature*, Vol. 35, No. 2, (1997), 688-726. (<https://EconPapers.repec.org/RePEc:aea:jeclit:v:35:y:1997:i:2:p:688-726>).
31. Levine, R., "Finance and growth: Theory and evidence", *Handbook of economic growth*, Vol. 1, (2005), 865-934. (<https://econpapers.repec.org/RePEc:eee:grochp:1-12>).
32. Levine, R. and Zervos S., "Stock markets, banks, and economic growth", *The American Economic Review*, Vol. 88, No. 3, (1998), 537-558. (<https://www.jstor.org/stable/116848>).
33. Manzour, D., Aghababayi, M.E. and Haghghi, I., "Analyzing the recursive effects of efficiency improvement in electricity consumption in Iran: Computable general balance patter", *Quarterly Journal of Energy Studies*, Vol. 8, No. 29, (2011), 1-23. (<http://noo.rs/8xLcE>).
34. Marin, D., "Is the export-led hypothesis valid for industrialize countries?", *Review of Economics and Statistics*, Vol. 74, (1992), 678-688. (<https://doi.org/10.2307/2109382>).
35. Medlock, K.B. and Soligo, R., "Economic development and end-use energy demand", *The Energy Journal*, Vol. 22, (2001), 77-105. (<https://www.jstor.org/publisher/iaee?refreqid=excelsior%3A76fb53a6726075823818c1df33e9bbae>).
36. Moradpour Oladi, M., Ebrahimi, M. and Tarkaman Ahmadi, M., "Financial market development and energy demand in Iran", *Quarterly Journal of Energy and Environmental Economics*, Vol. 2, No. 5, (2012), 187-209. (http://jiece.atu.ac.ir/article_779.html).
37. Narayan, P.K. and Smyth, R., "Electricity consumption, employment and real income in Australia evidences from multivariate granger causality tests", *Energy Policy*, Vol. 33, No. 9, (2005), 1109-1116. (<https://doi.org/10.1016/j.enpol.2003.11.010>).
38. Omri, A. and Chaibi, N., "Nuclear energy, renewable energy, and economic growth in developed and developing countries: A modelling analysis from simultaneous-equation models", *Ipag Business School, and Working Paper*, (2014), 2014-188. (<https://EconPapers.repec.org/RePEc:ipag:wpaper:2014-188>).
39. Pesaran, M., Shin, Y. and Smith, R., "Bounds testing approaches to the analysis of level relationships", *Journal of Applied Econometrics*, Vol. 16, (2001), 289-326. (<https://doi.org/10.1002/jae.616>).
40. Razmi, S.F., Ramezani Bajgiran, B., Behname, M., Ebrahimi Salari, T. and Razmi, S.M.J., "The relationship of renewable energy consumption to stock market development and economic growth in Iran", *Renewable Energy*, Vol. 145, (2020), 2019-2024. (<https://doi.org/10.1016/j.renene.2019.06.166>).
41. Sadeghi, S.K., Motefakker Azad, M.A., Pour Ebadolahian Kouch, M. and Shahbaz Zadeh, A., "Investigation the causal relationship between CO₂ emission, foreign direct investment, Energy consumption per capita and gross domestic production in Iran (Toda-Yamamoto causality test)", *Quarterly Journal of Energy and Environment Economics*, Vol. 1, No. 4, (2012), 101-116. (http://jiece.atu.ac.ir/article_601.html).
42. Sadorsky, P., "Financial development and energy consumption in central and eastern european frontier economies", *Energy Policy*, Vol. 39, (2011), 999-1006. (<https://doi.org/10.1016/j.enpol.2010.11.034>).
43. Sadorsky, P., "Correlations and volatility spillovers between oil prices and the stock prices of clean energy and technology companies", *Energy Economics*, Vol. 34, (2012), 248-255. (<https://doi.org/10.1016/j.eneco.2011.03.006>).
44. Saini, S. and Yadawananda, N., "Examining the linkages between financial development and energy consumption in India", *Proceedings of International Conference on Economics and Finance*, (2018), 119-130.
45. Salim, R.A., Hassan, K. and Shafiei, S., "Renewable and nonrenewable energy consumption and economic activities: Further evidence from OECD countries", *Energy Economics*, Vol. 44, (2014), 350-360. (<https://doi.org/10.1016/j.eneco.2014.05.001>).
46. Sbia, R., Shahbaz, M. and Hamdi, H., "A contribution of foreign direct investment, clean energy, trade openness, carbon emissions and economic growth to energy demand in UAE", *Economic Modeling*, Vol. 36, (2014), 191-197. (<https://doi.org/10.1016/j.econmod.2013.09.047>).
47. Serap, C. and Topcu, M., "The nexus between financial development and energy consumption in the EU: A dynamic panel data analysis", *Energy Economics*, Vol. 39, (2013), 81-88. (<https://doi.org/10.1016/j.eneco.2013.04.001>).
48. To, H., Wijeweera, A. and Charles, M.B., "Energy consumption and economic growth- The case of australia", *Proceedings of The 42nd Australian Conference of Economists, Conference Proceedings Beyond the Frontiers, New Directions in Economics*, Murdoch University, Perth, Western Australia, (2013).
49. Yue, S., Lu, R., Yongchan, Sh. and Hongtao, Ch., "How does financial development affect energy consumption? Evidence from 21 transitional countries", *Energy Policy*, Vol. 130, (2019), 253-262. (<https://doi.org/10.1016/j.enpol.2019.03.029>).
50. Zhang, Y.J., Fan, J.L. and Chang, H.R., "Impact of China's stock market development on energy consumption: An empirical analysis", *Energy Procedia*, Vol. 5, (2011), 1927-1931. (<https://doi.org/10.1016/j.egypro.2011.03.331>).



Application of Artificial Neural Networks to the Simulation of Climate Elements, Drought Forecast by Two Indicators of SPI and PNPI, and Mapping of Drought Intensity; Case Study of Khorasan Razavi

Mohammad Hossein Jahangir*, Mahnaz Abolghasemi, Seyedeh Mahsa Mousavi Reineh

Department of Renewable Energies and Environment, Faculty of New Sciences and Technologies, University of Tehran, Tehran, Iran.

PAPER INFO

Paper history:

Received 01 January 2020

Accepted in revised form 25 April 2020

Keywords:

Forecasting of Drought Intensity
Artificial Neural Network
Simulation
Multi-Layer Perceptron
Levenberg-Marquardt
Razavi Khorasan

ABSTRACT

Drought is considered as a destructive disaster that can have irreversible effects on different aspects of life. In this study, artificial neural network was used as a powerful means of modeling nonlinear and indefinite processes in order to simulate drought intensities at 7 synoptic stations of Khorasan Razavi from more than 35 years ago up to the year 2014. Input data were the calculations of the two indicators of PNPI and SPI by DIC software, and the output layer (drought intensity) was taken to the Matlab software and employed as the teaching data (from 25 years), experiment (from 5 years), and validation (from another 5 years). The 3-9-1 structure of the network of layers had the maximum accuracy with the error rate of less than 2 % and high correlation (more than 90 %). After trial and error for each station through sigmoid stimulation function in the Perceptron network, it was observed that the stations of Mashhad and Quchan had the minimum error and the maximum error was related to the station of Neyshabur. The results of comparisons and observations showed that the artificial neural network had high efficiency in simulation of the data. The obtained correlation amount of 0.999 for the base station represented the small error of the model in prediction. Drought forecasting was performed in this study by the trained algorithm in the artificial neural network without using the observation data. The results showed that rainfall, temperature, and speed models had a positive role in forecasting the provinces that would experience drought. Due to its lower amount of error, SPI indicator was selected for mapping, the findings of which showed that the highest drought intensity belonged to the near normal to normal wet lands.

1. INTRODUCTION

Forecasting the atmospheric processes in the planning and management of water resources is of high importance, especially in arid and semi-arid areas. In recent decades, most researchers have adopted multivariate regression and geostatistical models such as auto-regressive moving average and auto-regressive integrated moving average in the prediction and modeling of meteorological and hydrologic processes as well as characterization of flood and drought [1-3]. Decrease in atmospheric precipitation is the main reason of agricultural and hydrological drought, which in turn leads to increase in the evaporation of surface waters [4]. Most of the applied models in the literature enter the considered parameters into decision-making processes in a linear form, and they often cannot analyze complex climate and hydrology issues properly. Hence, it is necessary to introduce more efficient models to predict non-linear and complex phenomena [5]. For this reason, experts and scientists of hydrology and other related fields have intended to develop appropriate models for predicting when different hydrological events occur. Emergence of robust theories like phase algorithm and nervous network has brought a revolution in analyzing the behavior of dynamic systems in different scientific areas associated with the water issues. These methods are nowadays used for the prediction of meteorological parameters to attenuate the possibility of

human error, increase precision, and reduce the limitations of massive amounts of data and computations. One of the common methods for the prediction of meteorological parameters is artificial neural networks, which are powerful and flexible tools independent of the dynamic model system. It is an intelligent method that has improved the recognition and prediction of important parameters with widespread application to different forecasting fields comprising complex processes. The major superiorities of the method are the ability to learn, extensible distribution of information, parallel processing, and durability [6]. Also, artificial neural networks have great modelling capabilities that can be applied to the forecasting of climate and hydrological issues, especially when the adopted network is able to extract the governing law of data, even confusing data [7].

Many research studies have recently been conducted dealing with the prediction of river flow, rainfall-runoff modeling, and estimation of hydrologic parameters using neural networks and, in most cases, they have been proven effective in predicting and stimulating hydrologic parameters [8-11]. Some studies have aimed to forecast drought cycle and simulate climate elements using dynamic structures and develop models through artificial neural networks, e.g., the research conducted by Krisbo & Mooma (2003) in Spain [5] and those on Kanchoos river basin in Mexico [12], Kanabatis river basin in the east of India and Kamilo (2008), and Altotachos river basin. In Iran, different research studies have also addressed draught by adopting artificial neural networks and large-scale climate signals [13]. The obtained results of the neural models have shown that during the warm-phase

*Corresponding Author's Email: mh.jahangir@ut.ac.ir (M.H. Jahangir)

Table 1. Characteristics of the studied stations in the province [Source: weather.com].

Station	Geographical location	Elevation (m)
Mashhad	16' N 36° و E 59° 38'	999.2
Sarakhs	N 32' 36° و E 61° 10'	235.0
Quchan	N 4' 37° و E 30' 58°	1287.0
Sabzevar	N 12' 36° و E 39' 57°	972.0
Turbat-jam	N 16' 35° و E 13' 59°	1450.0
Kashmar	N 12' 35° و E 28' 58°	1109.7
Neyshabur	N 16' 36° و E 48' 58	1213.0

2.2. The mathematical theory of neural networks

The mathematical theory of neural networks is in fact a simplified model of information processing pattern in human brain. It enables performing processes and finding the favorite non-linear combination for the relation between input and output of each system. Also, through learning process, this network is trained with the available data to perform the future forecasting. Neurons in the neural network are very simplified representations of biological neurons with lower abilities (Figure 2). In fact, artificial neural network is a mathematical model with the ability of modeling and development of non-linear relations for interpolation.

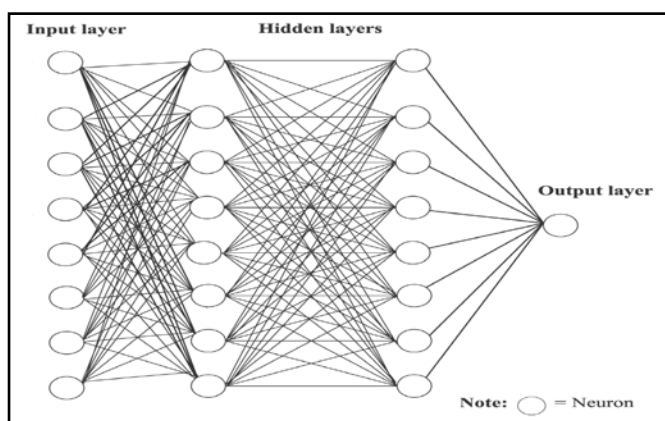


Figure 2. A schematic of the Multi-Layer Perceptron (MLP) neural network [Source: MSc thesis of the author, 2016].

Generally, every neural network consists of three layers. The first layer, namely the input layer, includes a few neurons, which in this study is devoted to average annual rainfall, average annual temperature, and average annual wind speed. The hidden layers include a few variable neurons, the optimal number of which is determined by examination and repetition for making the minimum error in terms of, e.g., RME. Efficiency of the neural network highly depends on appropriate selection of the number of neurons in the hidden layer. The last layer, i.e., output layer, is used to properly output the functions for increasing the speed of the network.

2.3. Architecture of the multi-layer neural network

In many extremely complicated mathematical problems that require complicated non-linear equations, a multilayer perceptron network can be simply used by defining weights and appropriate functions. Depending on the type of problem in neurons, various activation functions can be used. Demonstrating proximate hypothesis, Hernick and others

suggested that a novel neural network with a sigmoidal hidden layer and a linear output layer could predict each complicated mapping with a proximate degree of accuracy. This hypothesis involves the minimum number of hidden layers and, hence, it significantly decreases complexity of the model [21]. In recent years, several general raters have been proposed, e.g., Multi-Layered Perceptron (MLP) in which enough neurons can be considered. MLP is able to estimate an appropriate proximate for each function and use the available information in large numeral sets. It should be noted that, in general, one cannot suggest any appropriate number of neurons for the medial layer and this choice should be made by trial and error. In this research, three-layer network perceptron is considered by the training algorithm after emission of error.

2.4. Design stages and running of the neural network

To run the neural network, the following steps should be taken:

- Collecting and pre-processing the required data for the intended neural network.
- Determination of the appropriate type and structure of neural network and developing a network with high efficiency.
- Testing the network by a portion of the collected data (stage of training).
- Examination of the trained network by the rest of the data (examination level).
- Saving the network if the result of examination is acceptable; otherwise, repeating steps 2 to 4.

General characteristics of the studied neural network in forecasting the variation of draught are given in the following. Since certain laws are not available, several structures are required for training and designing the neural network in this study. Choosing data for meta-measurement different from those for training or learning of the artificial neural network, simultaneously, can help us take steps more confidently than when the developed models are not pre-trained [22, 23]. In this study, Multi-Layer Perceptron (MLP) network is used with Back Propagation (BP) and Levenberg-Marquardt (LM) learning tech. The effects of changes in parameters are surveyed in many repetitions and the coefficients with better results for training the network in the modelling are introduced. In order to simulate the climate elements and determine draught intensity, the two indicators of PNPI and SPI are employed.

For the synoptic situations of Khorasan Razavi province, meteorological information from 1980 to 2014 (35 years) was employed on an annual time scale. After determining input data (in three layers of average annual rainfall, average annual temperature, and average annual wind speed), target data (obtained by calculating the two indicators of PNPI and SPI through DIC software), and output layer (draught intensity) and normalizing them, information from 25 years was utilized for training, 5 years for examination, and the rest 5 years for validation. Finally, mapping of the present situation was carried out for zone evaluation measurements of the neural network.

2.5. Neural network performance evaluation criteria

To evaluate and compare the obtained results by the applied models and methods in this research, two measures, namely root mean square error in Equation (1) and correlation coefficient (random error (R^2)) in Equation (2), are employed as follows:

$$RMSE = \sqrt{\frac{\sum_{i=1}^N (obv - pr)^2}{N}} \quad (1)$$

$$R^2 = \frac{\sum_{i=1}^N (obv - \overline{obv})(pr - \overline{pr})}{\sqrt{\sum_{i=1}^N (obv - \overline{obv})^2 \sum_{i=1}^N (pr - \overline{pr})^2}} \quad (2)$$

In the above relations: obv is the observed values, \overline{obv} is average observed value, pr is pre-estimated values of network

models and N shows the number of total data of each stage of training data and examination data. The closer the value of RMSE to 0 and the numeral value to 1, the closer the observed and predicted data and the more accurate the answers at each stage. These measurements are made for important patterns at the test and training stages of the neural network.

3. RESULTS AND DISCUSSION

3.1. Identifying important patterns in training and testing

To forecast the course of draught intensity through the artificial network, statistics from synoptic stations of Khorasan Razavi province in a 35-year period (1980-2014) were used. The diagrams obtained by PNPI and SPI methods indicate that draught intensity has experienced a significant increase during the included years. This increasing trend is also predicted to continue in the following years (Figures 3 & 4).

Figures 5-8 display the obtained results by the neural network model using the two indicators of PNPI and SPI and compare them with real data (observed data) for different patterns from Mashhad station, proving high precision of the model and network (more than 99 %). Figure 5 shows the correlation value for PNPI indicator with four classes of data (training, testing, validation, and total) from Mashhad station.

The diagrams given in the below figures show high accuracy of the results of ANN.

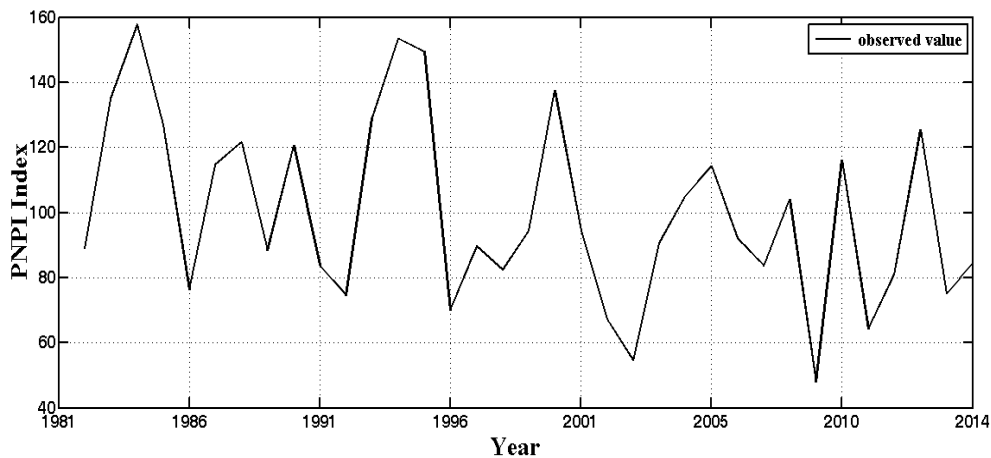


Figure 3. Draught intensity with the PNPI indicator in neural network during the statistic period (35 years).

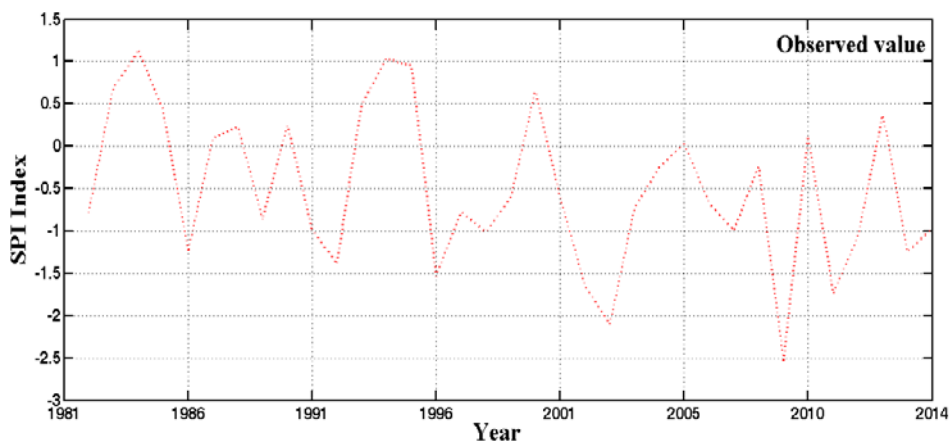


Figure 4. Draught intensity with the SPI indicator in neural network during the statistic period (35 years).

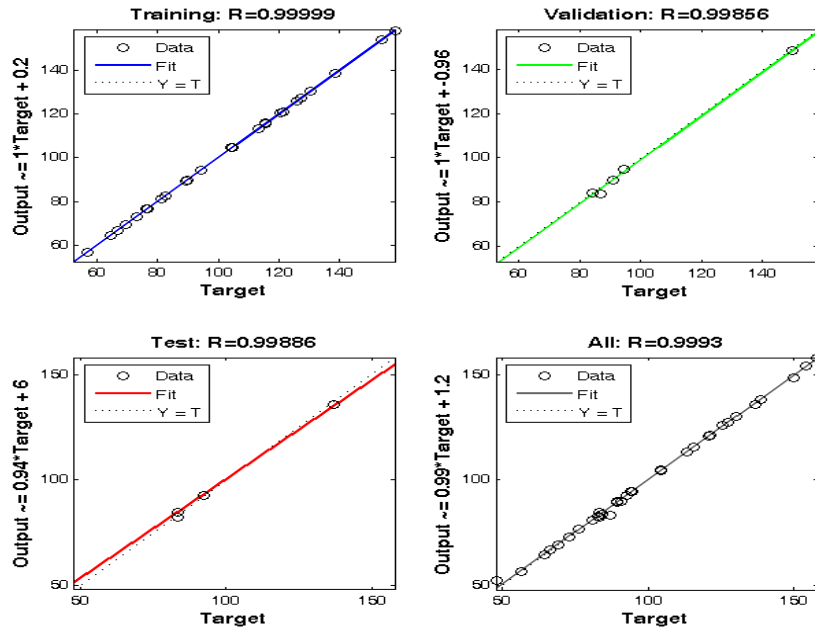


Figure 5. The correlation coefficient for PNPI index with four categories of data (training, testing, validation, and total) from Mashhad station.

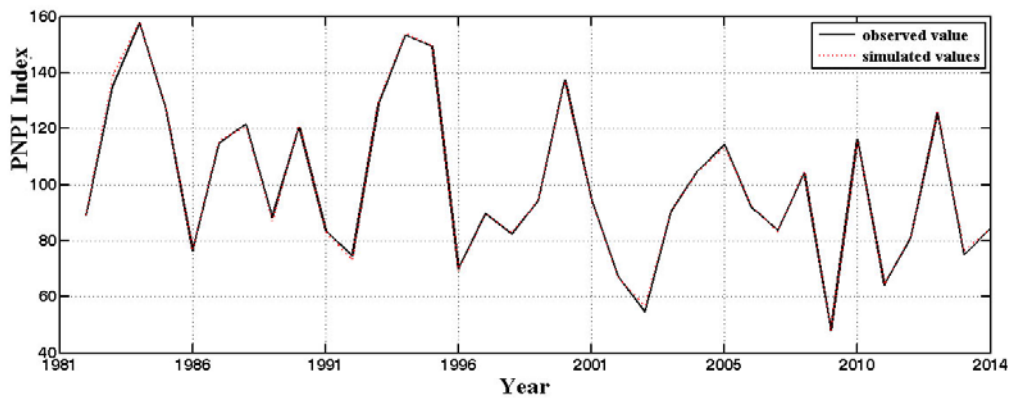


Figure 6. Comparison between PNPI and the observed results at Mashhad station.

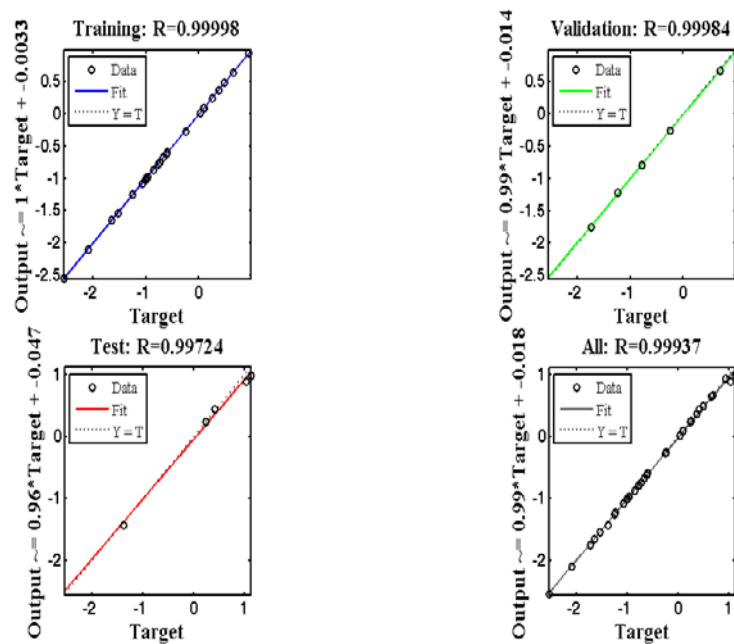


Figure 7. The correlation coefficient for SPI index with four categories of data (training, testing, validation, and total) from Mashhad station.

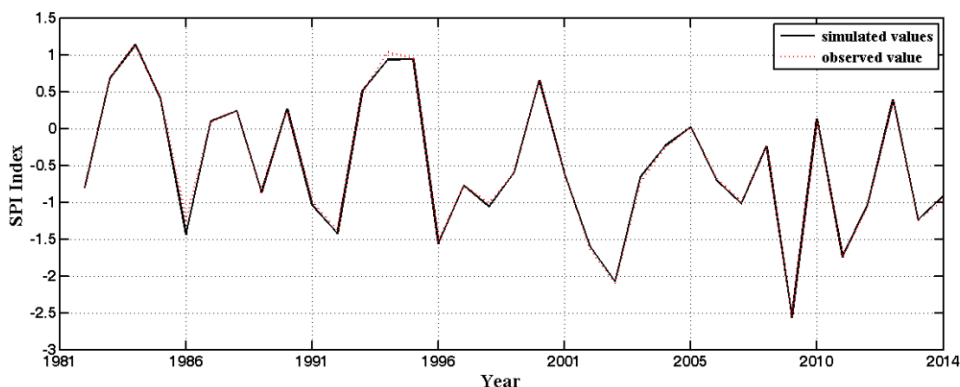


Figure 8. Comparison between SPI and the observed results at Mashhad station.

3.2. Determination of the appropriate indicator for forecasting draught intensity

One of the major concerns of draught studies is identifying the proper indicator that can evaluate intensity, stability, and magnitude of draught in a zone. Each indicator certainly uses different factors on each time scale. An appropriate draught indicator should be inclusive and reflect the short-term conditions of draught so that it reacts to different types of draught, e.g., agricultural, meteorological, and hydrological. Also, it should not be limited to any specific season and must be able to specify the draught regardless of whether it is, e.g., summer or winter; the same can be said about whether the indicator is dealing with a wet-climate region or a dry zone. In this research, RMSE and R^2 are employed as measures to forecast draught intensity. The closer the RMSE value to zero and the value of R^2 to 1, the better the indicator for forecasting draught. Both indicators, i.e., SPI and PNPI, have very good

correlation coefficients ($R^2=0.99$) and error of the indicators in different stations were from 0.0070 to 0.31, representing high precision of both indicators. However, since the error value for SPI is less than that for PNPI, SPI is used for mapping and other calculations.

3.3. Mapping

For mapping, the value of SPI was calculated for the available systems in DIC software and the required slope was developed in GIS software. Then, the map for the distribution of draught on surface zone was prepared by the Kriging methode (k), which is the best known and most widespread way of modeling draught. This way of interpolation is appropriate for the data collected through a locally defined procedure. As shown in Figure 9, the highest intensity of draught belongs to the nearly normal to normal wet levels.

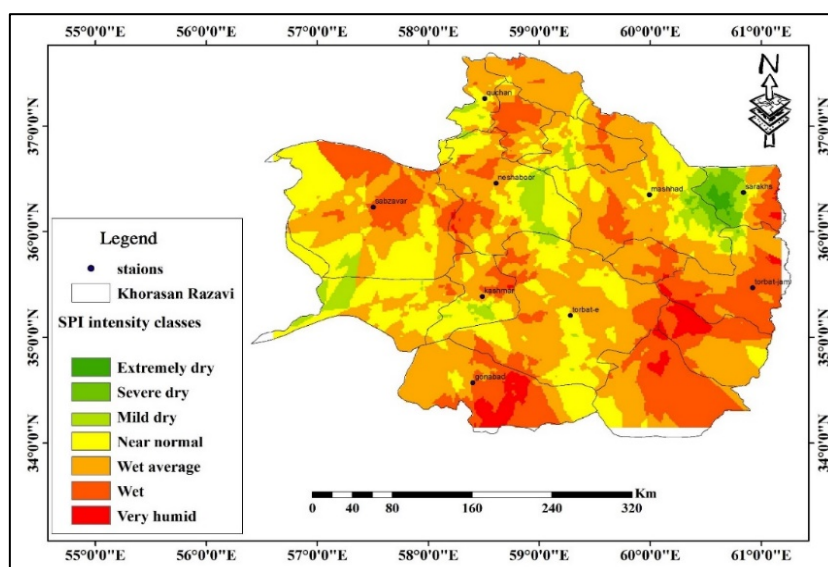


Figure 9. Zoning of the SPI index for stations in the basin.

To predict draught intensity in Khorasan Razavi province, artificial neural network was employed using the two indicators of normal rainfall (SPI) and percentage of normal rainfall (PNPI). After collecting data from synoptic stations, they were statistically examined and normalized for entering into the artificial neural network. At the next stage, the appropriate structure for the neural network, stimulation function, number of neurons, and the number of hidden, input, and output layers were selected. Then, three average annual

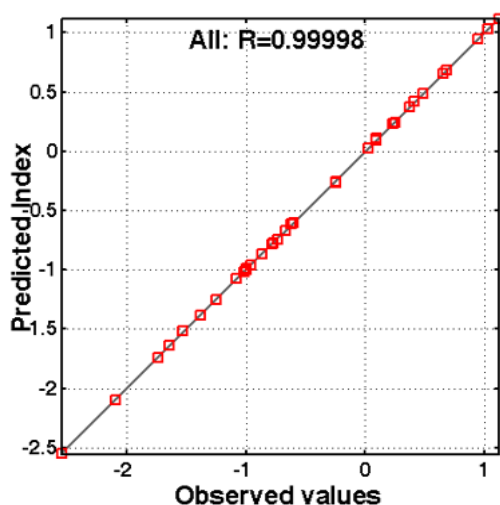
temperatures and three average wind speeds were considered for the prediction of draught intensity by the given two indicators. High correlation between the observed data and the predicted ones was observed. A summary of the considered structure for the neural network, neurons, and other information related to different stations as well as the general pattern of the stages (training, testing, and validation) is given in Table 2 in terms of error (RMSE) and correlation coefficient (R^2).

Table 2. Statistics for the general pattern of the model for the studied stations.

Station	Record data	Error		The correlation coefficient for total data		Layer structure	Trial and error	Type of algorithm
		SPI Index	PNPI Index	SPI Index	PNPI Index			
Mashhad	35	0.00070	0.027	0.99	0.99	1-9-3	4	LM
Sarakhs	30	0.003	0.03	0.99	1	1-9-2	3	LM
Quchan	30	0.0008	0.01	0.99	0.99	1-9-2	2	LM
Sabzevar	35	0.0004	0.3	0.99	0.99	1-9-2	5	LM
Turbat-jam	35	0.005	0.02	0.99	0.99	1-9-2	4	LM
Kashmar	28	0.004	0.31	0.99	0.99	1-9-2	2	LM
Neyshabur	24	0.06	0.001	0.99	1	1-9-2	3	LM

According to the obtained results for correlation coefficient and error with three input layers for Mashhad station and two for others, one output layer and nine hidden layers provided the maximum precision and minimum error (less than 2 %) with high correlation (more than 4 %). Evaluation of each station with sigmoidal stimulation function in the perceptron network shows that Mashhad and Quchan stations have the minimum error and Neyshabur station the highest error. Figures 6 and 8 show the simulated results of the model for the two indicators: (a) the comparison between SPI and the observed results at Mashhad station and also (b) the comparison between PNPI and the observed results at Mashhad station.

The curves and calculations in the drawn diagrams prove that artificial neural network has high efficiency in the simulation of the studied data. The correlation degree of 0.999 for the base station (Mashhad) indicates minimum error of the model in forecasting. Since the number of the studied stations was large, for the sake of conciseness, the results for correlation and the comparisons are given only for Mashhad station. Information on the two indicators for different stations is brought in Table 2, and Figure 10 shows the total correlation pattern for the simulated and observed values at Mashhad station.

**Figure 10.** Correlation diagram for SPI of simulated values at Mashhad station.

After determining the values of error and correlation coefficient, the next step is validation of the simulation and forecast, the results of which are represented in Table 2. As

observed, the network could perform the simulation with high precision and relatively high adaptability. The low value of error indicates that the network has high efficiency or, in another words, simulated results are well near real observations. The next step requires predicting values of the two indicators for the following year in a limited period by means of the neural network using the algorithm trained by the previous data. This forecast depends on the precision and error of the network for the previous data and as long as the obtained results represent a low amount of error, they are acceptable. MLP classifier makes use of the following algorithm for calculating the inputs receiving an individual knot:

$$\text{net}_j = \sum_i w_{ij} I_i \quad (3)$$

where net_j is the input parameter that receives the individual neuron j , W_{ij} shows the weights of neurons i and j , and I_i stands for the output of neuron i belonging to the sender, input or hidden layer. The output value derived from neuron j is computed through Equation (4).

$$f(\text{net}_j) = (1 + \exp(-\text{net}_j)) \quad (4)$$

The results of comparison between draught forecasting by the neural network and real draught statistics indicate no significant difference and imply that the amount of error is acceptable. Accordingly, artificial neural network can be considered as an efficient model for forecasting and simulation with high precision.

4. CONCLUSIONS

Natural disasters like flood and drought can lead to huge damages, e.g., agricultural, biological, etc., as well as social and economic effects, e.g., immigration of rural people from villages to the margins of the cities. Hence, the return period and intensity of such disasters should be identified to prevent the resulting damages and bad outcomes. In recent years, artificial neural network has been employed frequently to predict and model draught in different regions of the world.

The obtained results in this study indicated that artificial neural network was more efficient than linear models in forecasting the cycle and intensity of drought. Correlation coefficient and error were investigated with three input layers for Mashhad station and two for others, one output layer, and nine hidden layers. Trial and error with sigmoidal stimulation

function in perceptron network for each station showed that Mashhad and Quchan stations had the lowest error and Neyshabur station the highest error. Also, the findings of network training for the two indicators of PNPI and SPI by input data from 35 years (from 1980 to 2014) on average annual rainfall and average annual temperature were evaluated. The results of evaluation showed maximum precision of the model with an error amount less than 2 % and high correlation (more than 90 %). A correlation diagram was drawn between the real and forecasted values, which showed agreement to a great extent (more than 99 %). Overall, artificial neural network performed efficiently in forecasting draught in Khorsan Razavi province. According to the findings of mapping through Kriging method by the SPI indicator, the maximum draught intensity belonged to the near normal to normal wet zones.

As the final conclusion of this study, it can be stated that artificial neural network can have a broad extent of applications, for both seasonal and short-term forecasting, to water resource management, biological studies, extraction, draught management, and climate change studies.

5. ACKNOWLEDGEMENT

The authors would like to thank the journal editor and Faculty of New Sciences and Technologies, University of Tehran.

REFERENCES

- Zambrano, F., Vrieling, A., Nelson, A., Meroni, M. and Tadesse, T., "Prediction of drought-induced reduction of agricultural productivity in Chile from MODIS, rainfall estimates, and climate oscillation indices", *Remote Sensing of Environment*, Vol. 219, (2018), 15-30. (<https://doi.org/10.1016/j.rse.2018.10.006>).
- Hao, Z., Singh, V.P. and Xia, Y., "Seasonal drought prediction: Advances, challenges, and future prospects", *Reviews of Geophysics*, Vol. 56, No. 1, (2018), 108-141. (<https://doi.org/10.1002/2016RG000549>).
- Wang, W., Chau, K., Xu, D., Qiu, L. and Liu, C., "The annual maximum flood peak discharge forecasting using Hermite projection pursuit regression with SSO and LS method", *Water Resources Management*, Vol. 31, No. 1, (2017), 461-477. (<https://doi.org/10.1007/s11269-016-1538-9>).
- Miralles, D.G., Gentile, P., Seneviratne, S.I. and Teuling, A.J., "Land-atmospheric feedbacks during droughts and heatwaves: State of the science and current challenges", *Annals of the New York Academy of Sciences*, Vol. 1436, No. 1, (2019), 19. (<https://doi.org/10.1111/nyas.13912>).
- Kim, T.-W. and Valdés, J.B., "Nonlinear model for drought forecasting based on a conjunction of wavelet transforms and neural networks", *Journal of Hydrologic Engineering*, Vol. 8, No. 6, (2003), 319-328. ([https://doi.org/10.1061/\(ASCE\)1084-0699\(2003\)8:6\(319\)](https://doi.org/10.1061/(ASCE)1084-0699(2003)8:6(319))).
- Deka, P. and Chandramouli, V., "Fuzzy neural network model for hydrologic flow routing", *Journal of Hydrologic Engineering*, Vol. 10, No. 4, (2005), 302-314. ([https://doi.org/10.1061/\(ASCE\)1084-0699\(2005\)10:4\(302\)](https://doi.org/10.1061/(ASCE)1084-0699(2005)10:4(302))).
- Ardabili, S., Mosavi, A., Dehghani, M. and Várkonyi-Kóczy, A.R., "Deep learning and machine learning in hydrological processes climate change and earth systems: A systematic review", *Lecture Notes in Networks and Systems*, Vol. 101, (2020), 52-62. (https://doi.org/10.1007/978-3-030-36841-8_5).
- Pashazadeh, A. and Javan, M., "Comparison of the gene expression programming, artificial neural network (ANN), and equivalent Muskingum inflow models in the flood routing of multiple branched rivers", *Theoretical and Applied Climatology*, Vol. 139, No. 3-4, (2020), 1349-1362. (<https://doi.org/10.1007/s00704-019-03032-2>).
- Tokar, A.S. and Markus, M., "Precipitation-runoff modeling using artificial neural networks and conceptual models", *Journal of Hydrologic Engineering*, Vol. 5, No. 2, (2000), 156-161. ([https://doi.org/10.1061/\(ASCE\)1084-0699\(2000\)5:2\(156\)](https://doi.org/10.1061/(ASCE)1084-0699(2000)5:2(156))).
- Singh, P. and Deo, M.C., "Suitability of different neural networks in daily flow forecasting", *Applied Soft Computing*, Vol. 7, No. 3, (2007), 968-978. (<https://doi.org/10.1016/j.asoc.2006.05.003>).
- Wang, W., Van Gelder, P.H., Vrijling, J.K. and Ma, J., "Forecasting daily streamflow using hybrid ANN models", *Journal of Hydrology*, Vol. 324, No. 1-4, (2006), 383-399. (<https://doi.org/10.1016/j.jhydrol.2005.09.032>).
- Mishra, A.K. and Desai, V.R., "Drought forecasting using feed-forward recursive neural network", *Ecological Modelling*, Vol. 198, No. 1-2, (2006), 127-138. (<https://doi.org/10.1016/j.ecolmodel.2006.04.017>).
- Sedaghatkender, A. and Fattahi, E., "Indicators of drought in Iran", *Journal of Geography and Development*, Vol. 11, (2008), 59-76.
- Afkhami, H., Dastorani, M.T., Malekinejad, H. and Mobin, M.H., "The effect of climatic factors on the accuracy of artificial neural network based drought prediction in Yazd region", *Proceedings of 5th National Conference on Watershed Management Science and Engineering of Iran*, Iranian Watershed Association, Retrieved from (2009), 1-12. (https://www.civilica.com/Paper-WATERSHED05-WATERSHED05_278.html).
- Farahmand, F., Galka, F. and Farahmand, A., "Evaluation of artificial neural networks performance in modeling river water contamination using qualitative parameters", *First National Conference on New Technologies in Engineering Sciences, Islamic*, (2009).
- Dastjerdi, J. and Hoseini, S.M., "Application of artificial neural network in climate element simulation and drought cycle forecasting case study: Isfahan province", *Geography and Environmental Planning*, Retrieved from (2010), Vol. 21, No. 3, 107-120. (<http://ensani.ir/fa/article/231193>).
- Nasri, M., "Application of artificial neural networks (ANNs) in prediction models in risk management", *World Applied Sciences Journal*, Vol. 10, No. 12, (2010), 1493-1500. (<https://doi.org/10.1.1.390.3895>).
- Rezaeian-Zadeh, M. and Tabari, H., "MLP-based drought forecasting in different climatic regions", *Theoretical and Applied Climatology*, Vol. 109, No. 3-4, (2012), 407-414. (<https://doi.org/10.1007/s00704-012-0592-3>).
- Afkhami, H., Dastorani, M.T., Malekinejad, H. and Mobin, M.H., "Effects of climatic factors on accuracy of ANN-based drought prediction in Yazd area", TT. *JSTNAR*, Retrieved from <http://jstnar.iut.ac.ir/article-1-1215-fa.html>, (2010). (<http://jstnar.iut.ac.ir/article-1-1215-fa.html>).
- Mousavi, B.M. and Ashrafi, B., "The study of synoptic patterns that caused autumn and winter droughts in Khorasan Razavi Province", *Journal of Soil and Water Conservation*, Vol. 4, No. 18, (2011), 167-184.
- Bai, L., David, R. and Hernick, M., "Apparatus and method for controlling a fuel cell using the rate of voltage recovery", U.S. Patent 7,722,972, B2 Appl. NO.: 11/207,123, (2010).
- Schalkoff, R.J., *Artificial neural networks*, McGraw-Hill Higher Education, (1997). (<https://doi.org/10.5555/541158>).
- Maniezzo, V., "Genetic evolution of the topology and weight distribution of neural networks", *IEEE Transactions on Neural Networks*, Vol. 5, No. 1, (1994), 39-53. (<https://doi.org/10.1109/72.265959>).



A Review of Application of Experimental Design Techniques Related to Dark Fermentative Hydrogen Production

 Fatemeh Boshagh^a, Khosrow Rostami^{b*}
^a Department of Chemical Technologies, Iranian Research Organization for Science and Technology (IROST), P. O. Box: 3353-5111, Tehran, Iran.

^b Department of Biotechnology, Iranian Research Organization for Science and Technology (IROST), P. O. Box: 3353-5111, Tehran, Iran.

PAPER INFO

Paper history:

Received 12 December 2019

Accepted in revised form 26 April 2020

Keywords:

 Biohydrogen Production
 Dark Fermentation
 Experimental Design
 Optimization

ABSTRACT

The current review purpose is to present a general overview of different experimental design methods that are applied to investigate the effect of key factors on dark fermentation and are efficient in predicting the experimental data for biological hydrogen production. The methods of two levels full and fractional factorials, Plackett–Burman, and Taguchi were employed for screening the most important factors in dark fermentation. The techniques of central composite, Box–Behnken, Taguchi, and one factor at a time for optimization of the dark fermentation were extensively used. Papers on the three levels full and fractional factorials, artificial neural network coupled with genetic algorithm, simplex, and D-optimal for the optimization of the dark fermentation are limited, and no paper on the Dohrlert design has been reported to date. The artificial neural network coupled with genetic algorithm is a more suitable method than the RSM technique for the optimization of dark fermentation. Literature shows that the optimization of critical factors plays a significant role in dark fermentation and is useful to improve the hydrogen production rate and hydrogen yield.

1. INTRODUCTION

In recent years, hydrogen has received global recognition as a clean energy carrier with a potential to substitute liquid fossil fuels. Hydrogen can be useful for solving the problem of growing global warming and greenhouse gas emissions. Hydrogen is produced from fossil fuel, water, and biomass through physicochemical and biological methods [1]. One of hydrogen production methods is dark fermentation that occurs under facultative or strictly anaerobic conditions in the absence of light [2,3]. Dark fermentation as a complicated multiproduct process is affected by many variables such as temperature, pH, bioreactor configuration, hydrogen partial pressure, substrate type and concentration, nutrients, inhibitors, hydraulic retention time (HRT), and so on [4,5]. Thus, its production depends largely on the optimization of various controlling factors.

Experiments are described as tests that make purposeful changes in the factors (input variables) of a system or process, and effect of these changes in the responses (output variables) are noticed [6]. It is evident that if experiments are carried out randomly, the observed results will also be random and are affected by noise. Therefore, it is beneficial to fit the data with appropriate statistical methods [7]. Design of experiments (DOE) is a technique for systematically employing statistical methods to carry out experiments, that was proposed by Fisher in 1920 [8]. An appropriate DOE must avoid systematic error, be accurate, allow the estimation of the size of the random error, and have extensive validity [9]. Randomization, replication, and blocking are the three basic principles of DOE [10]. Design of experiments is employed for three experimental objectives including screening, optimization, and robustness testing. The screening stage is applied to recognize

the key factors that affect the results [11]. The two levels full factorial design (2-FFD), two levels fractional factorial design (2-PFD), and Plackett–Burman design (PBD) methods are mainly used for the screening stage [12]. Frequently, the initial estimate of the factor levels is far from the actual optimum values [6,13]. Thus, the approximate level of key factors generating optimal conditions can be estimated using approaches such as steepest ascent and descent. The optimization is a critical step to obtain appropriate levels of key factors to find the best possible response. The optimization represents increasing the efficiency of a product, a system, a procedure, or a process to receive the maximum benefit out of it [14] and is more implicated than the screening stage and requires more experiments to be performed [11]. The models of one factor at a time (OFAT), Taguchi design (TD), three levels full factorial design (3-FFD), three levels fractional factorial design (3-PFD), Box–Behnken design (BBD), central composite design (CCD), D-optimal (DO), Dohrlert design (DD), simplex method (SM), and artificial neural network (AAN) design are mainly used for the optimization stage. DOE methods are shown in Fig. 1. The choice of a suitable DOE method is a very intricate issue and depends on a set of criteria including type of problem, degree of optimization, time and cost constraints, number of factors under investigation and their interactions, the possible presence of identifiable and non-identifiable extraneous factors, ease of understanding and implementation, complexity of using each design, required training, statistical validity and robustness of approach, etc. [15,16]. Designing experiments presents more advantages such as reducing time, cost, resources, and effort than the univariate procedures that facilitate collecting large quantities of information while minimizing tedious experimental work [15].

Since DFHP is affected by many factors and depends largely on the optimization of controlling factors, there is a need to

*Corresponding Author's Email: Rostami 2002@ yahoo.com (Kh. Rostami)

have at hand a reliable technique of DOE for optimization of various controlling factors that can help facilitate a better understanding of individual and interactive effects of each factor on hydrogen production. The present study covers the conventional experimental design methods related to DFHP

that are currently employed to study the effect of key factors on dark fermentation. An appropriate DOE method can be used to find optimum conditions for maximizing hydrogen yield (HY) and hydrogen production rate (HPR).

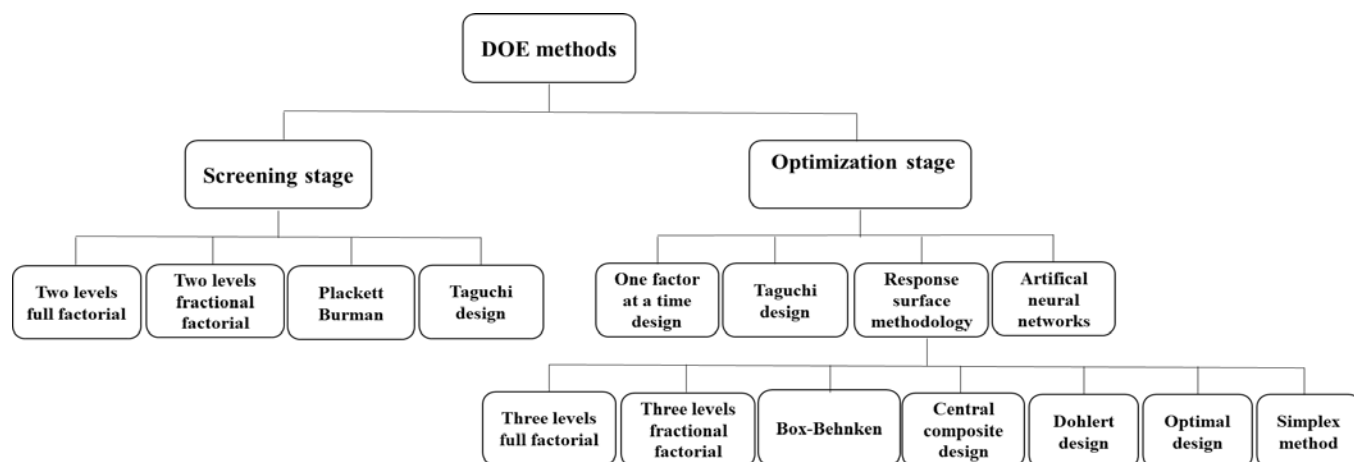


Figure 1. DOE methods.

2. DOE METHODS

2.1. Screening stage

2.1.1. Two levels full or fractional factorials

A factorial approach is classified into full and fractional factorial design. A full factorial design (FFD) consists of all possible combinations of factor levels to investigate the effect of the factors on a response simultaneously. In this approach, the total number of experiments for studying k factors, each at L levels, is L^k and for various levels (L_1, L_2, \dots, L_n) is obtained by multiplication of levels ($L_1 \times L_2 \times \dots \times L_n$). All interactions between factors are investigated in the FFD [17]. Frequently, experimenters do not have adequate time, cost, and resources to perform full factorial experiments [10]. The partial (fractional) factorial design (PFD) is used when the number of experiments of FFD is too large, which was first presented by Finney in 1945 [18]. PFD investigates the effect of factors on a response under an economical condition. A PFD is generally represented in the form of L^{k-p} , where k , L , and $1/L^p$ are the number of factors, levels, and the fraction of the full factorial L^k , respectively. The two levels full and fractional factorials are mainly used for screening the key factors, where the total number of experiments for k factors is 2^k and 2^{k-p} , respectively [19]. The number of experiments of 2^k and 2^{k-p} is given in Table 1. PFD does not enable the estimation of all major and interaction effects separately because some of them are estimated together [15].

Some of the studies on screening stage for dark fermentative hydrogen production are summarized in Table 2. Rasdi et al. [20] employed two-level FFD for the initial screening of the most influential variables, namely substrate concentration, pH, inoculum size, and heat treatment for hydrogen production from palm oil mill effluent. They illustrated that according to the 2^4 design, chemical oxygen demand (COD) of POME and pH significantly influenced hydrogen production. The factors with p -values less than 0.05 are considered significant, whereas values greater than 0.05 are insignificant. A CCD was applied after a two-level FFD to optimize selected variables. The preliminary screening of temperature, initial pH, inoculum size, and COD by two-level FFD was carried

out by Ismail et al. [21] and, later, CCD optimization for hydrogen production from food wastes was used. The results of 2^4 design showed that initial pH and temperature were selected as the most critical variables on hydrogen production individually and interactively.

Table 1. Comparison of the numbers of experiments of 2^k and 2^{k-p} (2 levels, k factors) design.

Factors	Reduced fraction ($1/2^p$)	Numbers of experiments in 2^k	Numbers of experiments in 2^{k-p}
6	1/2	$2^6=64$	$2^{6-1}=32$
6	1/4	$2^6=64$	$2^{6-2}=16$
6	1/8	$2^6=64$	$2^{6-3}=8$
6	1/16	$2^6=64$	$2^{6-4}=4$
5	1/2	$2^5=32$	$2^{5-1}=16$
5	1/4	$2^5=32$	$2^{5-2}=8$

2.1.2. Plackett-Burman design

Plackett-Burman design, which is a two levels design, is a useful alternative to a 2^{k-p} design and was introduced by Plackett and Burman in 1946 [22]. Method of PBD has been extensively used to screen a large number of factors for further investigations [23]. Generally, a first-order polynomial model as observed in Eq. (1) is applied to study experimental results of PBD, where y , β_0 , β_i , and X_i are the response, constant, linear coefficient, and coded factor, respectively [24]. The number of runs (N) of PBD for studying k factors is $N = (k + 1)$, which is equal to a multiple of 4 for a PBD [25]. The design have runs of 12, 20, 24, 28, etc. PBD method has one major drawback, that is to say, the interactions between factors are ignored [26].

$$y = \beta_0 + \sum_{i=1}^k \beta_i x_i \quad (1)$$

Costa et al. [27] used PBD for the screening of eleven variables of glycerol, peptone, yeast extract, temperature, initial pH, K_2HPO_4 , KH_2PO_4 , NH_4Cl , $(NH_4)_2SO_4$, $FeSO_4 \cdot 7H_2O$, and $MgSO_4 \cdot 7H_2O$ for hydrogen production by

Klebsiella pneumoniae BLb01 from residual glycerol from biodiesel plant. According to the PBD, nine variables present the most significant effect on hydrogen production. The factors having the important effect on hydrogen production (p -value < 0.05) were then detected through a 2-level FFD. Six factors of initial pH, temperature, glycerol, KH_2PO_4 , K_2HPO_4 , and yeast extract were investigated by 2-level FFD and the other three factors were fixed in their optimal values. According to the 2^{6-2} FFD, three factors of KH_2PO_4 , K_2HPO_4 , and temperature were considered as key factors. Then, the level of three factors was optimized by CCD. Jiang et al. [28] studied hydrogen production from glucose by *Clostridium butyrium*. The variables include concentration of glucose, K_2HPO_4 , KH_2PO_4 , yeast extract, tryptone, L-cysteine, $\text{MgSO}_4 \cdot 7\text{H}_2\text{O}$, and $\text{FeSO}_4 \cdot 7\text{H}_2\text{O}$ were investigated in 12 experimental runs by PBD. The results of PBD screening indicated that yeast extract and glucose concentration were statistically significant in the hydrogen production. After PBD, the CCD method was carried out to identify optimal values of the level of two factors. Varrone et al. [29] investigated the effect of five factors of temperature, tryptone, glycerol concentration, initial pH, and yeast extract on the dark fermentation by PBD. Based on PBD, temperature, glycerol concentration, and initial pH were considered as important factors. The temperature and initial pH indicated a positive effect on HY, while the concentration of glycerol showed a negative effect. BBD was then carried out for the optimization of level of key factors. The techniques of PBD

and BBD were used to screen important factors and identify the optimal condition of hydrogen production by *Ethanoligenens harbinense* B49. Initial screening of factors of K_2HPO_4 , $\text{ZnSO}_4 \cdot 7\text{H}_2\text{O}$, NaCl, MgCl_2 , $\text{FeSO}_4 \cdot 7\text{H}_2\text{O}$, and $\text{CaCl}_2 \cdot 2\text{H}_2\text{O}$ by PBD for hydrogen production was performed by Guo et al. [30]. The results of 12 experimental runs of PBD showed that MgCl_2 and $\text{FeSO}_4 \cdot 7\text{H}_2\text{O}$ significantly affected hydrogen production. Then, BBD was used to identify optimal values that promoted maximum hydrogen production. The methods of PBD followed by CCD were employed to screen the key factors and optimize their levels by Boonsayompo et al. [31]. Six factors of FeSO_4 , CaCl_2 , peptone, MgCl_2 , NiCl_2 , and NaHCO_3 were screened by PBD in 12 experimental runs. The results indicated that hydrogen production from the sweet sorghum bagasse by *thermoanaerobacterium thermosaccharolyticum* KCU19 was affected by key factors of FeSO_4 , CaCl_2 , MgCl_2 , and NaHCO_3 . Pan et al. [32] studied the effects of eight factors of glucose, yeast extract, initial pH, peptone, FeSO_4 , phosphate buffer, mineral salt solution, and vitamin solution, on DFHP by PBD in 12 experimental runs. The screening results showed that glucose, phosphate buffer, and vitamin solution had individual significant effect on DFHP. The optimal key factor level and effect of their interactions on production of hydrogen were further investigated by BBD. The application of PBD for screening the most important factors of DFHP by some researchers is reported in Table 2.

Table 2. Studies of screening stage on DFHP.

Inoculum	Substrate	Design	Studied factors	Ref.
Heat-treated palm oil mill sludge	Palm oil mill effluent	2-FFD (2^4)	Substrate concentration, pH, inoculum size, heat treatment	[20]
Heat-treated palm oil mill sludge	Food wastes	2-FFD (2^4)	Initial pH, temperature, inoculum size, COD	[21]
<i>Klebsiella pneumoniae</i> BLb01	Residual glycerol from biodiesel plant	2-PFD (2^{6-2})	Glycerol, initial pH, temperature, yeast extract, KH_2PO_4 , K_2HPO_4	[27]
<i>Klebsiella pneumoniae</i> BLb01	Residual glycerol from biodiesel plant	PBD	Glycerol, initial pH, temperature, K_2HPO_4 , KH_2PO_4 , $(\text{NH}_4)_2\text{SO}_4$, peptone, $\text{MgSO}_4 \cdot 7\text{H}_2\text{O}$, NH_4Cl , yeast extract, $\text{FeSO}_4 \cdot 7\text{H}_2\text{O}$	[27]
<i>Clostridium butyrium</i>	Glucose	PBD	Glucose, yeast extract, tryptone, K_2HPO_4 , KH_2PO_4 , L-cysteine, $\text{MgSO}_4 \cdot 7\text{H}_2\text{O}$, $\text{FeSO}_4 \cdot 7\text{H}_2\text{O}$	[28]
Mixed culture	Glycerol	PBD	Temperature, glycerol concentration, initial pH, tryptone, yeast extract	[29]
<i>Ethanoligenens harbinense</i> B49	Glucose	PBD	K_2HPO_4 , MgCl_2 , $\text{FeSO}_4 \cdot 7\text{H}_2\text{O}$, NaCl, $\text{ZnSO}_4 \cdot 7\text{H}_2\text{O}$, $\text{CaCl}_2 \cdot 2\text{H}_2\text{O}$	[30]
<i>Clostridium sp. Fanp2</i>	Glucose	PBD	Glucose, yeast extract, initial pH, peptone, FeSO_4 , phosphate buffer, mineral salt solution, vitamin solution	[32]
<i>Enterobacter aerogenes</i> MTCC 111	Glucose	PBD	Yeast extract, tryptone, initial pH, glucose, ferric chloride, inoculum size	[33]
<i>Enterobacter</i> MTCC 7104	Glucose, sucrose and xylose	PBD	Yeast extract, sucrose, initial pH, peptone, tryptone, xylose and glucose	[34]
Heat-treated sludge	Sweet sorghum syrup	PBD	Peptone, initial pH, sodium bicarbonate, total sugar, nutrient solution, iron (II) sulphate (FeSO_4)	[35]
<i>Enterobacter aerogenes</i>	Glucose and glycerol	PBD	Temperature, initial pH, yeast extract, tryptone, glycerol, glucose, agitation rate, inoculum size	[36]
<i>Thermoanaerobacterium thermosaccharolyticum</i> KCU19	Sweet sorghum bagasse	PBD	Peptone, FeSO_4 , CaCl_2 , NaHCO_3 , NiCl_2 , MgCl_2	[31]
<i>E. coli</i>	Formate	PBD	Formate, cell density, yeast extract, NaCl, tryptone, stirring speed	[37]
Mixed culture	Pineapple waste extract	PBD	Substrate concentration, initial pH FeSO_4 , NaHCO_3 , endo-nutrient	[38]
Mixed culture	Cow manure slurry	Taguchi	Temperature, pH, substrate concentration, agitation, ultrasound, KH_2PO_4	[39]

2.2. After screening: Method of steepest ascent/descent

The technique of steepest ascent/descent is applied to identify the region that contains the optimum operating conditions [40]. The variables screened by the screening methods can be further studied using steepest ascent/descent method. This approach is a simple and efficient method [24].

As presented in Table 3, the steepest ascent technique was applied by researchers after screening the most important factors of DFHP. Varrone et al. [29] employed the steepest ascent method after PBD to determine the design center of key

factors of initial pH, glycerol concentration, and temperature for dark fermentation. The path of steepest ascent was used to find the best starting point of two critical factors of HRT and pH by Lay et al. [41]. After screening of key factors by PBD, Boonsayompoo and Reungsang [31] determined the proper direction of changing the concentration of key factors, CaCl_2 , MgCl_2 , FeSO_4 , and NaHCO_3 , by the path of steepest ascent for DFHP. Experimental results showed that the steepest ascent technique was an effective method to determine region of optimal levels. However, the optimal values of factors need to be determined by the following optimization methods.

Table 3. Studies after screening stage (before optimization) by steepest ascent method in dark fermentation.

Inoculum	Substrate	Studied factors	Ref.
<i>Clostridium sp. Fanp2</i>	Glucose	Glucose, vitamin solution, phosphate buffer	[32]
<i>Clostridium butyrium</i>	Glucose	Glucose, yeast extract	[28]
Mixed culture	Glycerol	Glycerol concentration, initial pH, temperature	[29]
Heat-treated sludge	Sweet sorghum syrup	Initial pH, FeSO_4 , total sugar	[35]
<i>Enterobacter</i> MTCC 7104	Xylose	Xylose, initial pH, and peptone	[34]
<i>Enterobacter sp. CN1</i>	Xylose	Xylose, FeSO_4 , peptone	[42]
<i>Thermoanaerobacterium thermosaccharolyticum</i> KKU19	Sweet sorghum bagasse	FeSO_4 , MgCl_2 , CaCl_2 , NaHCO_3	[31]
Anaerobic digested sludge	Starch	pH and HRT	[41]

2.3. Optimization stage

2.3.1. One factor at a time design

The one factor at a time approach studies just one factor at a time while keeping the levels of the other factors constant [13]. The OFAT approach consists of selecting a baseline set of levels of each factor and changing each factor over its favorable range, while keeping the other factors constant at the baseline level [43]. The OFAT design is simple and easy. The technique has some major drawbacks, that is to say (a) interactions between factors are ignored, (b) the optimum can be missed, especially when the interactions among factors are significant, and (c) it presents a relatively large number of runs, is susceptible to high cost, and takes long time to perform especially when the number of factors is large [25,44].

There are a large number of studies available in the literature on OFAT method for dark fermentation, a few of which are reported in Table 4. Satar et al. [45] studied the effect of glucose concentration, feed flow rate, and fermentation time with around 20 runs on DFHP by *Enterobacter aerogenes* ATCC 13048 using OFAT design. Each time, only the effect of one factor on HY was studied and the levels of other factors were kept constant. Results showed that the optimal glucose concentration, feed flow rate and retention time were 8 g/L, 0.5 mL/min, and 24 h, respectively. In optimal conditions, hydrogen yield was 9.44 mmol/g glucose. The method of OFAT design was performed to study the effect of four factors of initial pH, starch, nitrogen, and iron concentration on DFHP from starch. The optimum pH, concentration of iron, nitrogen, and starch were calculated as 7–8, 10 mg/L, 5.64 g/L, and 15 g/L, respectively. Hydrogen yield in optimum conditions was reported as 178 mL/g starch [46].

Table 4. Studies in optimization stage on DFHP.

Inoculum	Substrate	Design	Studied factors	Ref.
Wasted activated sludge	Sucrose	Taguchi	Three phosphate sources, three carbonate sources, and a nutrient formulation	[92]
Wasted activated sludge	Sucrose	Taguchi	Concentration of 13 nutrients	[93]
<i>Pseudoalteromonas sp. BH11</i>	Glucose	Taguchi	Glucose, yeast extract, sea water, tryptone	[94]
<i>Thermoanaerobacterium thermosaccharolyticum</i> IIT BTST1	Glucose	Taguchi	Temperature, pH, glucose, FeSO_4 , yeast extract	[49]
Cow dung	Glucose	Taguchi	C/N ratio, pH, temperature, yeast extract	[50]
Wastewater	Potato starch	Taguchi	Ultrasonic frequency, energy, exposure time, starch concentration	[95]
Mixed consortia	Glucose and xylose	Taguchi	Glucose: xylose ratio, pH, inoculum size, and inoculum age	[96]
Mixed culture	Cane molasses	Taguchi	pH, recycle ratio, dilution rate	[97]
Mixed culture	Wastewater	Taguchi	Inoculums, pre-treatment, inlet pH and feed composition	[98]
Municipal wastewater	Xylose	3-PFD (3^{k-p})	pH, oleic acid concentration, biomass concentration	[55]
Brewery wastewater	Steam exploded corn stalk liquor	3-PFD (3^{k-p})	Temperature, pH, HRT	[54]

<i>Thermoanaerobacterium aotearoense</i> SCUT27/ Δ ldh	Sugarcane bagasse	3-FFD (3 ^k)	Sulfuric acid concentration, treatment time	[99]
<i>E. coli</i> (DJT 135)	Formate	3-FFD (3 ^k)	Substrate concentration, pH	[56]
Anaerobic sludge	Renewable waste	Simplex	Corn stalk, Bean husk, organic fraction of solid municipal waste	[80]
Buffalo dung compost	Renewable agri-waste	Simplex	Corn husk, ground nut shell, rice husk	[79]
Mixed culture	Co-digestion Mixture	Simplex	Cheese whey, crude glycerol, buffalo slurry	[81]
Mixed culture	Agricultural wastes	Simplex	Food waste, potato pulp, cattle manure, and pig manure	[100]
Mixed culture	Glucose	D-optimal	Substrate concentration, compost leachate concentration	[73]
<i>E. coli</i> (XL1-BLUE)	Formate	OFAT	Formate concentration	[37]
<i>Clostridium acetobutylicum</i> X9 and <i>Ethanoigenens harbinense</i> B2	Cellulose	OFAT	Substrate concentration, initial pH, C/N ratio, L-cysteine concentration, incubation time	[101]
Wastewater sludge	Sucrose	OFAT	Gas reflux, liquid reflux	[102]
Fermentative bacteria B49	Glucose	OFAT	Magnesium concentration, iron concentration, sparging gas type	[103]
Mixed culture	Starch	OFAT	Nitrogen concentration, iron concentration, initial pH, substrate concentration	[46]
<i>Escherichia coli</i> MC13-4	Glucose	OFAT	Immobilized gel bead size	[104]
<i>Enterobacter aerogenes</i> ATCC 13048	Glucose	OFAT	Glucose, feed flow rate, fermentation time	[45]
<i>Clostridium thermolacticum</i>	Lactose	OFAT	Dilution rate and pH	[105]
Mixed culture	Citric acid wastewater	OFAT	Organic loading rate	[106]
<i>Clostridium</i> sp. Fanp2	Glucose	BBD	Glucose, phosphate buffer, vitamin concentrations	[32]
Mixed culture	Glycerol	BBD	Glycerol concentration, initial pH, temperature	[29]
<i>Enterobacter aerogenes</i> MTCC 111	Glucose	BBD	Substrate concentration, initial pH, ferric chloride	
Heat-treated sludge	Sweet sorghum syrup	BBD	Initial pH, FeSO ₄ , total sugar	[35]
<i>Thermoanaero bacterium thermosaccharolyticum</i> IIT BTST1	Glucose	BBD	Temperature, pH, glucose, FeSO ₄ , yeast extract	[49]
Anaerobic sludge	Bean husk, corn stalk, solid municipal waste	BBD	Substrate concentration, HRT, pH, temperature	[80]
Mixed culture	Synthetic food waste	BBD	Initial pH, linoleic acid concentration, initial COD concentration	[60]
<i>Ethanoligenens harbinense</i> B49	Glucose	BBD	Glucose concentration, FeSO ₄ , 7H ₂ O, MgCl ₂	[30]
<i>Enterobacter aerogenes</i>	Glucose	BBD	Glucose concentration, pH, temperature	[107]
<i>Clostridium tyrobutyricum</i> JM1	Glucose	BBD	Glucose concentration, pH, temperature	[108]
<i>Escherichia coli</i> DJT135	Glucose	BBD	Glucose concentration, pH, temperature	[109]
Mixed culture	Glucose	BBD	Linoleic acid concentration, initial pH, number of glucose injections	[110]
<i>Klebsiella. pneumoniae</i> ECU-15	Glucose	BBD	Substrate concentration, ammonium sulfate concentration, trace elements concentration	[111]
Anaerobic sludge	Dairy wastewater	BBD	Substrate concentration, pH, COD/N ratio, COD/P ratio	[112]
Anaerobic sludge	Glucose	BBD	pH, microwave treatment duration, microwave intensity	[113]
Gamma irradiated sludge	Glucose	BBD	Temperature, initial pH, substrate concentration	[114]
Brewery wastewater	Steam exploded switchgrass liquor	BBD	pH, HRT, linoleic acid concentration	[74]
<i>Enterobacter</i> sp. CN1	Xylose	BBD	Xylose, FeSO ₄ , peptone	[42]
Anaerobic sludge	Brewery wastewater	BBD	Temperature, pH, brewery wastewater concentration	[115]
Heat-treated anaerobic sludge	<i>Laminaria japonica</i>	BBD	HCl concentration, heating temperature, reaction time	[116]
<i>Klebsiella pneumoniae</i> BLb01	Residual glycerol from biodiesel plant	CCD	Temperature, KH ₂ PO ₄ , K ₂ HPO ₄	[27]
<i>Thermoanaerobacterium thermosaccharolyticum</i> K KU19	Sweet sorghum bagasse	CCD	FeSO ₄ , MgCl ₂ , CaCl ₂ , NaHCO ₃	[31]
Mixed culture	Pineapple waste extract	CCD	Substrate concentration, initial pH, FeSO ₄	[38]
Heat-treated anaerobic granular sludge	Lactose, glucose, and cheese whey powder	CCD	Substrate concentration, initial pH	[117]
<i>Clostridium acidisoli</i> and <i>Rhodobacter Sphaeroides</i>	Sucrose	CCD	Sucrose concentration, initial pH, inoculum ratio	[64]
Mixed culture	Sucrose	CCD	Substrate concentration, initial pH	[118]
Seed sludge	Sucrose	CCD	Ultrasonic time, density	[119]
Anaerobic sludge	Wheat powder	CCD	C/N ratio and C/P ratio	[120]

Mixed culture	Food residues and manure	CCD	Temperature, HRT, N ₂ -flow rate	[121]
<i>Clostridium butyricum</i> EB6	Palm oil mill effluent	CCD	Temperature, pH, COD of POME	[122]
<i>Clostridium butyricum</i> EB6	Glucose	CCD	Glucose concentration, pH, iron concentration	[123]
Anaerobic digester sludge	Food waste with residual blood	CCD	HRT, total solids feed (% TS), proportion of residues (% Blood)	[124]
Anaerobic grass compost	Food wastes	CCD	PO ₄ ³⁻ , Fe ²⁺ , NH ₄ ⁺ concentrations	[125]
Mixed culture	Organic municipal solid waste	CCD	Organic municipal solid waste, pretreated anaerobic digestion sludge, amount of hydrogen-producing bacteria	[126]
Anaerobic digested sludge	Starch	CCD	HRT, pH	[127]
<i>Clostridium</i> sp.	Beer brewing industry wastewater	CCD	Glucose addition concentration, pH, temperature	[128]
Anaerobic sludge	Sucrose	CCD	Substrate concentration, HRT	[65]
Cow dung compost	Sucrose	CCD	Substrate concentration, initial pH	[118]
Anaerobic sludge	Palm oil mill effluent	CCD	C/N ratio, C/P ratio, Fe ⁺² concentration	[129]
Anaerobic sludge	Glucose	CCD	Substrate concentration, pH, temperature	[130]
Anaerobic sludge	Glucose	CCD	Substrate concentration, pH, temperature	[131]
Anaerobic sludge	Sucrose	CCD	Substrate concentration, pH, temperature	[132]
Mixed culture	Swine manure, fruit, and vegetable market waste	CCD	HRT, substrates ratio	[133]
Lesser panda manure	Corn stalk	CCD	Temperature, time, solid state compound enzyme	[134]
Anaerobic sludge	Glycerin (standard or residual)	CCD	pH, glycerin concentration, volatile suspended solids	[135]
Mixed culture	Cow manure slurry	CCD	pH, temperature	[39]
Anaerobic sludge	Sugarcane bagasse hydrolysate	CCD	Substrate concentration, substrate: buffer ratio, inoculum: substrate ratio	[136]
<i>Escherichia coli</i> WDHL	Wheat straw hydrolysate	CCD	Temperature, pH, total reducing sugars	[137]
<i>Clostridium butyrium</i>	Glucose	CCD	Glucose, yeast extract	[28]
Anaerobic sludge	Glucose	CCD	pH and autoclave	[138]
Anaerobic hydrogen producing bacteria	Starch	CCD	Starch concentration, ferrous iron concentration, L-cysteine concentration	[139]
<i>Clostridium pasteurianum</i>	Crude glycerol	CCD	Temperature, initial pH, glycerol concentration	[140]
Granular sludge	Cassava's stillage	CCD	Initial pH, MoO ₄ ⁻² concentration	[141]
Digested anaerobic granular sludge	Glucose	CCD	Glucose concentration, initial pH, nickel nanoparticles concentration	[142]
Heat-treated POME sludge	Palm oil mill effluent	CCD	Substrate concentration, pH	[20]
<i>Enterobacter</i> MTCC 7104	Xylose	CCD	Xylose concentration, initial pH, peptone concentration	[34]
Mixed culture	Waste glycerol and sludge	CCD	Waste glycerol concentration, sludge concentration, and amount of Endo-nutrient addition	[143]
Mixed culture	Sugar refinery wastewater	CCD	pH, HRT, organic loading rate	[63]
Anaerobic seed sludge	Food waste	CCD	Inoculums concentration, substrate concentration, citrate buffer concentration	[144]
Anaerobic sludge	Starch	CCD	Starch concentration, Fe, Ni	[145]
Anaerobic seed sludge	Palm oil mill effluent	CCD	Substrate concentration, initial pH, temperature, inoculum volume	[146]
Anaerobic activated sludge	Sugar refinery wastewater	ANN	VLR, ORP, pH, alkalinity	[147]
Sewage sludge	Sucrose	ANN	HRT, sucrose concentration, sucrose degradation, biomass concentrations, ethanol, acetate, propionate and butyrate concentrations. ORP, pH, recycle ratio, alkalinity	[148]
<i>Enterobacter</i> MTCC 7104	Xylose	ANN	Xylose concentration, initial pH, peptone concentration	[34]
<i>E. coli</i>	Cheese Whey	ANN	ORP, pH, dissolved CO ₂	[149]
Thermal preheated sludge	Starch	ANN	Organic loading rate, pH, VSS yield	[150]
Mixed culture	Thin stillage, glucose, sucrose	ANN	Initial pH, substrate concentration, temperature, maximum fermentation time, biomass concentration	[87]
Buffalo dung compost	Glucose and xylose	ANN-GA	Inoculum age, inoculum size, pH, glucose: xylose ratio	[91]
Anaerobic digested sludge	Glucose	ANN-GA	Temperature, pH, substrate concentration	[151]
Anaerobic digested sludge	Sucrose	ANN-GA	Organic loading rate, HRT, influent alkalinity	[152]

2.3.2. Taguchi design

The Taguchi design was applied in screening and optimization stages, which was introduced by Genechi Taguchi in the 1950s [16]. In this approach, the application of orthogonal array reduces the number of runs [23]. The Taguchi approach can recognize key factors and best level of a factor from a pre-determined number of levels. However, the actual optimal value of the level of a factor cannot be determined using this approach. This problem can be modified using techniques such as neural network [16]. The technique can help reduce the number of experiments significantly and minimize the operational time and cost [47]. Naturally, it is susceptible to several limitations, that is, it is only effective when employed in the early design of process or product. If the design variables and their nominal values are determined, Taguchi method may not be cost effective. This approach may not be a proper choice for a continuous variable. Also, the method is not always accurate and actual optimal factor levels may not be guaranteed [48]. The number of experiments covered by Taguchi technique is reported in Table 5.

Wang et al. [39] carried out screening of factors with Taguchi method followed by CCD optimization. They used the Taguchi design L₁₈ orthogonal array to screen variables of temperature, pH, substrate concentration, agitation, ultrasound, and KH₂PO₄ at three levels. The results indicated that temperature and pH were selected as key factors. Roy et al. [49] studied the effect of glucose concentration, temperature, pH, yeast extract concentration, and FeSO₄ at three levels by the Taguchi technique. A L₂₇ orthogonal array with three degrees of freedom was applied to evaluate the effect of factors on DFHP by *Thermoanaerobacterium thermosaccharolyticum* IIT BT-ST1. According to Taguchi method, temperature was found as the most important variable followed by pH and glucose concentration. The effect of factors of temperature, yeast extract concentration, substrate

concentration, pH, and carbon to nitrogen (C/N) ratio on hydrogen production using cow dung was investigated with Taguchi design by Kumari and Das [50]. Statistical analysis indicated that the C/N ratio was the essential factor in hydrogen production. The similar studies are reported in Table 4.

Table 5. Number of experiments of Taguchi technique.

Number of factors	Number of levels			
	2	3	4	5
2	L4	L9	L16	L25
3	L4	L9	L16	L25
4	L8	L9	L16	L25
5	L8	L18	L16	L25
6	L8	L18	L32	L25
7	L8	L18	L32	L50
8	L12	L18	L32	L50
9	L12	L18	L32	L50
10	L12	L27	L32	L50

2.3.3. Response surface methodology

The response surface methodology (RSM) is a collection of the mathematical and statistical methods that are useful for the optimization of an interest response, which is affected by several factors [51]. The RSM techniques of three levels full or fractional factorial, central composite design, Box-Behnken design, Doehlert design, simplex design, and optimal design are widely used in the optimization stage. Finding a suitable relation between the response and the factors for the RSM methods is necessary. Generally, a linear polynomial model (first-order: Eq. (1)) or quadratic polynomial model (second-order: Eq. (2)) is used to explain the effect of key variables on a response [52].

Table 6. Comparison of the efficiency of 3- FFD, CCD, BBD, and DD [53].

Factors (K)	Number of coefficients	Number of experiments				Efficiency			
		3- FFD	CCD	BBD	DD	3- FFD	CCD	BBD	DD
2	6	9	9	-	7	0.67	0.67	-	0.86
3	10	27	15	13	13	0.37	0.67	0.77	0.77
4	15	81	25	25	21	0.18	0.60	0.60	0.71
5	21	243	43	41	31	0.09	0.49	0.61	0.68
6	28	729	77	61	43	0.04	0.36	0.46	0.65
7	36	2187	143	85	57	0.02	0.25	0.42	0.63
8	45	6561	273	113	73	0.0069	0.16	0.4	0.62

The efficiency of an experimental design is defined as the number of coefficients in the estimated model divided by the number of runs. It is concluded from Table 6 that the efficiency DD > BBD > CCD > 3-FFD [53]. However, it is seen that CCD is extensively applied to optimization.

$$y = \beta_0 + \sum_{i=1}^k \beta_i x_i + \sum_{i=1}^k \beta_{ii} x_i^2 + \sum_{i < j} \beta_{ij} x_i x_j + \varepsilon \quad (2)$$

2.3.3.1. Three levels full or fractional factorial design

The full and fractional factorial designs with three levels (-1, 0, +1) are used to study quadratic effects and are mainly applied in the optimization stage. The total number of experiments for k factors is 3^k and 3^{k-p} in the 3-FFD and 3-PFD, respectively. A 3^k or 3^{k-p} design might need too many runs, depending on the values of k and p [18]. Since the factorial design for more than two factors requires a

considerable number of experiments, designs those offer a smaller number of runs such as the BBD, CCD, and DD are applied more often.

After screening key factors (pH, HRT, and temperature), a 3-PFD was employed by Shanmugam et al. [54] to optimize hydrogen production from lignocellulosic biomass. A 3³⁻¹ analysis indicated that the hydrogen yield was affected by all the experimental variables. However, the effect of temperature was greater than HRT and pH. Chaganti et al. [55] investigated the effect of pH, concentration of oleic acid (OA), and biomass on DFHP from xylose by a 3-PFD. According to a 3³⁻¹ design, the terms of linear and quadratic OA and pH were significant, and the concentration of biomass was insignificant. A 3-FFD (3²) was applied by Bakonyi et al. [56] to determine the optimum conditions of two operational variables (pH and substrate concentration) to obtain maximum

hydrogen yield from formate by both strains of *E. coli* (XL1-BLUE) and *E. coli* (DJT 135). The total number of 12 experimental runs (including 3 replications in the center point) were performed for both strains of wild-type and metabolic engineering. The results showed that pH and formate concentration were statistically important. However, the effect of formate concentration was much higher than pH.

2.3.3.2. Box-Behnken design

The Box-Behnken approach is a class rotatable (or nearly rotatable) second-order design [57], introduced by Box and Behnken in 1960 [58]. The BBD is based on three levels (-1, 0, +1) fractional factorial design and can be applied to problems having three or more factors. The number of required experiments in this design is $2k(k-1) + n_c$, where k and n_c are the number of factors and central points, respectively [57]. The technique is more efficient and economical in terms of the number of required experiments and is a spherical design with all points lying on a sphere of radius 2. The BBD does not require any run where all factors are simultaneously at their highest or lowest levels. Therefore, this design can be considered appropriate when unsatisfactory results occur at the extreme points of the experimental region [59].

As presented in Table 4, many research studies have employed BBD to optimize DFHP from various substrates. Having performed initial screening by PBD, Long et al. [42] applied BBD in 15 runs of experiment to optimize the most important operational variables of concentration of substrate, FeSO_4 , and peptone on hydrogen production from xylose using *Enterobacter* sp. CN1. The results show the initial concentration of xylose and FeSO_4 and their substantial effect on hydrogen production, while peptone remains unaffected. Under the optimal medium condition, hydrogen yield of 2 mol H_2 /mol xylose was obtained. The effects of individual and interaction of three key factors, namely concentration of linoleic acid (LA), initial pH, and chemical oxygen demand (COD), on DFHP using a BBD in 13 runs of experiments were studied by Pendyala et al. [60]. The results indicated that pH, concentration of LA, COD, and their interactions affected hydrogen production. A PBD followed by BBD was performed to screen important parameters and identify the optimal value of key factors, glucose concentration, Mg^{2+} , and Fe^{2+} , in dark fermentation by *E. harbinense* B49. According to 17 runs of experiment of BBD, optimal concentrations were obtained and, under the optimal condition, HY was 2.2 mol/mol glucose. Among the studied factors, Mg^{2+} and Fe^{2+} had significant individual effect, while their interactions were no significance [30].

2.3.3.3. Central composite design

The central composite design is a favorite class of experimental design and is employed for fitting the second-order model that was introduced by Box and Wilson in 1951 [40]. The CCD investigates each factor at five levels (- α , -1, 0, +1, + α), where α is the distance of the axial runs from the design center. The number of experiments in this design is $2^k + 2k + n_c$, where k and n_c are the number of factors and central points, respectively [61]. Two variables of α and n_c in this design must be determined [53]. Generally, three to five center runs are suggested. α value depends on the number of factors and can be calculated by $\alpha = 2^{0.25k}$, where for two, three, and four factors is 1.41, 1.68, and 2, respectively [62].

Hydrogen production in an anaerobic sequencing batch bioreactor was optimized using CCD by Won et al. [63]. Three operational variables (pH, HRT, and OLR) were studied in 18 experimental runs. Results showed that HRT had lower significant effect on hydrogen production than pH and OLR, whereas OLR had much effect on hydrogen production rate. A CCD after PBD screening was used to evaluate the effects of the most important variables, namely sucrose concentration, inoculum ratio, and initial pH, on hydrogen production by co-culture of *Clostridium acidisoli* and *Rhodobacter sphaeroides*. According to 15 experimental runs, all of the key factors individually affected hydrogen yield, and pH and sucrose concentration interacted interdependently [64]. Zao et al. [65] employed CCD to evaluate both interactive and individual effects of HRT and sucrose concentration on DFHP from sucrose. The results indicated that under optimum conditions, HY of 1.62 mol H_2 /mol hexose was obtained. Both HRT and sucrose concentration present a significant individual effect on hydrogen yield. However, their interactions have no significant effect on the hydrogen yield. There are many reports available in the literature on the application of CCD to optimize hydrogen production from various substrates, as depicted in Table 4.

2.3.3.4. Dohrlert design

An advantage of experimental design for second-order models is the uniform shell design, introduced by Doehlert in 1970. Dohrlert design is polyhedron based on hyper triangles with a hexagonal structure in the simplest case [66]. The number of experiments in this design is $k^2 + k + n_c$, where k and n_c are the number of factors and central points, respectively. Unlike CCD and BBD, Dohrlert design is neither orthogonal nor rotatable [67] and has more advantages than CCD and BBD such as DD requires less number of experiments [12]. As shown in Table 7, a DD presents different number of levels for all factors, which is an interesting property. Thus, the factors that are considered more important can be measured at more levels [67]. Another attractive feature of DD is the possibility of introducing new factors during an experimental design without losing the runs already performed [53]. As seen in Figure 2, it is also feasible to displace the experimental region to another place. To the best of our present knowledge, Dohrlert design has not been used to meet the objective of dark fermentation to date.

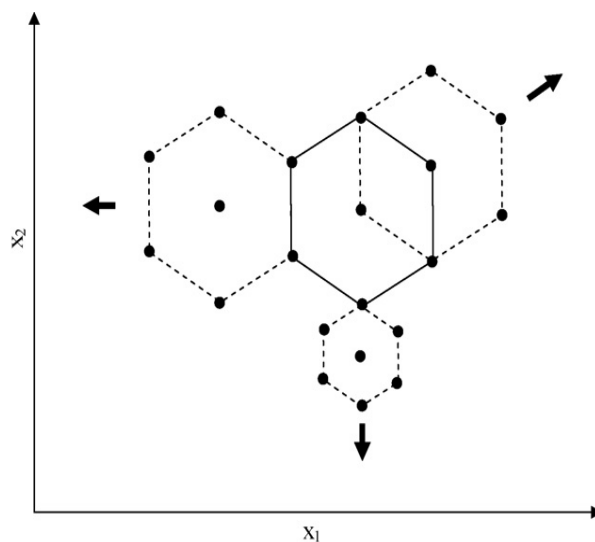


Figure 2. Displacement ability of Dohrlert design [14].

Table 7. Number of levels of DD generated for two to six factors [53].

Factors	Number of levels of factors
2	3,5
3	3,7,5
4	3,7,7,5
5	3,7,7,7,5
6	3,7,7,7,7,5

2.3.3.5. Optimal design

Typically, there is a standard response surface design such as CCD and BBD, provided that the experimental region is a cube or a sphere. However, sometimes, an experimenter encounters a situation where a standard response surface design may not be the best choice [6]. A certain approach to handling the irregular experimental region is using creation of computer-aided optimal design. The optimal designs represent a class of DOE, which is optimal with respect to some statistical criteria. The designs are particularly useful when the factor space is not uniformly accessible, qualitative factors have more than two levels, and so on. In optimal designs, the best sets of experiments are chosen based on some criteria. There are several popular designs related to optimality criteria such as A-optimality, G-optimality, E-optimality, D-optimality, and so on, where the D-optimality is the criterion that receives the most attention in the literature among them [68,69]. A design is expressed as D-optimal if $|(X X^T)^{-1}|$ is minimized, where X is the matrix of design points and T denotes the transpose [70]. The D-optimal designs are used for multi-factor experiments with both quantitative and qualitative factors, while the factors can be studied at a mixed number of levels [71]. The number of experiments of D-optimal is lower than FFD and PFD. The design can be considered very efficient if its efficiency is 0.8, 0.9 or higher [72].

Liu et al. [73] used D-optimal method to find optimal operating conditions for DFHP from the co-fermentation of glucose and leachate by anaerobic sludge. The results showed that the HY was affected by the glucose concentration and organic loading of leachate. According to a two-factor D-optimal design, the cubic model was suggested and a hydrogen yield of 1.6 mol H₂/ mol glucose was predicted at 6174.93 mg/L glucose and 3383.20 mg COD/L leachate. D-optimal design is also applicable to the validation stage. A validation study was carried out for variables of temperature, pH, and HRT by the D-optimality procedure after a 3-PFD design. The index of D-optimality is between 0 and 1, where a value closer to 1 shows a completely favorable solution. In the validation study, the value of D-optimality of 1 was obtained with a HY of 100 mL/g TVS at 9.5 h HRT, pH 4.5, and 53 °C [54]. Veeravalli et al. [74] employed D-optimality analysis to perform the validation of optimal level for the three factors of HRT, pH, and LA after BBD. Results of D-optimality showed that maximum hydrogen yield was 99.86 mL H₂/g TVS at HRT 10 h, pH 5, and LA concentration of 1.75 g/L.

2.3.3.6. Simplex method (mixture designs)

The Nelder-Mead simplex design proposed by John Nelder and Roger Mead (1965) is used for performing nonlinear unconstrained optimization [75] and is different from the simplex of Dantzig for linear programming [76]. A Nelder-Mead simplex has a geometric shape with k+1 corners, where k is the number of factors. As illustrated in Figure 3- (a) and

(b), a simplex is an equilateral triangle and tetrahedron in two and three dimensions, respectively [26]. The simplex is a stepwise technique by which the runs are carried out one by one. The direction for improvement is obtained by moving away from the vertex with the smallest value [77]. The principles for a simplex optimization with two factors are illustrated in Figure 3-(c). Further application of the simplex optimization is employed to investigate the effects of mixture components on the variable of response. The total amount of components is kept constant (100 %) in the mixture designs. There are several different types of mixture designs where simplex lattice and centroid are the most common ones [78]. The contour plot of simplex lattice design is depicted in Figure 3-(d).

Prakasham et al. [79] studied hydrogen production from buffalo dung compost with untreated mixed renewable agro-residues. Corn husk (CH), ground nut shell (GNS), and rice husk (RH) were used as the substrate sources of agri-residues. A mixture design demonstrated that a partial supplementation of rice husk or ground nut shell to corn husk enhanced hydrogen yield. Maximum hydrogen production of 65.78 mL H₂/ g TVS with a 70:16:12 (CH: RH: GNS) without any material treatment was determined. A simplex design was applied by Sekoai et al. [80] to obtain the optimum proportions of agro-municipal waste (corn stalk (CS), bean husk (BH), and organic fraction of solid municipal waste (OFSMW)). The results indicated that the optimum hydrogen production was observed at a ratio of 30: 0: 0 (OFSMW: BH: CS) without any material treatment or at a ratio of 15: 15: 0 (OFSMW: BH: CS) in optimum conditions of the process. Marone et al. [81] reported hydrogen production from different substrate mixtures, namely cheese whey (CW), buffalo slurry (BS), and crude glycerol (CG). Mixture design was employed to determine the optimal three-substrate composition and distinguish the effect of the mixing ratio on the hydrogen yield. The optimum hydrogen production was obtained at a ratio of 66:33:0 (BS: CW: CG).

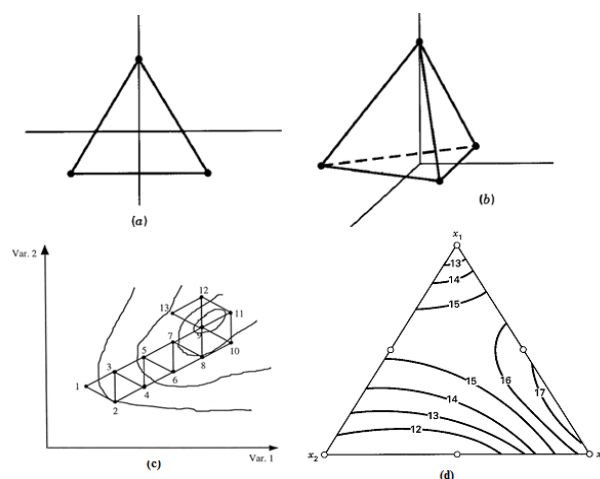


Figure 3. Simplex designs in two dimensions (a) and three dimensions (b), illustration of a simplex optimization with two factors (c), contour plot of simplex lattice design (d) [52, 77].

2.3.4. Artificial neural networks

An artificial neural network (ANN), introduced by Rosenblatt (1959) and Widrow and Hoff (1960) [82], simulates the brain's learning process by mathematically modeling the network structure of interconnected nerve cells. As depicted in Figure 4, the configuration of an ANN consists of an input

layer, one or more hidden layers, and an output layer. The essential processing elements of ANN are called artificial neurons or nodes. The neurons in the hidden layer are connected to the neurons in the input and output layers by adjustable weights that enable the network to compute complicated associations between the factors and response. The input of each neuron in the hidden and output layers is summed up, and the activation function is applied to process the resulting summation. Initially, the weights are randomly chosen and, then, an iterative algorithm is employed to obtain the weights that minimize the differences between the network calculated and actual outputs. The application of conventional optimization methods including gradient-based technique to optimize an ANN model is complex because it is difficult to calculate the derivatives of the model [25,83–85]. The genetic algorithm (GA) as a strong optimization method was introduced by Holland (1975) [86], which mimics the process of natural evolution. The neural network coupled with genetic algorithm optimization model (ANN-GA) has been successfully employed to optimize complex processes [83].

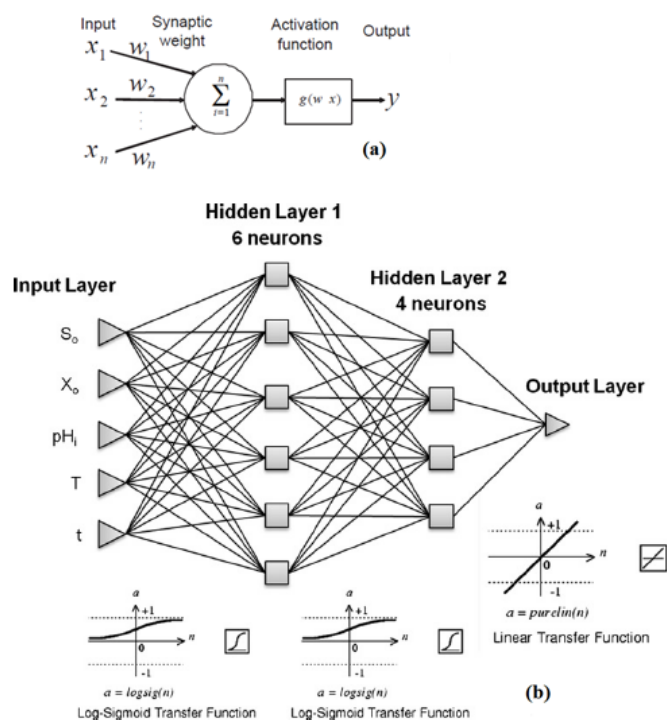


Figure 4. Artificial neural network configuration, (a) operation of a single neuron (b) operation of a three layers (input, hidden, output) network [87].

Nasr et al. [87] used a feed-forward network with back propagation algorithm (configuration of 5-6-4-1 layers) to model the profile of hydrogen production in batch experiments. The input and output layers consisted of five neurons (biomass concentrations, substrate, initial pH, temperature, and time) and one neuron (hydrogen production with time), respectively. 60, 20, and 20 % of the data sets were used for training, testing, and validation, respectively. R^2 of training, testing, and validating data was observed as 0.988, 0.996, and 0.987, respectively. Results depicted that a correlation coefficient of 0.976 was obtained for predicting the profile of hydrogen production with time. Karthic et al. [34] employed ANN (configuration of 3-8-1 layers) to model the hydrogen yield in batch experiments. The input and output

layers were three neurons (peptone concentration, xylose concentration, and initial pH), and one neuron (hydrogen yield), respectively. Method of CCD was also applied to investigate the effect of the aforementioned variables. The modeling ability of RSM and ANN was investigated in predicting the HY at the estimated values of root mean square error (RMSE), standard error of prediction (SEP), and correlation coefficients (R^2). The reported values of RMSE, SEP, and R^2 of RSM and ANN showed that the accuracy of fitness and prediction of ANN were higher than that of RSM design. An ANN method can approximate all kinds of non-linear functions including quadratic functions, whereas RSM is useful only for quadratic approximations [88]. It is reported that the ANN is a suitable method compared to the RSM technique in terms of the modeling and optimization of fermentation processes [89,90]. Prakasham et al. [91] employed an ANN-GA (configuration of 4-10-1 layers) to predict hydrogen production by mixed anaerobic consortia. The age and size of the inoculum, pH, and glucose to xylose ratio as four input parameters and HY as one output parameter were considered. 80 and 20 % of the data sets were applied to training and verification, respectively. The optimum conditions were obtained after performing GA evaluation of 300 generations. After optimization, HY increased from 325.35 to 378.29 mL/g substrate, showing an increase of approximately 16 %. More studies are reported in Table 4.

3. DISCUSSION

The experimental design approaches have been successfully employed for the optimization of dark fermentation. The dark fermentative hydrogen production is a complicated multi-product process that depends on different variables. The optimization purpose of the DFHP process is to improve data analysis, design, and operation and ultimately to enhance the hydrogen production rate and yield. In order to optimize DFHP, the selection of factors and levels is more important and, then, choosing an appropriate experimental design method is necessary to fit with a mathematical function. The quality and accuracy of the fitted model to predict the experimental data is investigated by regression coefficients and interpreted in a response contour plot. Analysis of variance (ANOVA) is a collection of statistical techniques used to analyze the differences between group means and their associated procedures. ANOVA is essential to investigate the significance and adequacy of the model. Screening methods are employed for a large number of process or design variables to identify the most important variables that have significant effect on the process performance. In the case of the DFHP, methods such as Plackett–Burman, two levels full or fractional factorial, and Taguchi design are used for screening the key factors. The methods of Plackett–Burman and two levels full or fractional factorial at two levels for each factor are economical and efficient. When there are few factors, the two levels FFD can be employed for screening key factors. When the number of factors increases, two levels fractional factorial or Plackett–Burman can be used for screening. Further, the DFHP is followed by the steepest ascent/descent technique to approach the neighborhood of the optimal conditions. Subsequently, the optimization methods are applied. As illustrated in Table 8, each experimental design method is characterized by certain advantages and limitations. The OFAT was widely employed to evaluate the effect of various factors on DFHP. However, the technique

has some major disadvantages: (a) disregard for interactions between factors and (b) requiring a rather large number of experiments, being expensive, taking long time, and highly consuming materials. The OFAT design is always less efficient than other DOE methods. The literatures indicate that, among the RSM methods, CCD and BBD are more applicable than DD, simplex, D-optimal, and three levels full or fractional factorial for DFHP optimization. The CCD as a very effective method for fitting the second-order model for the optimization of DFHP is widely used. The application of BBD is often recommended owing to its economic advantages. The BBD and DD approaches are slightly more useful than CCD. However, they are more effective than the 3-FFD and 3-PFD. The three levels factorial designs have limited application in DFHP when the number of factors is larger than two, because the number of required experiments for more than two factors is very large. Generally, the FFD for more than two factors requires a large number of experiments, which is not economically and practically feasible. Therefore, an FFD method is useful when there are few factors and levels involved. The reviewed papers show that there has been no report on the DD to date for the optimization of the DFHP. The DD has two attractive features (different number of levels

for each factor and displacement ability) that provides a specific advantage in some studies. Thus, the DD method of optimization is suggested for DFHP. Some studies have reported on the optimization of substrate mixture with simplex method of optimization. In the mixture designs, the total amount of components is constant. The D-optimal for optimization and model validation has been used. An irregular experimental region can be handled with the D-optimal design. The D-optimality as a favorable index varies between zero (worst case) and one (ideal case). The Taguchi design for the screening and optimization of the DFHP has been applied. Taguchi approach is able to identify the key factors and the best level of factors from a pre-determined number of levels. However, the approach cannot guarantee determining the optimal condition. This problem can be modified using methods such as ANN. The ANN as a well-known technique to solve the complex non-linear optimization problems is an effective method to optimize several responses simultaneously and also optimize DFHP. It appears that ANN and ANN-GA are more suitable methods than the RSM technique for DFHP optimization. Although the studies of the ANN-GA, simplex, and D-optimal for the optimization of the DFHP are limited. Therefore, more studies covering these aspects are suggested.

Table 8. Advantages and disadvantages of experimental design methods.

Design method	Advantages	Disadvantages	Application
2-FFD	➤ Identification of main effect and the interaction of factors	✓ Large number of runs, time, cost, and consumed materials ✓ Only two levels	Screening
2-PFD	➤ Smaller number of runs compare to 2-FFD for the equal number of factors	✓ Only two levels ✓ Effect of interaction of factors is limited and may be unobserved	Screening
PBD	➤ Good screening tool ➤ Minimum number of required runs for large number of factors	✓ Ignoring interactions between factors ✓ Only two levels	Screening
OFAT	➤ Simple and easy	✓ Ignoring interactions between factors ✓ Large number of experiments, time, cost, and consumed materials ✓ Less efficient than other methods of DOE ✓ Optimum can be missed	Optimization
TD	➤ Using orthogonal array ➤ Reducing number of runs significantly ➤ Minimizing the operational time and cost ➤ Applicable to industrial process	✓ Cannot guarantee the determination of optimal conditions	Optimization and Screening
CCD	➤ Rotatable ➤ Estimate curvature	✓ Moderate number of runs	Optimization
BBD	➤ Rotatable (or nearly rotatable) ➤ Small number of runs in relation to CCD ➤ Estimate curvature	✓ Less coverage than central composite	Optimization
DD	➤ Smaller number of experiments in relation to CCD and BBD ➤ Different number of levels for each factor ➤ Displacement ability	✓ Neither orthogonal nor rotatable	Optimization
3-FFD	➤ Identification of main effect and the interaction of factors	✓ Large number of runs, time, cost, and consumed material ✓ Is not rotatable	Optimization
3-PFD	➤ Smaller number of runs than 3-FFD for the equal number of factors	✓ Is not rotatable ✓ Effect of interaction of factors is limited	Optimization
DO	➤ Applicable to any experimental region (such as irregular experimental region) ➤ Applicable to combination of quantitative and qualitative factors ➤ Number of experiments is lower than FFD and PFD	✓ It does not always lead to a good design	Optimization
SM	➤ The variables are not independent (total amount of the factors must be 1) ➤ Applicable to quantitative factors	✓ Not very efficient for problems having multiple responses that need to be simultaneously optimized	Optimization

ANN	<ul style="list-style-type: none"> ➤ Handling large amounts of data easily ➤ Optimize several responses simultaneously ➤ Suitable to optimize complex processes and all kinds of non-linear functions 	<ul style="list-style-type: none"> ✓ Can be overtrained ✓ Training process can be time consuming ✓ It usually requires a lot of data ✓ Selection of layers, neurons, activation function may be mistaken 	Optimization
-----	--	--	--------------

4. CONCLUSIONS

The present review highlights the recent studies on experimental design approaches to hydrogen production by dark fermentation. The CCD, BBD, OFAT techniques for the optimization of the DFHP were extensively used. The 3-FFD and 3-PFD are not applied frequently, the application of which has been limited to the optimization of two factors. The papers on the ANN-GA, simplex, and D-optimal for the optimization of the DFHP are limited and no paper on the DD has been reported so far. Therefore, more studies covering these aspects are required. The ANN coupled with GA is a more suitable method than the RSM technique for the optimization of dark fermentation. The RMSE and the SEP for the ANN method were much smaller than those for the RSM, indicating that the ANN had a much higher modeling ability and accuracy than the RSM approach. Therefore, more research studies covering these aspects are required. Further comparative studies of these techniques are suggested. Most of the optimization studies presented here were carried out in the batch mode of operation. Thus, the DOE methods used to investigate the effect of the key factors on DFHP in both batch and continuous operations are recommended.

5. ACKNOWLEDGEMENT

The authors wish to express their gratitude to Iranian Research Organization for Science and Technology (IROST) for the support of the present study.

REFERENCES

- Das, D.D., Khanna, N. and Nag, C., Biohydrogen production: Fundamentals and technology advances, First edition, CRC Press, (2014).
- Boshagh, F., Rostami, K. and Moazami, N., "Biohydrogen production by immobilized *Enterobacter aerogenes* on functionalized multi-walled carbon nanotube", *International Journal of Hydrogen Energy*, Vol. 44, (2019), 14395-14405. (DOI: 10.1016/j.ijhydene.2018.11.199).
- Boshagh, F., Rostami, K. and Moazami, N., "Immobilization of *Enterobacter aerogenes* on carbon fiber and activated carbon to study hydrogen production enhancement", *Biochemical Engineering Journal*, Vol. 144, (2019), 64-72. (DOI: 10.1016/j.bej.2019.01.014).
- Jang, K.-W., Kim, D., Kim, S. and Shin, H.-S., "Bioreactor design for continuous dark fermentative hydrogen production", *Bioresour Technol*, Vol. 102, (2011), 8612-8620.
- Show, K., Lee, D. and Chang, J., "Bioreactor and process design for biohydrogen production", *Bioresour Technol*, Vol. 102, (2011), 8524-8533. (DOI: 10.1016/j.biortech.2011.04.055).
- Montgomery, D.C., Design and analysis of experiments, Eighth edition, John Wiley & Sons Inc., (2013).
- Cavazzuti, M., Design of experiments, Optimization methods: From theory to design scientific and technological aspects in mechanics, Springer Science & Business Media, (2012), 13-42.
- Tanco, M., Viles, E. and Pozueta, L., Comparing different approaches for design of experiments (DoE), Advances in electrical engineering and computational science, Lecture notes in electrical engineering, Springer Science & Business Media, 611-621.
- Oehlert, G.W., A first course in design and analysis of experiments, 1st edition, (2010).
- Jiju, A., Design of experiments for engineers and scientists, Elsevier Science & Technology Books, (2003).
- Eriksson, L., Johansson, E., Kettaneh-Wold, N., Wikström, C. and Wold, S., Design of experiments, principles and applications., 3rd edition, Umetrics AB, (2008).
- Callao, M.P., "Multivariate experimental design in environmental analysis", *TrAC-Trends in Analytical Chemistry*, Vol. 62, (2014), 86-92. (DOI: 10.1016/j.trac.2014.07.009).
- Wang, J. and Yin, Y., Biohydrogen production from organic wastes, Singapore: Springer Singapore, (2017).
- Bezerra, M.A., Santelli, R.E., Oliveira, E.P., Villar L.S. and Escalera L.A., "Response surface methodology (RSM) as a tool for optimization in analytical chemistry", *Talanta*, Vol. 76, (2008), 965-977. (DOI: 10.1016/j.talanta.2008.05.019)
- Candiotti, L.V., De Zan, M.M., Camara, M.S. and Goicoechea, H.C., "Experimental design and multiple response optimization, Using the desirability function in analytical methods development", *Talanta*, Vol. 124, (2014), 123-38. (DOI: 10.1016/j.talanta.2014.01.034).
- Antony, J., "Taguchi or classical design of experiments: A perspective from a practitioner", *Sensor Review*, Vol. 26, No. 3, (2006), 227-230.
- Shirakura, T., "Fractional factorial designs of two and three levels", *Discrete Mathematics*, Vol. 116, (1993), 99-135.
- Ryan, T.P., Modern experimental design, John Wiley & Sons Inc., Hoboken, New Jersey, (2007).
- Davim, J.P., Design of experiments in production engineering, Switzerland: Springer International Publishing, (2016).
- Rasdi, Z., Aini, N., Rahman, A., Abd-aziz, S., Lai-ye, P., Zulkhairi, M., Yusoff, M., Mei-ling, C. and Hassan, M.A., "Statistical optimization of biohydrogen production from palm oil mill effluent by natural microflora", *The Open Biotechnology Journal*, Vol. 3, (2009), 79-86. (DOI: 10.2174/1874070700903010079).
- Ismail, F., Abd-Aziz, S., MeiLing, C. and Hassan, M.A., "Statistical optimization of biohydrogen production using food waste under thermophilic conditions", *Open Renewable Energy Journal*, Vol. 2, (2009), 124-131. (DOI: 10.2174/1876387100902010124).
- Plackett, R.L. and Burman, J.P., "The design of multifactorial experiments", *Biometrika*, Vol. 33, (1946), 305-325.
- Nath, K. and Das, D., "Modeling and optimization of fermentative hydrogen production", *Bioresour Technol*, Vol. 102, (2011), 8569-8581. (DOI: 10.1016/j.biortech.2011.03.108).
- Box, G.E., Hunter, W.G. and Hunter, J.S., Statistics for experimenters design, innovation, and discover, 2nd edition, (1978).
- Wang, J. and Wan, W., "Experimental design methods for fermentative hydrogen production: A review", *International Journal of Hydrogen Energy*, Vol. 34, (2009), 235-244. (DOI: 10.1016/j.ijhydene.2008.10.008).
- Kennedy M. and Krouse, D., "Strategies for improving fermentation medium performance: A review", *Journal of Industrial Microbiology & Biotechnology*, Vol. 23, (1999), 456-475. (DOI: 10.1038/sj.jim.2900755).
- Costa, J.B., Rossi, D.M., De Souza, E.A., Samios, D., Bregalda, F., Do Carmo Ruaro Peralba, M., Flores, S.H., and Ayub, M.A.Z., "The optimization of biohydrogen production by bacteria using residual glycerol from biodiesel synthesis", *Journal of Environmental Science and Health-Part A Toxic/Hazardous Substances and Environmental Engineering*, Vol. 46, (2011), 1461-1468. (DOI: 10.1080/10934529.2011.609036).
- Jiang, D., Fang, Z., Chin, S.X., Tian, X.F. and Su, T.C., "Biohydrogen production from hydrolysates of selected tropical biomass wastes with *Clostridium Butyricum*", *Scientific Reports*, Vol. 6, (2016), 1-11. (DOI: 10.1038/srep27205).
- Varrone, C., Giussani, B., Izzo, G., Massini, G., Marone, A., Signorini, A. and Wang, A., "Statistical optimization of biohydrogen and ethanol production from crude glycerol by microbial mixed culture", *International Journal of Hydrogen Energy*, Vol. 37, (2012), 16479-16488. (DOI: 10.1016/j.ijhydene.2012.02.106).
- Guo, W., Ren, N., Wang, X., Xiang, W., Ding, J., You, Y. and Liu, B.-F., "Optimization of culture conditions for hydrogen production by

- Ethanoligenens harbinense* B49 using response surface methodology", **Bioresource Technology**, Vol. 100, (2009), 1192-1196. (DOI: 10.1016/j.biortech.2008.07.070).
31. Boonsayompoo, O. and Reungsang, A., "Thermophilic biohydrogen production from the enzymatic hydrolysate of cellulose fraction of sweet sorghum bagasse by *Thermoanaerobacterium thermosaccharolyticum* KKU19: Optimization of media composition", **International Journal of Hydrogen Energy**, Vol. 38, (2013), 15777-15786. (DOI: 10.1016/j.ijhydene.2013.04.129).
 32. Pan, C.M., Fan, Y.T., Xing, Y., Hou, H.W. and Zhang, M.L., "Statistical optimization of process parameters on biohydrogen production from glucose by *Clostridium* sp. Fanp2", **Bioresource Technology**, Vol. 99, (2008), 3146-3154. (DOI: 10.1016/j.biortech.2007.05.055).
 33. Karthic, P., Joseph, S. and Arun, N., "Optimization of process variables for biohydrogen production from glucose by *Enterobacter aerogenes*", **Open Access Scientific Reports**, Vol. 1, (2012), 142. (DOI: 10.4172/scientificreports.1).
 34. Karthic, P., Joseph, S., Arun, N. and Kumaravel, S., "Optimization of biohydrogen production by *Enterobacter* species using artificial neural network and response surface methodology", **Renewable and Sustainable Energy**, Vol. 5, (2013), 1-13. (DOI: 10.1063/1.4803746).
 35. Saraphirom, P. and Reungsang, A., "Optimization of biohydrogen production from sweet sorghum syrup using statistical methods", **International Journal of Hydrogen Energy**, Vol. 35, (2010), 13435-13444. (DOI: 10.1016/j.ijhydene.2009.11.122).
 36. Puad, N.I.M., Mamat, N.A. and Azmi, A.S., "Screening of various parameters of *Enterobacter aerogenes* batch culture for biohydrogen production", **International Proceedings of Chemical, Biological and Environmental Engineering**, Vol. 93, (2016), 55-61. (DOI: 10.7763/IPCBE. 2016. V93. 8).
 37. Bakonyi, P., Nemestothy, N., Lovitusz, E. and Belafi-Bako, K., "Application of Plackett - Burman experimental design to optimize biohydrogen fermentation by *E. coli* (XL1-BLUE)", **International Journal of Hydrogen Energy**, Vol. 36, (2011), 13949-13954. (DOI: 10.1016/j.ijhydene.2011.03.062).
 38. Reungsang, A. and Sreela-or, C., "Bio-hydrogen production from pineapple waste extract by anaerobic mixed cultures", **Energies**, Vol. 6, (2013), 2175-2190. (DOI: 10.3390/en6042175).
 39. Wang, K.S., Chen, J.H., Huang, Y.H. and Huang, S.L., "Integrated Taguchi method and response surface methodology to confirm hydrogen production by anaerobic fermentation of cow manure", **International Journal of Hydrogen Energy**, Vol. 38, (2013), 45-53. (DOI: 10.1016/j.ijhydene.2012.03.155).
 40. Box, G.E.P. and Wilson, K.B., *On the experimental attainment of optimum conditions*, Breakthroughs in statistics, Springer, New York, N.Y., (1992), 270-310.
 41. Lay, J., "Modeling and optimization of anaerobic digested sludge converting starch to hydrogen", **Biotechnology and Bioengineering**, Vol. 68, (2000), 269-278. (DOI: 10.1002/(SICI)1097-0290(20000505)68:3<269::AID-BIT5>3.0.CO;2-T).
 42. Long, C., Cui, J., Liu, Z., Liu, Y., Long, M. and Hu, Z., "Statistical optimization of fermentative hydrogen production from xylose by newly isolated *Enterobacter* sp. CN1", **International Journal of Hydrogen Energy**, Vol. 35, (2010), 6657-6664. (DOI: 10.1016/j.ijhydene.2010.04.094).
 43. Wahid, Z. and Nadir, N., "Improvement of one factor at a time through design of experiments", **World Applied Sciences Journal**, Vol. 21, (2013), 56-61. (DOI: 10.5829/idosi.wasj.2013.21.mae.99919).
 44. Taylor, P. and Czitrom, V., "One-factor-at-a-time versus designed experiments", **The American Statistician**, Vol. 53, (2013), 16-131. (DOI: 10.1080/00031305.1999.10474445).
 45. Satar, I., Ghasemi, M., Aljilil, S.A., Nor, W., Wan, R., Abdalla, A.M., Alam, J., Daud, W.R.W., Yarmo, M.A. and Akbarzadeh, O., "Production of hydrogen by *Enterobacter aerogenes* in an immobilized cell reactor", **International Journal of Hydrogen Energy**, Vol. 42, (2017), 9024-9030. (DOI: 10.1016/j.ijhydene.2016.04.150).
 46. Liu, G.G.Z. and Shen, J.J.Q., "Effects of culture and medium conditions on hydrogen production from starch using anaerobic bacteria", **Journal of Bioscience and Bioengineering**, Vol. 98, (2004), 251-256. (DOI: 10.1263/jbb.98.251).
 47. Gundogdu, T.K., Deniz, I., Caliskan, G., Sahin, E.S. and Azbar, N., "Experimental design methods for bioengineering applications", **Critical Reviews in Biotechnology**, Vol. 36, (2016), 368-388. (DOI: 10.3109/07388551.2014.973014).
 48. Roy, R., *A primer on the Taguchi method*, 2nd edition, Society of Manufacturing Engineers, (2010).
 49. Roy, S., Vishnuvardhan, M. and Das, D., "Improvement of hydrogen production by newly isolated *Thermoanaerobacterium thermosaccharolyticum* IIT BT-ST1", **International Journal of Hydrogen Energy**, Vol. 39, (2014), 7541-7552. (DOI: 10.1016/j.ijhydene.2013.06.128).
 50. Kumari, S. and Das, D., "Improvement of biohydrogen production using acidogenic culture", **International Journal of Hydrogen Energy**, Vol. 42, (2017), 4083-4094. (DOI: 10.1016/j.ijhydene.2016.09.021).
 51. Myers, R.H., Montgomery, D.C. and Anderson-Cook, C.M., *Response surface methodology, process and product optimization using designed experiments*, 3rd edition, New York, Wiley, (2009).
 52. Ferreira, S.L.C., Bruns, R.E., da Silva, E.G.P., dos Santos, W.N.L., Quintella, C.M., David, J.M., de Andrade, J.B., Breitkreitz, M.C., Fontes Jardim, I.C.S. and Barros Neto, B., "Statistical designs and response surface techniques for the optimization of chromatographic systems", **Journal of Chromatography A**, Vol. 1158, (2007), 2-14. (DOI: 10.1016/j.chroma.2007.03.051).
 53. Ebrahimi-Najafabadi, H., Leardi, R. and Jalali-Heravi, M., "Experimental design in analytical chemistry, part I: Theory", **Journal of AOAC International**, Vol. 97, (2014), 3-11. (DOI: 10.5740/jaoacint.SGEEbrahimi1).
 54. Shanmugam, S.R., Rao, S., Lalman, J.A. and Heath, D.D., "Using a statistical approach to model hydrogen production from a steam exploded corn stalk hydrolysate fed to mixed anaerobic cultures in an ASBR", **International Journal of Hydrogen Energy**, Vol. 39, (2014), 10003-10015. (DOI: 10.1016/j.ijhydene.2014.04.115).
 55. Chaganti, S.R., Kim, D., Lalman, J.A. and Ayele, W., "Statistical optimization of factors affecting biohydrogen production from xylose fermentation using inhibited mixed anaerobic cultures", **International Journal of Hydrogen Energy**, Vol. 37, (2012), 11710-11718. (DOI: 10.1016/j.ijhydene.2012.05.036).
 56. Bakonyi, P., Nemestothy, N. and Belafi-Bako, K., "Comparative study of various *E. coli* strains for biohydrogen production applying response surface methodology", **The Scientific World Journal**, Vol. 2012, (2012). (DOI: 10.1100/2012/819793).
 57. Ferreira, S.L.C., Bruns, R.E., Ferreira, H.S., Matos, G.D., David, J.M., Brandao, G.C., da Silva, E.G.P., Portugal, L.A., dos Reis, P.S., Souza, A.S. and dos Santos, W.N.L., "Box-Behnken design: An alternative for the optimization of analytical methods", **Analytica Chimica Acta**, Vol. 597, (2007), 179-186. (DOI: 10.1016/j.aca.2007.07.011).
 58. Box, G.E.P. and Behnken, D.W., "Some new three level designs for the study of quantitative variables", **Technometrics**, Vol. 2, (1960), 455-475.
 59. Bruns, R.E., Scarminio, I.S. and de Barros, N.B., *Statistical design-chemometrics*, Vol. 25, Elsevier, (2006).
 60. Pendyala, B., Rao, S., Lalman, J.A., Heath, D.D., Shanmugam, S.R. and Veeravalli, S.S., "Using a food and paper-cardboard waste blend as a novel feedstock for hydrogen production: Influence of key process parameters on microbial diversity", **International Journal of Hydrogen Energy**, Vol. 38, (2013), 6357-6367. (DOI: 10.1016/j.ijhydene.2013.03.003).
 61. Sharif, K.M., Rahman, M.M., Azmir, J., Mohamed, A., Jahurul, M.H.A., Sahena, F. and Zaidul, I.S.M., "Experimental design of supercritical fluid extraction - A review", **Journal of Food Engineering**, Vol. 124, (2014), 105-116. (DOI: 10.1016/j.jfoodeng.2013.10.003).
 62. Asghar, A., Abdul Raman, A.A. and Daud, W.M.A.W., "A comparison of central composite design and Taguchi method for optimizing fenton process", **The Scientific World Journal**, Vol. 2014, (2014), 869120. (DOI: 10.1155/2014/869120).
 63. Won, S.G., Baldwin, S.A., Lau, A.K. and Rezadehbash, M., "Optimal operational conditions for biohydrogen production from sugar refinery wastewater in an ASBR", **International Journal of Hydrogen Energy**, Vol. 38, (2013), 13895-13906. (DOI: 10.1016/j.ijhydene.2013.08.071).
 64. Sun, Q., Xiao, W., Xi, D., Shi, J., Yan, X. and Zhou, Z., "Statistical optimization of biohydrogen production from sucrose by a co-culture of *Clostridium acidisoli* and *Rhodobacter sphaeroides*", **International Journal of Hydrogen Energy**, Vol. 35, (2010), 4076-4084. (DOI: 10.1016/j.ijhydene.2010.01.145).
 65. Zhao, B., Yue, Z., Zhao, Q., Mu, Y., Yu, H., Harada, H. and Li, Y.Y., "Optimization of hydrogen production in a granule-based UASB

- reactor", *International Journal of Hydrogen Energy*, Vol. 33, (2008), 2454-2461. (DOI: 10.1016/j.ijhydene.2008.03.008).
66. Doehlert, D.H., "Uniform shell designs", *Applied Statistics*, Vol. 19, (1970), 231.
 67. Hibbert, D.B., "Experimental design in chromatography: A tutorial review", *Journal of Chromatography B*, Vol. 910, (2012), 2-13. (DOI: 10.1016/j.jchromb.2012.01.020).
 68. Rady, E.A., Abd El-Monsef, M.M.E. and Seyam, M.M., "Relationships among several optimality criteria", *Interstat Journals*, Vol. 247, (2009), 1-11.
 69. Allen-Zhu, Z., Li, Y., Singh, A. and Wang, Y., "Near-optimal discrete optimization for experimental design: A regret minimization approach", *ArXiv Preprint ArXiv: 1711.05174*, (2017).
 70. Mousavi, L., Tamiji, Z. and Khoshayand, M.R., "Applications and opportunities of experimental design for the dispersive liquid-liquid microextraction method - A review", *Talanta*, Vol. 190, (2018), 335-356. (DOI: 10.1016/j.talanta.2018.08.002 TAL18923).
 71. D-Optimal designs, (1992), 1-23.
 72. Wong, W.K., "G-optimal designs for multi-factor experiments with heteroscedastic errors", *Journal of Statistical Planning and Inference*, Vol. 40, (1994), 127-133. (DOI: 10.1016/0378-3758(94)90146-5).
 73. Liu, Q., Zhang, X., Zhou, Y., Zhao, A., Chen, S., Qian, G. and Ping, Z., "Optimization of fermentative biohydrogen production by response surface methodology using fresh leachate as nutrient supplement", *Bioresour Technology*, Vol. 102, (2011), 8661-8668. (DOI: 10.1016/j.biortech.2011.03.002).
 74. Veeravalli, S.S., Chaganti, S.R., Lalman, J.A. and Heath, D.D., "Optimizing hydrogen production from a switchgrass steam exploded liquor using a mixed anaerobic culture in an upflow anaerobic sludge blanket reactor", *International Journal of Hydrogen Energy*, Vol. 39, (2014), 9994-10002. (DOI: 10.1016/j.ijhydene.2013.12.057).
 75. Nelder, J.A. and Mead, R., "A Simplex method for function minimization", *The Computer Journal*, Vol. 7, (1965), 308-313. (DOI: 10.1093/comjnl/7.4.308).
 76. Lagarias, J.C., Reeds, J.A., Wright, M.H. and Wright, P.E., "Convergence properties of the Nelder-Mead simplex method in low dimensions", *SIAM Journal on Optimization*, Vol. 9, (1998), 112-147. (DOI: 10.1137/S1052623496303470).
 77. Lundstedt, T., Seifert, E., Abramo, L., Thelin, B., Nystrom, A., Pettersen, J. and Bergman, R., "Experimental design and optimization", *Chromometrics and Intelligent Laboratory Systems*, Vol. 42, (1998), 3-40. (DOI: 10.1007/978-3-540-49148-4-3).
 78. Bondari, K., "Mixture experiments and their applications in agricultural research", *Proceedings of The 30th Annual SAS Users Group International Conference (SUGI 30), Statistics and Data Analysis*, (2005), 1-8.
 79. Prakasham, R.S., Sathish, T., Brahmaiah, P., Subba, C., Rao, R.S. and Hobbs, P.J., "Biohydrogen production from renewable agri-waste blend: Optimization using mixer design", *International Journal of Hydrogen Energy*, Vol. 34, (2009), 6143-6148. (DOI: 10.1016/j.ijhydene.2009.06.016).
 80. Sekoai, P.T. and Kana, E.B.G., "A two-stage modelling and optimization of biohydrogen production from a mixture of agromunicipal waste", *International Journal of Hydrogen Energy*, Vol. 38, (2013), 8657-8663. (DOI: 10.1016/j.ijhydene.2013.04.130).
 81. Marone, A., Varrone, C., Fiocchetti, F., Giussani, B., Izzo, G., Mentuccia, L., Rosa, S. and Signorini, A., "Optimization of substrate composition for biohydrogen production from buffalo slurry co-fermented with cheese whey and crude glycerol, using microbial mixed culture", *International Journal of Hydrogen Energy*, Vol. 40, (2015), 209-218. (DOI: 10.1016/j.ijhydene.2014.11.008).
 82. Shapiro, A.F., "Capital market applications of neural networks, fuzzy logic and genetic algorithms", *Proceedings of The 13th International AFIR Colloquium*, Vol. 1, (2003), 493-514.
 83. Nagata, Y. and Chu, K.H., "Optimization of a fermentation medium using neural networks and genetic algorithms", *Biotechnology Letters*, Vol. 25, (2003), 1837-1842. (DOI: 10.1023/A:1026225526558).
 84. Tahmasebi, P. and Hezarkhani, A., "A hybrid neural networks-fuzzy logic-genetic algorithm for grade estimation", *Computers and Geosciences*, Vol. 42, (2012), 18-27. (DOI: 10.1016/j.cageo.2012.02.004).
 85. Fan, M., Hu, J., Cao, R., Ruan, W. and Wei, X., "A review on experimental design for pollutants removal in water treatment with the aid of artificial intelligence", *Chemosphere*, Vol. 200, (2018), 330-343. (DOI: 10.1016/j.chemosphere.2018.02.111).
 86. Holland, J.H., "Adaptation in natural and artificial systems: An introductory analysis with applications to biology, control, and artificial intelligence", Vol. 69, MIT Press, (1992).
 87. Nasr, N., Hafez, H., El Naggat, M.H. and Nakhla G., "Application of artificial neural networks for modeling of biohydrogen production", *International Journal of Hydrogen Energy*, Vol. 38, (2013), 3189-3195. (DOI: 10.1016/j.ijhydene.2012.12.109).
 88. Desai, K.M., Survase, S.A., Saudagar, P.S., Lele, S.S. and Singhal, R.S., "Comparison of artificial neural network (ANN) and response surface methodology (RSM) in fermentation media optimization: Case study of fermentative production of scleroglucan", *Biocatalysis-from Discovery to Application*, Vol. 41, (2008), 266-273. (DOI: 10.1016/j.bej.2008.05.009).
 89. Bas, D. and Boyac, I.H., "Modeling and optimization II: Comparison of estimation capabilities of response surface methodology with artificial neural networks in a biochemical reaction", *Journal of Food Engineering*, Vol. 78, (2007), 846-854. (DOI: 10.1016/j.jfoodeng.2005.11.025).
 90. Lou, W. and Nakai, S., "Application of artificial neural networks for predicting the thermal inactivation of bacteria: A combined effect of temperature, pH and water activity", *Food Research International*, Vol. 34, (2001), 573-579. (DOI: 10.1016/S0963-9969(01)00074-6).
 91. Prakasham, R.S., Sathish, T. and Brahmaiah, P., "Imperative role of neural networks coupled genetic algorithm on optimization of biohydrogen yield", *International Journal of Hydrogen Energy*, Vol. 36, (2011), 4332-4339. (DOI: 10.1016/j.ijhydene.2011.01.031).
 92. Lin, C.Y. and Lay, C.H., "Effects of carbonate and phosphate concentrations on hydrogen production using anaerobic sewage sludge microflora", *International Journal of Hydrogen Energy*, Vol. 29, (2004), 275-281. (DOI: 10.1016/j.ijhydene.2003.07.002).
 93. Lin, C.Y. and Lay, C.H., "A nutrient formulation for fermentative hydrogen production using anaerobic sewage sludge microflora", *International Journal of Hydrogen Energy*, Vol. 30, (2005), 285-292. (DOI: 10.1016/j.ijhydene.2004.03.002).
 94. Hosseinkhani, B., Hennebel, T. and Boon, N., "Potential of biogenic hydrogen production for hydrogen driven remediation strategies in marine environments", *New Biotechnology*, Vol. 31, (2014), 445-450. (DOI: 10.1016/j.nbt.2014.04.005).
 95. Hsia, S. and Chou, Y., "Optimization of biohydrogen production with biomechatronics optimization of biohydrogen production with biomechatronics", *Journal of Nanomaterials*, Vol. 2014, (2014), 1-11. (DOI: /10.1155/2014/721267).
 96. Prakasham, R.S., Sathish, T. and Brahmaiah, P., "Biohydrogen production process optimization using anaerobic mixed consortia: A prelude study for use of agro-industrial material hydrolysate as substrate", *Bioresour Technology*, Vol. 101, (2010), 5708-5711. (DOI: 10.1016/j.biortech.2010.01.145).
 97. Roy, S., Vishnuvardhan, M. and Das, D., "Continuous thermophilic biohydrogen production in packed bed reactor", *Applied Energy*, Vol. 136, (2014), 51-58. (DOI: 10.1016/j.apenergy.2014.08.031).
 98. Mohan, S.V., Raghavulu, S.V., Mohanakrishna, G., Srikanth, S. and Sarma, P.N., "Optimization and evaluation of fermentative hydrogen production and wastewater treatment processes using data enveloping analysis (DEA) and Taguchi design of experimental (DOE) methodology", *International Journal of Hydrogen Energy*, Vol. 34, (2009), 216-226. (DOI: 10.1016/j.ijhydene.2008.09.044).
 99. Lai, Z., Zhu, M., Yang, X., Wang, J. and Li, S., "Optimization of key factors affecting hydrogen production from sugarcane bagasse by a thermophilic anaerobic pure culture", *Biotechnology for Biofuels*, Vol. 7, (2014), 1-11. (DOI: 10.1186/s13068-014-0119-5).
 100. Shuang, L., Chunying, W., Lili, Y., Wenzhe, L., Zhongjiang, W. and Lina, L., "Optimization of hydrogen production from agricultural wastes using mixture design", *International Journal of Agricultural and Biological Engineering*, Vol. 10, (2017), 246-254. (DOI: 10.3965/j.ijabe.20171003.2688).
 101. Bao, H., Chen, C., Jiang, L., Liu, Y., Shen, M., Liu, W. and Wang, A., "Optimization of key factors affecting biohydrogen production from microcrystalline cellulose by the co-culture of *Clostridium acetobutylicum* X9+ *Ethanoigenens harbinense* B2", *RSC Advances*, Vol. 6, (2016), 3421-3427. (DOI: 10.1039/C5RA14192C).
 102. Lee, K.S., Lo, Y.S., Lo, Y.C., Lin, P.J. and Chang, J.S., "Operation strategies for biohydrogen production with a high-rate anaerobic

- granular sludge bed bioreactor", *Enzyme and Microbial Technology*, Vol. 35, (2004), 605-612. (DOI: 10.1016/j.enzmictec.2004.08.013).
103. Wang, X.J., Ren, N.Q., Xiang W.S. and Qian Guo, W., "Influence of gaseous end-products inhibition and nutrient limitations on the growth and hydrogen production by hydrogen-producing fermentative bacterial B49", *International Journal of Hydrogen Energy*, Vol. 32, (2007), 748-754. (DOI: 10.1016/j.ijhydene.2006.08.003).
104. Ishikawa, M., Yamamura, S., Takamura, Y., Sode, K., Tamiya, E. and Tomiyama, M., "Development of a compact high-density microbial hydrogen reactor for portable bio-fuel cell system", *International Journal of Hydrogen Energy*, Vol. 31, (2006), 1484-1489. (DOI: 10.1016/j.ijhydene.2006.06.014).
105. Collet, C., Adler, N., Schwitzguebel, J.P. and Peringer, P., "Hydrogen production by *Clostridium thermolacticum* during continuous fermentation of lactose", *International Journal of Hydrogen Energy*, Vol. 29, (2004), 1479-1485. (DOI: 10.1016/j.ijhydene.2004.02.009).
106. Yang, H., Shao, P., Lu, T., Shen, J., Wang, D., Xu, Z. and Yuan, X., "Continuous bio-hydrogen production from citric acid wastewater via facultative anaerobic bacteria", *International Journal of Hydrogen Energy*, Vol. 31, (2006), 1306-1313. (DOI: 10.1016/j.ijhydene.2005.11.018).
107. Jo, J.H., Lee, D.S., Park, D., Choe, W. and Park, J.M., "Optimization of key process variables for enhanced hydrogen production by *Enterobacter aerogenes* using statistical methods", *Bioresource Technology*, Vol. 99, (2008), 2061-2066. (DOI: 10.1016/j.biortech.2007.04.027).
108. Hye, J., Sung, D., Park, D. and Moon, J., "Statistical optimization of key process variables for enhanced hydrogen production by newly isolated *Clostridium tyrobutyricum* JM1", *International Journal of Hydrogen Energy*, Vol. 33, (2008), 5176-5183. (DOI: 10.1016/j.ijhydene.2008.05.012).
109. Ghosh, D. and Hallenbeck, P.C., "Response surface methodology for process parameter optimization of hydrogen yield by the metabolically engineered strain *Escherichia coli* DJT135", *Bioresource Technology*, Vol. 101, (2010), 1820-1825. (DOI: 10.1016/j.biortech.2009.10.020).
110. Ray, S., Reaume, S.J. and Lalman, J.A., "Developing a statistical model to predict hydrogen production by a mixed anaerobic mesophilic culture", *International Journal of Hydrogen Energy*, Vol. 35, (2010), 5332-5342. (DOI: 10.1016/j.ijhydene.2010.03.040).
111. Xiao, Y., Zhang, X., Zhu, M. and Tan, W., "Effect of the culture media optimization, pH and temperature on the biohydrogen production and the hydrogenase activities by *Klebsiella pneumoniae* ECU-15", *Bioresource Technology*, Vol. 137, (2013), 9-17. (DOI: 10.1016/j.biortech.2013.03.109).
112. Gadhe, A., Sonawane, S.S. and Varma, M.N., "Optimization of conditions for hydrogen production from complex dairy wastewater by anaerobic sludge using desirability function approach", *International Journal of Hydrogen Energy*, Vol. 38, (2013), 6607-6617. (DOI: 10.1016/j.ijhydene.2013.03.078).
113. Faloye, F.D., Kana, E.B.G. and Schmidt, S., "Optimization of biohydrogen inoculum development via a hybrid pH and microwave treatment technique - semi pilot scale production assessment", *International Journal of Hydrogen Energy*, Vol. 39, (2014), 5607-5616. (DOI: 10.1016/j.ijhydene.2014.01.163).
114. Yin, Y. and Wang, J., "Optimization of hydrogen production by response surface methodology using gamma irradiated sludge as inoculum", *Energy & Fuels*, Vol. 30, (2016), 4096-4103. (DOI: 10.1021/acs.energyfuels.6b00262).
115. Shi, X., Jin, D., Sun, Q. and Li, W., "Optimization of conditions for hydrogen production from brewery wastewater by anaerobic sludge using desirability function approach", *Renewable Energy*, Vol. 35, (2010), 1493-1498. (DOI: 10.1016/j.renene.2010.01.003).
116. Jung, K., Kim, D., Kim, H. and Shin, H., "Optimization of combined (acid+thermal) pretreatment for fermentative hydrogen production from *Laminaria japonica* using response surface methodology (RSM)", *International Journal of Hydrogen Energy*, Vol. 36, (2011), 9626-9631. (DOI: 10.1016/j.ijhydene.2011.05.050).
117. De Leo, A., Davila-vazquez, G. and Alatrisme-mondrago, F., "Fermentative hydrogen production in batch experiments using lactose, cheese whey and glucose: Influence of initial substrate concentration and pH", *International Journal of Hydrogen Energy*, Vol. 33, (2008), 4989-4997. (DOI: 10.1016/j.ijhydene.2008.06.065).
118. Fan, Y., Li, C. and Lay, J., "Optimization of initial substrate and pH levels for germination of sporing hydrogen-producing anaerobes in cow dung compost", *Bioresource Technology*, Vol. 91, (2004), 189-193. (DOI: 10.1016/S0960-8524(03)00175-5).
119. Guo, Y., Kim, S., Sung, S. and Lee, P., "Effect of ultrasonic treatment of digestion sludge on bio-hydrogen production from sucrose by anaerobic fermentation", *International Journal of Hydrogen Energy*, Vol. 35, (2010), 3450-3455. (DOI: 10.1016/j.ijhydene.2010.01.090).
120. Argun, H., Kargi, F., Kapdan, I.K. and Oztekin, R., "Biohydrogen production by dark fermentation of wheat powder solution: Effects of C/N and C/P ratio on hydrogen yield and formation rate", *International Journal of Hydrogen Energy*, Vol. 33, (2008), 1813-1819. (DOI: 10.1016/j.ijhydene.2008.01.038).
121. Karlsson, A., Vallin, L. and Ejlertsson, J., "Effects of temperature, hydraulic retention time and hydrogen extraction rate on hydrogen production from the fermentation of food industry residues and manure", *International Journal of Hydrogen Energy*, Vol. 33, (2008), 953-962. (DOI: 10.1016/j.ijhydene.2007.10.055).
122. Chong, M., Aini, N., Rahman, A., Abdul, R., Abdul, S., Shirai, Y. and Hassan, M.A., "Optimization of biohydrogen production by *Clostridium butyricum* EB6 from palm oil mill effluent using response surface methodology", *International Journal of Hydrogen Energy*, Vol. 34, (2009), 7475-7482. (DOI: 10.1016/j.ijhydene.2009.05.088).
123. Chong, M.-L., Abdul Rahman, N.A., Yee, P.L., Abd Aziz, S., Abdul Rahim, R., Shirai, Y. and Hassan, M.A., "Effects of pH, glucose and iron sulfate concentration on the yield of biohydrogen by *Clostridium butyricum* EB6", *International Journal of Hydrogen Energy*, Vol. 34, (2009), 8859-8865. (DOI: 10.1016/j.ijhydene.2009.08.061).
124. Cuertos, M.J., Gomez, X., Escapa, A. and Moran, A., "Evaluation and simultaneous optimization of bio-hydrogen production using 3² factorial design and the desirability function", *Journal of Power Sources*, Vol. 169, (2007), 131-139. (DOI: 10.1016/j.jpowsour.2007.01.050).
125. Lay, J.J., Fan, K.S., Hwang, J.I., Chang, J.I. and Hsu, P.C., "Factors affecting hydrogen production from food wastes by *Clostridium*-rich composts", *Journal of Environmental Engineering-Asce*, Vol. 131, (2005), 595-602. (DOI: 10.1061/(ASCE)0733-9372).
126. Lay, J., Lee, Y. and Noike, T., "Feasibility of biological hydrogen production from organic fraction of municipal solid", *Water Research*, Vol. 33, (1999), 2579-2586. (DOI: 10.1016/S0043-1354(98)00483-7).
127. Lay, J., "Modeling and optimization of anaerobic digested sludge converting starch to hydrogen", *Biotechnology and Bioengineering*, Vol. 68, (2000), 269-278. (DOI: 10.1002/(SICI)1097-0290(20000505)68:3<269::AID-B>).
128. Boboescu, I.Z., Ilie, M., Gherman, V.D., Mirel, I., Pap, B., Negrea, A., Kondrosi, E., Biro, T. and Maroti, G., "Revealing the factors influencing a fermentative biohydrogen production process using industrial wastewater as fermentation substrate", *Biotechnology for Biofuels*, Vol. 7, (2014), 1-15. (DOI: 10.1186/s13068-014-0139-1).
129. O-Thong, S., Prasertsan, P., Intrasingkha, N., Dhamwichukorn, S. and Birkeland, N.K., "Optimization of simultaneous thermophilic fermentative hydrogen production and COD reduction from palm oil mill effluent by *Thermoanaerobacterium*-rich sludge", *International Journal of Hydrogen Energy*, Vol. 33, (2008), 1221-1231. (DOI: 10.1016/j.ijhydene.2007.12.017).
130. Wang, J. and Wan, W., "Optimization of fermentative hydrogen production process by response surface methodology", *International Journal of Hydrogen Energy*, Vol. 33, (2008), 6976-6984. (DOI: 10.1016/j.ijhydene.2008.08.051).
131. Mu, Y., Zheng, X. and Yu, H., "Determining optimum conditions for hydrogen production from glucose by an anaerobic culture using response surface methodology (RSM)", *International Journal of Hydrogen Energy*, Vol. 34, (2009), 7959-7963. (DOI: 10.1016/j.ijhydene.2009.07.093).
132. Mu, Y., Wang, G. and Yu, H., "Response surface methodological analysis on biohydrogen production by enriched anaerobic cultures", *Enzyme and Microbial Technology*, Vol. 38, (2006), 905-913. (DOI: 10.1016/j.enzmictec.2005.08.016).
133. Tenca, A., Schievano, A., Perazzolo, F., Adani, F. and Oberti, R., "Biohydrogen from thermophilic co-fermentation of swine manure with fruit and vegetable waste: Maximizing stable production without pH control", *Bioresource Technology*, Vol. 102, (2011), 8582-8588. (DOI: 10.1016/j.biortech.2011.03.102).
134. Xing, Y., Fan, S., Zhang, J., Fan, Y. and Hou, H., "Enhanced bio-hydrogen production from corn stalk by anaerobic fermentation using response surface methodology", *International Journal of Hydrogen*

- Energy*, Vol. 36, (2011), 12770-12779. (DOI: 10.1016/j.ijhydene.2011.07.065).
135. De Oliveira, M. and Ferreira-leitao, V.S., "Optimization of biohydrogen yield produced by bacterial consortia using residual glycerin from biodiesel production", *Bioresource Technology*, Vol. 219, (2016), 365-370. (DOI: 10.1016/j.biortech.2016.07.141).
 136. Sangyoka, S., Reungsang, A. and Lin, C., "Optimization of biohydrogen production from sugarcane bagasse by mixed cultures using a statistical method", *Sustainable Environment Research*, Vol. 26, (2016), 235-242. (DOI: 10.1016/j.serj.2016.05.001).
 137. Lopez-hidalgo, A.M., Sanchez, A. and De Leon-Rodriguez, A., "Simultaneous production of bioethanol and biohydrogen by *Escherichia coli* WDHL using wheat straw hydrolysate as substrate", *Fuel*, Vol. 188, (2017), 19-27. (DOI: 10.1016/j.fuel.2016.10.022).
 138. Faloye, F.D., Kana, E.B.G. and Schmidt, S., "Optimization of hybrid inoculum development techniques for biohydrogen production and preliminary scale up", *International Journal of Hydrogen Energy*, Vol. 38, (2013), 11765-11773. (DOI: 10.1016/j.ijhydene.2013.06.129).
 139. Thi, H., Kieu, Q., Nguyen, Y.T., Dang, Y.T. and Nguyen, B.T., "Optimization of culture conditions for hydrogen production by an anaerobic bacteria strain on soluble starch using response surface methodology", *Bioprocessing & Biotechniques*, Vol. 5, (2015). (DOI: 10.4172/2155-9821.1000265).
 140. Sarma, S., Kumar, V. and Moholkar, V.S., "Kinetic and thermodynamic analysis (with statistical optimization) of hydrogen production from crude glycerol using *Clostridium pasteurianum*", *International Journal of Hydrogen Energy*, Vol. 441, (2016), 19972-19989. (DOI: 10.1016/j.ijhydene.2016.08.204).
 141. Dong-jie, N., Jing-yuan, W., Bao-ying, W. and You-cai, Z., "Effect of Mo-containing additives on biohydrogen fermentation from cassava's stillage", *International Journal of Hydrogen Energy*, Vol. 36, (2011), 5289-5295. (DOI: 10.1016/j.ijhydene.2011.01.139).
 142. Mullai, P., Yogeswari, M.K. and Sridevi, K., "Optimization and enhancement of biohydrogen production using nickel nanoparticles-A novel approach", *Bioresource Technology*, Vol. 141, (2013), 212-219. (DOI: 10.1016/j.biortech.2013.03.082).
 143. Sittijunda, S. and Reungsang, A., "Biohydrogen production from waste glycerol and sludge by anaerobic mixed cultures", *International Journal of Hydrogen Energy*, Vol. 37, (2012), 13789-13796. (DOI: 10.1016/j.ijhydene.2012.03.126).
 144. Sreela-or, C., Imai, T., Plangklang, P. and Reungsang, A., "Optimization of key factors affecting hydrogen production from food waste by anaerobic mixed cultures", *International Journal of Hydrogen Energy*, Vol. 36, (2011), 14120-14133. (DOI: 10.1016/j.ijhydene.2011.04.136).
 145. Taherdanak, M., Zilouei, H. and Karimi, K., "Investigating the effects of iron and nickel nanoparticles on dark hydrogen fermentation from starch using central composite design", *International Journal of Hydrogen Energy*, Vol. 40, (2015), 12956-12963. (DOI: 10.1016/j.ijhydene.2015.08.004).
 146. Akhbari, A., Ibrahim, S., Zinatizadeh, A.A., Bonakdari, H., Ebtehaj, I., Khozani, Z.S., Vafaeifard, M. and Gharabaghi, B., "Evolutionary prediction of biohydrogen production by dark fermentation", *Clean-Soil, Air, Water*, Vol. 47, (2019). (DOI: 10.1002/clen.201700494).
 147. Shi, Y., Gai, G.S., Zhao, X.T., Zhu, J.J. and Zhang, P., "Back propagation neural network (BPNN) simulation model and influence of operational parameters on hydrogen bio-production through integrative biological reactor (IBR) treating wastewater", *Proceedings of 4th International Conference on Bioinformatics and Biomedical Engineering, iCBBE*, (2010).
 148. Ozkaya, B., Visa, A., Lin, C., Puhakka, J.A. and Yli-harja, O., "An artificial neural network based model for predicting H₂ production rates in a sucrose-based bioreactor system", *International Journal of Mathematical Physical and Engineering Sciences*, Vol. 2, (2008), 20-25.
 149. Rosales-Colunga, L.M., Garcia, R.G. and De Leon Rodriguez, A., "Estimation of hydrogen production in genetically modified *E. coli* fermentations using an artificial neural network", *International Journal of Hydrogen Energy*, Vol. 35, (2010), 13186-13192. (DOI: 10.1016/j.ijhydene.2010.08.137).
 150. Nasr, M., Tawfik, A., Ookawara, S. and Suzuki, M., "Prediction of hydrogen production from starch wastewater using artificial neural networks", *International Water Technology Journal*, Vol. 4, (2014), 36-44. (DOI: 10.13140/RG.2.1.2582.3845).
 151. Wang, J. and Wan, W., "Optimization of fermentative hydrogen production process using genetic algorithm based on neural network and response surface methodology", *International Journal of Hydrogen Energy*, Vol. 34, (2009), 255-261. (DOI: 10.1016/j.ijhydene.2008.10.010).
 152. Mu, Y. and Yu, H., "Simulation of biological hydrogen production in a UASB reactor using neural network and genetic algorithm", *International Journal of Hydrogen Energy*, Vol. 32, (2007), 3308-3314. (DOI: 10.1016/j.ijhydene.2007.05.021).



Energy Modeling and Techno-Economic Analysis of a Biomass Gasification-CHAT-ST Power Cycle for Sustainable Approaches in Modern Electricity Grids

Saeed Hosseinpour^a, Seyed Alireza Haji Seyed Mirza Hosseini^{a*}, Ramin Mehdipour^b, Amir Hooman Hemmasi^a, Hassan Ali Ozgoli^c

^a Department of Energy Engineering, Faculty of Natural Resources and Environment, Science and Research Branch, Islamic Azad University, Tehran, Iran.

^b Department of Mechanical Engineering, Tafresh University, Tafresh, Iran.

^c Department of Mechanical Engineering, Iranian Research Organization for Science and Technology (IROST), Tehran, Iran.

PAPER INFO

Paper history:

Received 03 February 2020

Accepted in revised form 26 April 2020

Keywords:

Biomass Gasifier
 Cascaded Humidified Advanced Turbine
 Steam Turbine
 Combined Cycle
 Economic Analysis

ABSTRACT

In this study, an advanced combined power generation cycle was evaluated to obtain sustainable energy with high power and efficiency. This combined cycle includes biomass gasification, the Cascaded Humidified Advanced Turbine (CHAT), and the steam turbine. The fuel consumed by the system is derived from the gas produced in the biomass gasification process. The biomass consumed in this study is wood because of its reasonable supply and availability. The economic analysis conducted in the present research has produced significant gains. The proposed cycle with current prices intended to sell electricity in Iran has a positive Net Present Value (NPV). Therefore, the presented cycle in terms of energy supply has good economic value. Due to the significantly higher purchase/sale price of electricity from renewable power plants in developed countries in Europe or the United States, the power generation cycle proposed in this study may be more economically feasible in other regions than Iran. Of course, with a slight price increase in electricity sales in Iran (3 USC kWh⁻¹), the proposed system will have acceptable NPV. Because of the complicated equipment used in high-pressure and low-pressure turbines and compressors sets, the equipment used in this cycle requires a higher initial investment cost than conventional power generation systems. The results showed that the investment cost per unit of energy was approximately 909 USD kW⁻¹.

1. INTRODUCTION

According to the report of international energy outlook [1], CO₂ emissions, which are related to energy production, will increase to 43.2 b tons in 2035. One of the major contributors to climate change is greenhouse gas emissions through consuming fossil fuels to generate power, therefore making a big change and shift from conventional to renewable energy sources, particularly solar, wind, biomass, and hydropower is necessary [2].

Since biomass resources are distributed almost everywhere and also are usually abundantly available, they are significantly used as one of the renewable energies.

It is a fact that biomass energy is the most important energy source after fossil energy sources (oil, natural gas, and coal) which approximately provides 10 % of the world's energy consumption. Besides, municipal and industrial wastes along with agricultural biomass wastes can supply almost 1/4 of the primary energy in 2050 [3-6]. The output power efficiency of a gas turbine can be increased by humidifying the working fluid. Many different cycles have been suggested with a water or steam injection system. Although only a smaller number of the proposed cycles in the previous researches have been commercialized and used in the power plants yet. The humidification of the gas turbines leads to special benefits such as achieving high electrical efficiency and specific energy efficiency, reducing specific investment costs,

reducing the formation of nitrogen oxides (NO_x) in the combustion process, and reducing the degradation of energy output due to high ambient temperatures or low ambient pressure. Improved system performance under part-load conditions compared to the combined cycle is another characteristic of humidified gas turbines. One of the most efficient humidified gas turbine cycles is Cascaded Humidified Advanced Turbine (CHAT) which is considered in this research using biomass gasification as the fuel supply system.

Studies that have been reported in this paper demonstrate energy and economic analysis and also important aspects of a novel integrated biomass gasification as a power system. Since such important issues concerning cost estimation are associated with the capital investment in the humidified turbine-based system, the electricity and heat generation costs in the mentioned combined cycle power plants must be taken into account. The investment cost in the advanced turbine-based cycle according to the Brayton-Rankine system usually consumes approximately 40 % of the overall expenditure in a conventional power system. However, only the gas turbine needs about 30 % of the total investment cost. Additionally, the implementation and installment activities constitute 30 % of the remaining investment cost, which consists of remarkably about two-third of the physical functions that need to be allocated in the works involving the combined power systems. As a result, the specific investment cost that means unit cost per electrical power in simple gas turbine systems is approximately two times smaller than the combined cycle cost that includes steam or district heating bottoming systems [7-9]. Thus, attempts have been made to find alternative ways to

*Corresponding Author's Email: a-mirzahoseini@srbiau.ac.ir (S.A. Haji Seyed Mirza Hosseini)

reduce the electricity cost and heat generation related to the turbine-based cycles installed in the integrated and combined heat and power plants.

Jitka Hrbek [10] compared different thermal gasification projects that operate as a power generator. The main objective of this study is to explain the principals of the mentioned systems and describe relevant actual projects. The economic feasibility of gasification-based power technology plants has been described in this research. He found that the most important factors influencing the price of the biomass gasification outlets included the cost of renewable power, biomass cost, size of gasification unit, and number of operating hours per year. Also, the author showed that in a power to gas project, the total cost is between 5.7 and 7.1 €t kWh⁻¹, which is 2-3 times higher than the price of a project that uses fossil fuels.

In a review study by Bocci et al. [11], some aspects of power plants using biomass gasifier due to energy and economic analysis have been considered. They expressed that biomass gasification power plants based on downdraft gasifier and internal combustion engines were considered, and the results showed that the electrical and cogeneration efficiencies were about 20 % and 80 % with a global capital cost of about 500-1000 € kW⁻¹. The application of fluidized bed technologies causes a significant increase in the total capital cost of the power plant. They indicated that a micro gas turbine-fuel cell-based power generator attached to a fluidized bed biomass gasifier would require about 10000-15000 €kW⁻¹ capital investment.

In research presented by Omar et al. [12], a detailed thermodynamic and economic analysis of a combined power cycle was conducted, which integrated a topping cycle with the M-cycle heat exchanger. The proposed cycle experienced a 6 % improvement in the overall thermal efficiency compared to the conventional combined cycle, and the corresponding electricity cost reduction was 3.8 USD MWh⁻¹.

A novel combined cycle using biogas to supply the required fuel of the system was proposed by Ghavami et al. [13]. They performed a 4E optimization method, while the mentioned system operated as a multi-generation power cycle. The results demonstrated that cooling capacity, heating capacity, and net power were 123.59 MW, 0.73 MW, and 280.35 MW, respectively. Also, the results of economic analysis demonstrated 6.79 USD GJ⁻¹ as unit product cost.

Dibyendu et al. [14] presented a techno-economic assessment and environmental investigation of a power plant that includes biomass gasification which is integrated with a solid oxide fuel cell, a gas turbine based on external fired combustion system, and an organic Rankine cycle. Their economic analysis results predicted that, in this plant, the minimum power generation cost could be 0.086 USD kWh⁻¹.

A humidified advanced turbine (HAT) cycle combined with a micro gas turbine and a solar collector system was proposed by Li et al. [15]. Also, an organic Rankin cycle was proposed to increase power generation capacity by recovering heat losses of the cycle. Thermodynamic and economic analysis of this power system was performed. The presented plant generates approximately 254 kW power, of which almost half of the produced electricity is related to gas turbine and the rest of that is produced due to heat recovery of exhaust gasses by the bottoming cycle. Economic studies in this research showed that the specific plant cost in the main scenario was 0.2 USD kWh⁻¹.

According to previous studies, the economic aspects of advanced humidified power cycles coupled with biomass gasification units have not been received much deliberation. It appears that due to the complexity of these systems and the integration issues, concerted efforts have been directed at efficiency and power outputs. Furthermore, alternative renewable energy sources have not received much attraction compared with conventional power generators consuming fossil fuels because of lower calorific values, lower delivered power, and thus lower financial incomes. Hence, not only should the enrichment of energy capacity approaches in the biomass-based power plants be determined, but also the economic advantages must be considered to make a competitive observation for the investors.

This paper discusses the economic field related to the biomass gasification application in a power plant that uses a cascaded humidified advanced turbine (CHAT) as a top cycle and a steam turbine (ST) as a bottoming cycle, which offers a new aspect in the current research. For this purpose, the entire cost of purchased equipment in each part of the comprehensive cycle has been calculated based on the empirical formulations. In return, total capital investment is obtained by considering other direct and indirect costs to implement a power plant. Establishing a relationship with fixed capital functions is one of the main tasks of this study. Another important matter is that the total variable cost could be estimated when some parameters have been defined such as labor, fuel, utilities, maintenance, etc. Therefore, all principal variable cost factors have been selected in this study to increase the accuracy rank of the prediction. One of the important matters here is to develop a mathematical model to explain the economic profitable conditions of this advanced cycle. For this purpose, some popular financial indicators have been calculated by running the computational model. Net present value, internal rate of return, payback period time, and specific unit cost are common indicators whose values are presented in this research. Moreover, some parametric studies have been carried out to illustrate how the proposed cycle could compete with conventional power plants.

2. TECHNOLOGY DEVELOPMENT

According to the scientific documents, gasification technology was proposed to produce electricity from solid fuels in 1792 for the first time. Moreover, the next step was the installation of a gasifier plant, performed by Siemens in 1861. Meanwhile, the first fluidized bed gasifier unit was implemented in 1926, and the first installation of coal gasification was done in 1999. Accordingly, the fluctuation of fossil fuel prices, specifically oil, at the end of the previous century and climate change concerns are the reasons why biomass gasification has been introduced as an interesting approach to generating heat and power in the current era [16].

Generally, biomass gasification is explained as thermochemical oxidation that is executed partially and biomass is converted into synthesis gas (which usually called syngas). This process happens in the presence of gasifying agents, e.g., pure oxygen, air, steam, carbon dioxide, and maybe a mixture of the mentioned agents [17]. The syngas obtained in this process is a mixture of combustible components (especially hydrogen, carbon monoxide, carbon dioxide, and methane, along with ethane and propane as hydrocarbons). This process also produces char and tars that should be left from the gasifier reactor. Biomass feed material

combustion chamber of the HP turbine. The T-S diagram of the CHAT cycle is shown in Figure 2. The NO_x proportion in the CHAT cycle exhaust gas is significantly lower than the GT simple cycle since water vapor acts as a heat sink in the combustion air [27-31].

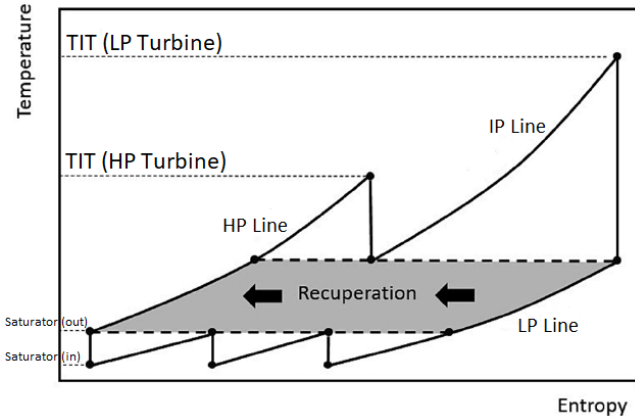


Figure 2. T-S diagram of the CHAT cycle.

The electrical efficiency of the whole cycle can be presented as follows:

$$\eta_{el} = \frac{P_{out} - P_{aux}}{\text{Biomass LHV}} = \frac{P_{net}}{\text{Biomass LHV}} \quad (2)$$

In addition, the total efficiency of the proposed cycle is defined by Equation (3) below:

$$\eta_{total} = \frac{P_{out} - P_{aux} + Q_{useful}}{\text{Biomass LHV}} \quad (3)$$

where Q_{useful} is the amount of useful heat that is consumed in the combined cycle to increase power generation. The conceptual diagram of the proposed cycle in this study is displayed in Figure 3.

3. ECONOMIC ANALYSIS APPROACH

In the present study, the economic analysis of a proposed cogeneration system based on the advanced CHAT gas turbine cycle, with the specified power generation capacity, along with the required fuel by the biomass gasification mechanism, which is presented in earlier parts of the paper, has been comprehensively carried out. Then, based on international fuel and electricity prices, economic indices such as internal rate of return (IRR) and net present value (NPV) of the power plant are calculated, and the level of competitiveness of the system with conventional power generation systems is investigated.

In general, the objectives of the economic model for the comprehensive cycle can be stated as follows:

1. Due to the necessity to develop an economic model in the field of investment cost analysis, the formulation of the purchase cost of system components is calculated.
2. From a systematic perspective, the costs studied including both direct and indirect costs have been examined and calculated. Typically, working capital expenses, startup costs, production costs, and general costs have been included in economic analysis. In previous studies, these parameters are often not considered for gasification-based combined systems, while they are generally presented in other studies. Therefore, the reliability of the obtained

results has also been investigated by comparing the unit cost of the power generation.

3. Given the general use of this cycle as a power generation system and its impact on the geographical area in terms of energy carrier prices, this approach has been taken into account when the cycle operation is evaluated based on the current conditions of electricity and fuel prices in European and American countries. The analysis of these results provides a good understanding of the current utility of the system and its economic future.

The economic feasibility of the comprehensively presented cycle is estimated by considering criteria such as NPV, IRR, and total unit cost for the minimum fuel calorific value. The amount of initial investment required to pay back the equipment cost used in the proposed cycle is also economically analyzed in this model, and the results are shown in a comparative diagram [32, 33].

3.1. Total investment cost

Before the power plant can be used, there are different costs involved in purchasing and installing different machinery and equipment. The sum of fixed investment costs and working capital is known as total investment costs. The fixed costs of power plant setup and operation can be divided into two parts. Some of the costs are directly related to the type of equipment and how the cycle operates; for example, the costs of tools, founding, and site preparation are just a few instances of the costs required to prepare power plant units. These costs, which are usually spent to purchase and install equipment, are called direct costs. The other part of fixed investment costs can be costs that are not directly related to the power plant's performance; however, should be added to the fixed costs of the industrial units overhead. Such costs can be called indirect costs [34-36].

3.1.1. Gas turbine cost functions

The main parts of the GT system are the gas turbine and compressor, where cost relations are shown in Equations 4 and 5. Based on these relationships, the turbine and compressor shaft work are the parameters that influence the cost of the GT system [37].

$$C_{GT} = [(-98.328 \ln(W_{GT}) + 1318.5) W_{GT}] \quad (4)$$

$$C_{comp} = 91562 \left[\frac{W_{comp}}{445} \right]^{0.67} \quad (5)$$

3.1.2. Steam turbine cost functions

The main components of the ST system are the turbine and the condenser, which are cost formulated in a system using 6 to 7 relationships. Based on these relationships, the shaft work of the turbine based on horsepower is the parameter that affects the cost of the ST system [38].

$$C_{ST} = 20000 (P)^{0.41} \quad (6)$$

$$C_{CO} = 3000 \left(\frac{Q_{CO}}{10} \right)^{0.6} \quad (7)$$

$$Q_{CO} = \dot{m} (h_{in} - h_{out}) \quad (8)$$

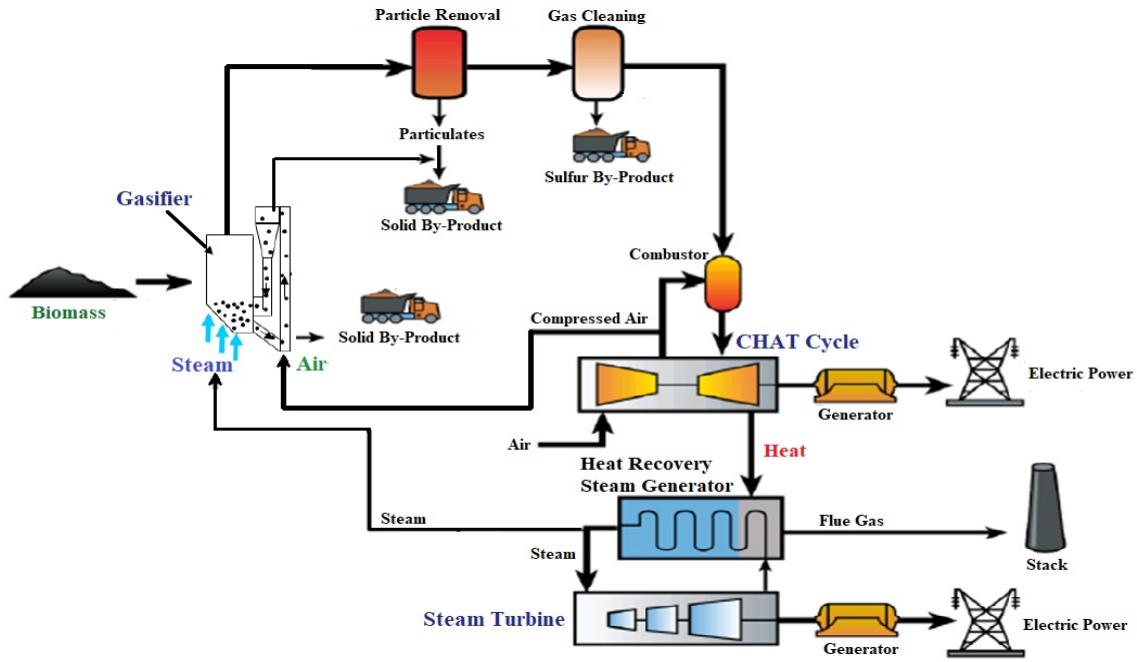


Figure 3. Conceptual view of the proposed combined cycle.

3.1.3. Fluidized bed gasifier cost function

Fluidized bed gasification systems including biomass gasifier and ash output cyclone based on Equations 9 and 10 have been studied in the cost calculations of equipment supply. Moreover, the scale coefficient was calculated 0.67 based on the mentioned references [39].

$$C_g = 1600 (m_g)^{0.67} \quad (9)$$

$$C_{cyclone} = \exp \left\{ \begin{array}{l} 8.9845 - 0.7892[\ln(S)] \\ + 0.08487[\ln(S)]^2 \end{array} \right\} \quad (10)$$

In Equation 10, the size factor is equal to the volume of discharged gas in $\text{ft}^3 \text{min}^{-1}$.

3.1.4. Gas cleaning cost functions

Equations 11 and 12 are used to calculate the cost of the gas treatment system. Cyclic separator with ceramic border plus filter was used for desulphurization and particle separation from bio syn-gas.

$$C_{sep} = 35 A_{mem} \quad (11)$$

$$C_{filter} = 3800 A_{filter}^{0.52} \quad (12)$$

The cost of other major equipment used in the cycle in the proposed power generation system is estimated using the relationships 13 to 26 present in Table 1 [36].

3.2. Total variable costs

Estimating the investment cost is only a part of the process of completing the cost analysis. Another important part is to calculate costs associated with power plant operation and electricity sales. These costs are known in a general classification as total variable costs, which are divided into two categories: production costs and general costs. Production costs are also known as performance costs. The variable cost in this study has been considered annually [34].

Table 1. Cost functions of the economic study for the present combined cycle.

Cost function	Parameter	No.
HRSG parameters		
$3650 \sum_i (f_{P_i} f_{T_{i,steam}} f_{T_{i,gas}} K^{0.8})_i$	$C_{HE(HRSG)}$	(13)
$0.0971(P_i/30)+0.9029$	f_{P_i}	(14)
$1+\exp(T_{out,steam}-830/500)$	$f_{T_{i,steam}}$	(15)
$1+\exp(T_{out,gas}-990/500)$	$f_{T_{i,gas}}$	(16)
$(Q_i / DT_{Lm,i})$	K_i	(17)
$11820 \sum_j (f_{P_{j,steam}})$	C_{piping}	(18)
$0.0971(P_j/30)+0.9029$	f_{P_j}	(19)
$685 m_{gas}^{1.2}$	C_{gas}	(20)
$C_{HE(HRSG)} + C_{piping} + C_{gas}$	C_{HRSG}	(21)
Other equipment's cost		
$130(A_{HE}/0.093)^{0.78}$	C_{HE}	(22)
$442(\dot{W}_{pump})^{0.71} 1.41f_h$	C_{pump}	(23)
$\exp \left\{ \begin{array}{l} 10.158 + 0.1003[\ln(A)] \\ + 0.04303[\ln(A)]^2 \end{array} \right\}$	C_{dryer}	(24)
$760 V^{0.22}$	C_{shs}	(25)
0.04 HRSG Cost	$C_{HRSGstack}$	(26)

3.3. Assumptions

Technical and operation assumptions of the proposed cycle have been presented in reference [26]. In this study, to solve the presented economic model, the following assumptions are applied:

- The lifespan of the cycle is assumed to be 25 years.
- In this study, the discount rate is set at 8 %.
- According to the available information on the guaranteed purchase price of renewable energy sources in industrial units in Iran, the value of USD kWh⁻¹ is considered to be 0.037. Because of the considerable difference between the price of electricity sales in most European countries and that in the United States, electricity prices are also calculated based on both European and American criteria. The average selling price of electricity to industries in Europe is 0.1 USD kWh⁻¹ and in the US is 0.07 USD kWh⁻¹.
- The biomass fuel used in the calculations of the proposed power generation system is wood chips, and information about its constituents and characteristics is accessible in reference [40]. The biomass fuel price is set at 20 USD ton⁻¹.

3.4. NPV and IRR calculation

Net cash flows are calculated based on the plant's annual revenue and expenses. Annual costs of the system include fuel costs and total variable costs annually. To compare different options, it is necessary to convert all cash flows to a specific factor. This is because the liquidity available today may be more valuable than its value in the future. To calculate the Net Cash Flow (NCF) value per year, Relation (27) is used [36].

$$\text{NCF} = (\text{Electricity Gross Payments} - \text{TVC} - \text{Fuel Cost}) \quad (27)$$

According to the values obtained for NCF, the NPV value for the performance cycle is obtained through Relation (28).

$$\text{NPV} = \sum_{n=1}^m \frac{\text{CF}_n}{(1+R)^n} - \text{TCI} \quad (28)$$

In this study, the value of m is equal to 25 in Equation 28.

The IRR criterion is the rate of interest that gives the system performance at the expected current cash flow value, compared to the current cash flow. The IRR is equal to the interest rate that results in zero NPV.

4. RESULTS AND DISCUSSION

The overall results of simulation are presented in Table 2. According to the simulated results, the overall vapor rate in the gasifier is about 1.275 kg s⁻¹, whereas the biomass flow rate and air mass flow rate in the gasifier are about 7.63 kg s⁻¹ and 4 kg s⁻¹, respectively. Inlet mass flow of fuel is about 4 kg s⁻¹. The overall process efficiency is over 56 % and cycles of electrical efficiency are 56.64 %. The electrical efficiency of the proposed model is about 2.2 times that of the simple IBG-GT cycle, which is quite impressive.

Parametric analysis was performed to calculate NPV and IRR changes based on electricity price variations in the considered geographical areas. The price range of electricity from 0.03 USD kWh⁻¹ to 0.1 USD kWh⁻¹, which is its selling price in Iran and its average price in the EU and the US respectively, is considered in the model. As shown in Figure 4, the variation of the NPV value calculated for the duration of

the cycle operation is shown. It should be noted that negative NPV values indicate that the cycle is uneconomical under these conditions and, therefore, is not considered as acceptable outputs of the model.

Also, the IRR is obtained at the point where the NPV is zero based on the considered interest rate. These results are presented in Figure 5. As can be seen, the current cycle with the current prices intended for electricity sales in Europe and the United States has the best positive NPV and the acceptable positive value in Iran.

Table 2. The main results of the integrated biomass gasification-cascaded humidified advanced turbine-steam turbine simulation [26].

Parameter (unit)	Value
HP generator electricity generation (kW)	12,497.13
LP generator electricity generation (kW)	15,721.31
Steam turbine electricity generation (kW)	5411.80
HP turbine outlet temperature (K)	1088.28
LP turbine outlet temperature (K)	957.92
FICFB syngas outlet temperature (K)	1094.55
FICFB syngas outlet flow rate (kg s ⁻¹)	4.15
Inlet air flow rate (kg s ⁻¹)	39.15
Gasifier cold gas efficiency (%)	80.71
Gasifier hot gas efficiency (%)	89.22
Gasifier thermal efficiency (%)	79.62
Hydrogen production potential (%)	83.79
Electrical energy efficiency (%)	56.54
Net energy efficiency (%)	50.33
Heat energy efficiency (%)	6.12
Total energy efficiency (%)	56.45

As noted above, the results presented in Figures 4 and 5 show a better economic status in Europe and the United States than in Iran. This is due to the higher selling price of electricity from renewable power plants in these countries.

Additionally, Table 3 shows the payback period time of the system capital for different values of electricity price for the sample cycle performance case studies mentioned earlier. According to Table 3, the Break-Even Point (B.E.P.) return of capital for the cycle operation in Iran has been estimated at the current electricity price of approximately 5 years.

Table 3. The Break-Even Point value of the payback period for the sample case studies.

Electricity price (USD kWh ⁻¹)	B.E.P. (year)
0.03	7.5
0.037 (Guaranteed electricity purchase price in Iran)	5.0
0.07	1.9
0.1	1.3

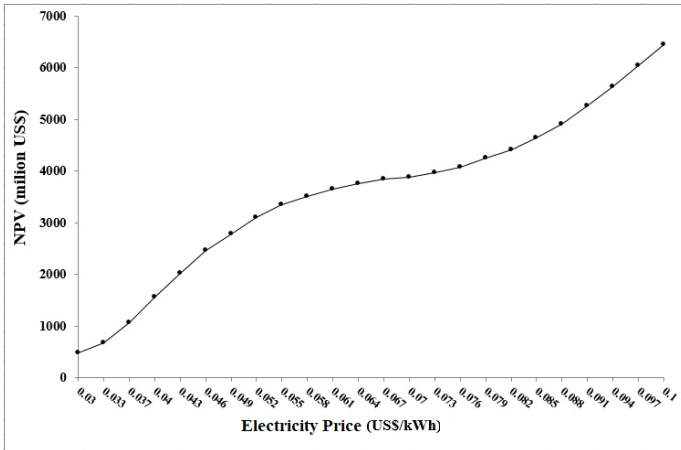


Figure 4. NPV changes for sample case studies based on different electricity sales prices.

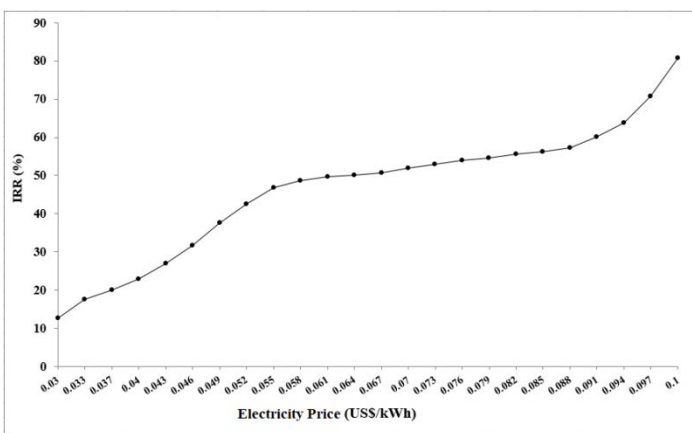


Figure 5. IRR changes for sample case studies based on different electricity sales prices.

Table 4 shows the values of the EPC estimated for the different units of the cogeneration system, as discussed in the previous sections. The purchased cost of the CHAT system for generating electricity, as shown in Table 4 and Figure 6, is substantially higher than the cost of other parts of the plant.

Table 4. The equipment purchase cost for the proposed combined heat and power system.

Equipment	Cost (USD)
Gas turbines and compressors	10,982,973.3
Steam turbine and condenser	839,761.11
Heat recovery steam generators	607,986.7
Gasifier	1,526,758.25
Heat exchangers	12,421.16
Other equipment	145,295.41
Total equipment purchased cost	14,115,195.9

The values of the required parts following TCI estimation are presented in Table 5. A significant increase in the proportion of direct costs versus indirect costs to calculate fixed investment costs indicates the importance of cost parameters in this section. Among the parameters affecting the estimation of direct costs, as can be predicted through the

relations presented in Table 5, the EPC has the highest amount.

The results of estimating variable costs and startup costs are also shown in Table 5. Based on the results of the present study, the production cost per unit of energy is approximately 909 USD kW⁻¹.

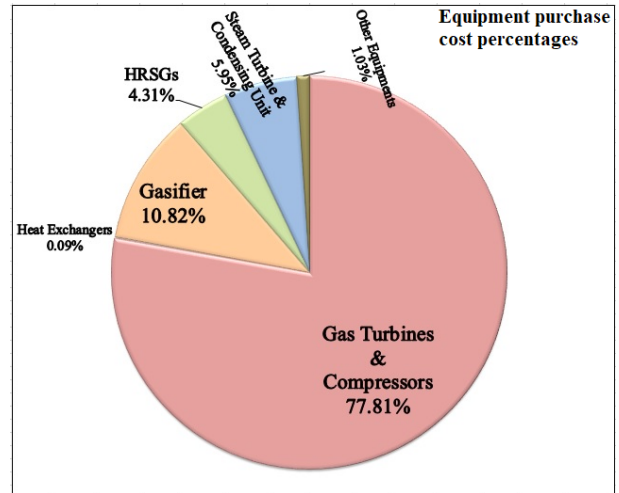


Figure 6. The proportion of equipment purchase cost of the proposed power generation system.

Table 5. TCI & TVC results for the proposed combined cycle.

Cost factor	Cost (USD)
Fixed capital investment	24,755,230
Direct costs	22,302,009
Equipment purchase costs	14,115,195
Installation cost for equipments	3,528,798
Total instrumentation and control cost	846,911
Piping cost	1,411,519
Electrical installation	141,151
Building including services	141,151
Yard improvements	141,151
Service facilities	1,411,519
Land	564,607
Indirect costs	2,453,221
Engineering and supervision	1,115,100
Construction expenses	892,080
Contractor's fee	446,040
Contingency	245,322
Working capital	2,475,523
Total capital investment	27,230,753
Manufacturing cost	1,263,837
Direct variable costs	840,383
Raw materials	-
Operating labor	84,691
Direct supervisory and clerical labor	8469

Utilities	169,382
Maintenance and repairs	495,104
Operating supplies	74,265
Laboratory charges	8469
Fixed charges	338,764
Depreciation	141,151
Local taxes	141,151
Insurance	56,460
General expenses	152,444
Administrative costs	33,876
Distribution and selling costs	33,876
Research and development costs	84,691
Financing	-
Total variable cost	2,426,012
Startup cost	30,000

The Levelized Cost of Electricity (LCOE) calculates by first taking the net present value of the total cost of building and operating the power generating asset. According to Equation 29, this value is divided by the total electricity generation over its lifetime [34].

$$\text{LCOE} = \frac{\text{NPV of Total Cost Over Lifetime}}{\text{NPV of Electrical Energy Produced Over Lifetime}} \quad (29)$$

Based on the above relation, the amount of LCOE is 0.66 USD kWh⁻¹.

$$\text{NCF} = (\text{Electricity Gross Payments} - \text{TVC} - \text{Fuel Cost}) \quad (30)$$

The notable points about the presented results are as follows:

1. Power plant operation is considered to take 365 days and 24 hours; therefore, no shutdown costs are incurred during repairs.
2. Costs such as patents, franchise costs, and depreciation costs for buildings have also been excluded from the calculation of total variable costs because of their insignificance values.

5. CONCLUSIONS

From the economic analysis carried out in the present study, the following conclusion can be considered as the most important achievements of this evaluation:

1. As can be observed from the results, the presented cycle at current prices intended for electricity sales in Europe and the United States has the best positive NPV and in Iran the acceptable positive value. Here are two things to consider: first, the price of electricity in several countries around the world is now above 0.1 USD kWh⁻¹ and, secondly, inevitable increase in energy consumption and consequently the price of electricity in the coming years is expected. Therefore, the presented cycle in terms of energy supply has favorable economic benefits, and hence its justification for industries with the amount of electricity consumed by the proposed cogeneration system is reasonable.

2. Based on the results presented in this study, at present, the proposed power-generation cycle may be more favorable in economic terms in other areas studied than in Iran. One of the important reasons could be a substantial increase in the purchase/sale price of electricity from renewable power plants in such countries, along with the stability of financial markets. Also, due to the low fuel price in Iran, if the guaranteed purchase price of renewable electricity or the sale of electricity with full implementation of the subsidy targeting law increases, the NPV and IRR values are higher than those in the other two case studies. On the other hand, with an increase in electricity sales price in Iran to only about 3 USC kWh⁻¹, the proposed system will reach NPV with high positive values. However, the Break-Even Point value based on the current guaranteed electricity purchase price in Iran is approximately 5 years.
3. The main reason for the higher cost of purchasing equipment in the proposed cycle than conventional power generation systems is the use of complicated equipment used in high-pressure and low-pressure turbines and compressors sets. The results indicated that investment cost to generate electricity per unit of energy was approximately 909 USD kW⁻¹ in the proposed power plant. Also, levelized cost of electricity was obtained 0.66 USD kWh⁻¹. However, in recent years, numerous efforts were made by manufacturers to reduce the cost of biomass gasifier implementation and set targets for reduction below half of the current value. Similarly, a list of estimated prices for other cycle equipment, steam turbine, and condenser assembly and the steam recovery generator are in the next category of expensive equipment, respectively, due to the presence of removable components or high heat-resistant components.

Based on the aforementioned results and sustainable energy targets, the integration of advanced power generation systems into highly efficient biomass gasifiers will be comparative in the future world energy market.

6. ACKNOWLEDGEMENT

We thank our colleagues who provided insight and expertise that greatly assisted the research.

REFERENCES

1. "International energy outlook 2019 with projections to 2050", U.S. Energy Information Administration, Office of Energy Analysis, U.S. Department of Energy, Washington, D.C., (2020).
2. Moghadasi, M., Ghadamian, H., Farzaneh, H., Moghadasi M. and Ozgoli, H.A., "CO₂ capture technical analysis for gas turbine flue gases with complementary cycle assistance including non linear mathematical modeling", *Procedia Environmental Sciences*, Vol. 17, (2013), 648-657. (DOI: 10.1016/j.proenv.2013.02.081).
3. Akia, M., Yazdani, F., Motae, E., Han, D. and Arandiyani, H., "A review on conversion of biomass to biofuel by nanocatalysts", *Biofuel Research Journal*, Vol. 1, (2014), 16-25. (DOI: 10.18331/BRJ2015.1.1.5).
4. Din, Z.U. and Zainal, Z.A., "Biomass integrated gasification-SOFC systems: Technology overview", *Renewable & Sustainable Energy Reviews*, Vol. 53, (2016), 1356-1376. (DOI: 10.1016/j.rser.2015.09.013).
5. Gottumukkala, L.D., Haigh, K., Collard, F.X., van Rensburg, E. and Görgens, J., "Opportunities and prospects of biorefinery-based

- valorisation of pulp and paper sludge", *Bioresource Technology*, Vol. 215, (2016), 37-49. (DOI: 10.1016/j.biortech.2016.04.015).
6. Saidur, R., Abdelaziz, E.A., Demirbas, A., Hossain, M.S. and Mekhilef, S., "A review on biomass as a fuel for boilers", *Renewable & Sustainable Energy Reviews*, Vol. 15, (2011), 2262-2289. (DOI: 10.1016/j.rser.2011.02.015).
 7. Bauen, A., Berndes, G., Junginger, M., Londo, M., Vuille, F., Ball, R., Bole, T., Chudziak, C., Faaij, A. and Mozaffarian, H., *Bioenergy: A sustainable and reliable energy source, A review of status and prospects*, IEA Bioenergy, USA, (2009).
 8. Razak, A.M.Y., *Industrial gas turbines performance and operability*, Woodhead Publishing Ltd., Oxford, UK, (2007).
 9. Ghadamian, H., Hamidi, A.A., Farzaneh, H. and Ozgoli, H.A., "Thermo-economic analysis of absorption air cooling system for pressurized solid oxide fuel cell/gas turbine cycle", *Journal of Renewable and Sustainable Energy*, Vol. 4, (2012) 1-14. (DOI: 10.1063/1.4742336).
 10. Hrbek, J., *Thermal gasification based hybrid systems*, IEA Bioenergy Task 33 special project, Vienna University of Technology, Austria, (2015).
 11. Bocci, E., Sisinni, M., Moneti, M., Vecchione, L., Di Carlo, A. and Villarini, M., "State of art of small biomass gasification power systems: A review of the different typologies", 68th Conference of the Italian Thermal Machines Engineering Association (ATI2013), *Energy Procedia*, Vol. 45, (2014), 247-256. (DOI: 10.1016/j.egypro.2014.01.027).
 12. Omar, A., Saghafifar, M. and Gadalla, M., "Thermo-economic analysis of air saturator integration in conventional combined power cycles", *Applied Thermal Engineering*, Vol. 107, (2016), 1104-1122. (DOI: 10.1016/j.applthermaleng.2016.06.181).
 13. Ghavami Gargari, S., Rahimi, M. and Ghaebi, H., "Energy, exergy, economic and environmental analysis and optimization of a novel biogas-based multigeneration system based on Gas Turbine-Modular Helium Reactor cycle", *Energy Conversion and Management*, Vol. 185, (2019), 816-835. (DOI: 10.1016/j.enconman.2019.02.029).
 14. Dibyendu, R., Samiran, S. and Sudip, G., "Techno-economic and environmental analyses of a biomass based system employing solid oxide fuel cell, externally fired gas turbine and organic Rankine cycle", *Journal of Cleaner Production*, Vol. 225, (2019), 36-57. (DOI: 10.1016/j.jclepro.2019.03.261).
 15. Li, J., Mohammadi, A. and Maleki, A., "Techno-economic analysis of new integrated system of humid air turbine, organic Rankine cycle, and parabolic trough collector", *Journal of Thermal Analysis and Calorimetry*, (2019). (DOI: 10.1007/s10973-019-08855-9).
 16. Basu, P., *Biomass gasification and pyrolysis: Practical design and theory*, Academic Press, (2010). (DOI: 10.1016/C2009-0-20099-7).
 17. Ruiz, J.A., Juárez, M.C., Morales, M.P., Muñoz, P. and Mendiivil, M.A., "Biomass gasification for electricity generation: Review of current technology barriers", *Renewable & Sustainable Energy Reviews*, Vol. 18, (2013), 174-183. (DOI: 10.1016/j.rser.2012.10.021).
 18. Parthasarathy, P. and Narayanan, K.S., "Hydrogen production from steam gasification of biomass: Influence of process parameters on hydrogen yield-a review", *Renewable Energy*, Vol. 66, (2014), 570-579. (DOI: 10.1016/j.renene.2013.12.025).
 19. Molino, A., Chianese, S. and Musmarra, D., "Biomass gasification technology: The state of the art overview", *Journal of Energy Chemistry*, Vol. 25, (2016), 10-25. (DOI: 10.1016/j.jechem.2015.11.005).
 20. Heidenreich, S. and Foscolo, P.U., "New concepts in biomass gasification", *Progress in Energy and Combustion Science*, Vol. 46, (2015), 72-95. (DOI: 10.1016/j.peccs.2014.06.002).
 21. Sikarwar, V.S., Zhao, M., Clough, P., Yao, J., Zhong, X., Memon, M.Z., Shah, N., Anthony, E. and Fennell, P., "An overview of advances in biomass gasification", *Energy & Environmental Science*, Vol. 9, (2016), 2939-2977. (DOI: 10.1039/C6EE00935B).
 22. Kirnbauer, F., Wilk, V., Kitzler, H., Kern, S. and Hofbauer, H., "The positive effects of bed material coating on tar reduction in a dual fluidized bed gasifier", *Fuel*, Vol. 95, (2012), 553-562. (DOI: 10.1016/j.fuel.2011.10.066).
 23. Gomez, E., Rani, D.A., Cheeseman, C.R., Deegan, D., Wise, M. and Boccaccini, A.R., "Thermal plasma technology for the treatment of wastes: A critical review", *Journal of Hazardous Materials*, Vol. 161, (2009), 614-626. (DOI: 10.1016/j.jhazmat.2008.04.017).
 24. Udomsirichakorn, J., Basu, P., Salam, P.A. and Acharya, B., "Effect of CaO on tar reforming to hydrogen-enriched gas with in-process CO₂ capture in a bubbling fluidized bed biomass steam gasifier", *International Journal of Hydrogen Energy*, Vol. 38, (2013), 14495-14504. (DOI: 10.1016/j.ijhydene.2013.09.055).
 25. Ozgoli, H.A., Moghadasi, M., Farhani, F. and Sadigh, M., "Modeling and simulation of an integrated gasification SOFC-CHAT cycle to improve power and efficiency", *Environmental Progress & Sustainable Energy*, Vol. 36, (2017), 610-618. (DOI: 10.1002/ep.12487).
 26. Hosseinpour, S., Mehdipour, R., Haji Seyed Mirzahosseini, A., Hemmasi, A.H. and Ozgoli, H.A., "Propose and analysis of an integrated biomass gasification-CHAT-ST cycle as an efficient green power plant", *Environmental Progress & Sustainable Energy*, Vol. 38, (2019), 13184. (DOI:10.1002/ep.13184).
 27. Goswami, D.Y., *The CRC handbook of mechanical engineering*, CRC Press, USA, (2004). (DOI: 10.1201/9781420041583).
 28. Nakhmkin, M., Swensen, E.C., Touchton, G., Cohn, A. and Polsky, M., "CHAT technology: An alternative approach to achieve advanced turbine systems efficiencies with present combustion turbine technology", *Proceedings of International Gas Turbine & Aeroengine Congress & Exhibition*, Orlando, USA, (1997). (DOI: 10.1115/98-GT-143).
 29. Wolk, R., Nakhmkin, M. and Goldstein, H.N., "Evaluation of cascaded humidified advanced turbine (CHAT) cycles for natural gas and syngas", *Proceedings of USDOE Turbine Power Systems Conference*, Galveston, TX., USA, (2002).
 30. Nakhmkin, M., Swensen, E., Wilson, L.M., Gaul, G. and Polsky, M., "The cascaded humidified advanced turbine (CHAT)", *Journal of Engineering for Gas Turbines and Power*, Vol. 118, (1996), 565-571. (DOI: 10.1115/1.2816685).
 31. Wolk, R. and Nakhmkin, M., "12 Megawatt cascaded humidified advanced turbine (CHAT) plant general overview", *Advanced Turbine Systems Annual Program Review Meeting*, US Department of Energy, Washington, D.C., USA, (1999).
 32. Ozgoli, H.A. and Ghadamian, H., "Energy price analysis of a biomass gasification-solid oxide fuel cell-gas turbine power plant", *Iranian Journal of Hydrogen & Fuel Cell*, Vol. 3, (2016), 45-58.
 33. Ozgoli, H.A., Ghadamian, H. and Pazouki, M., "Economic analysis of biomass gasification-solid oxide fuel cell-gas turbine hybrid cycle", *International Journal of Renewable Energy Research (IJRER)*, Vol. 7, (2017), 1007-1018.
 34. Ulrich, K.T., *Product design and development*, McGraw-Hill, USA, (2000).
 35. Garrett, D.E., *Chemical engineering economics*, Springer Netherlands, (1989). (DOI: 10.1007/978-94-011-6544-0).
 36. Seider, W.D., Lewin, D.R., Seader, J.D., Widagdo, S., Gani, R. and Ming Ng, K., *Product and process design principles: Synthesis, analysis, and evaluation*, Wiley, USA, (2016).
 37. Arsalis, A., "Thermoeconomic modeling and parametric study of hybrid SOFC-gas turbine-steam turbine power plants ranging from 1.5 to 10MWe", *Journal of Power Sources*, Vol. 181, (2007), 313-326. (DOI: 10.1016/j.jpowsour.2007.11.104).
 38. Boehm, R.F., *Design analysis of thermal systems*, Wiley, USA, (1987).
 39. Caputo, A.C., Palumbo, M., Pelagagge, P.M. and Scacchia, F., "Economics of biomass energy utilization in combustion and gasification plants: Effects of logistic variables", *Biomass and Bioenergy*, Vol. 28, (2005), 35-51. (DOI: 10.1016/j.biombioe.2004.04.009).
 40. Toonssen, R., "Sustainable power from biomass: Comparison of technologies for centralized or de-centralized fuel cell systems", Ph. D. Thesis, Delft University of Technology, Netherlands; (2010).



A Novel Local Control Technique for Converter-Based Renewable Energy Resources in the Stand-Alone DC Micro-Grids

Arash Abedi, Behrooz Rezaie*, Alireza Khosravi, Majid Shahabi

Department of Control, Faculty of Electrical and Computer Engineering, Babol Noshirvani University of Technology, Babol, Iran.

PAPER INFO

Paper history:

Received 12 February 2020

Accepted in revised form 12 May 2020

Keywords:

DC/DC Converter
Stability Analysis
Stand-Alone DC Micro-Grid
Switching Function

ABSTRACT

This paper presents a novel local control method for the converter-based renewable energy resources in a stand-alone DC micro-grid based on energy analysis. The studied DC micro-grid comprises the renewable energy resources, back-up generation unit, and battery-based energy storage system, which are connected to the common DC-bus through the buck and bidirectional buck-boost converters. The proposed control method satisfies the stability of the micro-grid output variables, along with current control and voltage regulation by controlling the switching functions of the converters, regardless of the energy resource dynamics. The dynamic component of the switching function is extracted as a control signal using the state-feedback through a mathematical method. The control inputs are designed based on Lyapunov stability theorem to guarantee the stability of output variables (DC-bus voltage and generated currents) in a stand-alone DC micro-grid through an energy analysis. The proposed distributed controller can be easily generalized as a platform with all kinds of the stand-alone DC micro-grids comprising any type or number of distributed generations such as renewable energy resources, fossil-fuel-based generations, and energy storage units. Other features of this local control method are simplicity, celerity, comprehensiveness, and independence of the distributed generations. The dynamic performance assessment of the proposed controller is verified through a simulation in MATLAB/SIMULINK® environment. The results validate the accuracy and stability of the proposed control strategy in various operating conditions.

1. INTRODUCTION

Recently the global efforts to reduce the use of fossil fuels, growing energy demand, increased number of renewable energy resources (RERs) [1] and more important advancements in power electronics have led to the modernization of the existing power system [2]. Introduction of AC and DC micro-grids including distributed generations (DGs) such as RERs, energy storage systems (ESS), gas-micro-turbine generators, etc. made it possible for engineers to reshape the conventional power system [3].

The micro-grids are emerging in the modern power system and becoming an attractive choice due to the integration of DGs such as photovoltaics, wind-turbines, storage devices, and controllable loads, which can operate in either isolated or grid-connected mode. However, the issue of reliability and stability has not been accomplished yet within these small-scale distribution grids [4]. In a grid-connected AC micro-grid, the main grid standards for frequency and voltage are utilized, and energy stability is important for power quality [5]. However, in the stand-alone operation mode, the frequency and the voltage must be stabilized and regulated via a control system [6-8].

In a stand-alone micro-grid supplying a residential area, most of the consumptions are DC loads, such as electronic, telecommunication and audio-visual devices. Moreover, the other loads can be supplied either by AC or DC such as air-conditioning or lighting devices [9]. In fact, distributing energy in DC form is in favor of distribution suppliers due to

the reduced number of converters, limited frequency control challenges, higher efficiency, and minimized costs. Thus, DC micro-grids is a proper choice for providing remote residential areas. Still, in such networks, the voltage regulation, voltage stabilization, and energy management are vital to improve the power quality and provide a reliable and efficient power [10, 11]. Therefore, proposing comprehensive methods for controlling and stability of the stand-alone DC micro-grids is of great importance.

Some studies in the literature have been devoted to the DC voltage control strategies and energy management control systems. In [12], the authors employed a three-level control strategy to stabilize the DC-bus voltage in various operation conditions (i.e. load change, generation fluctuations) in a DC micro-grid with variable sources and loads. In this study, a control program based on PI and droop controllers has been presented. However, the stability has not been guaranteed. Augustine et al. [13] developed an adaptive droop control technique to manage the current sharing and voltage regulation in a low voltage DC micro-grid. There are three points to note about this reference. First, in this study, the researchers have not addressed the issues of micro-grid stability. Besides, only two DGs with the same type of converter have been studied. Finally, the authors have neglected the role of energy storage units which is vital in the stand-alone micro-grids with RERs, because the challenges of bidirectional power flow are crucial in energy analysis and stability studies. Dizqah et al. [14] proposed a control strategy based on model predictive control (MPC) to manage the voltage stability and energy flow between wind, solar and battery devices, as well as battery management in a DC micro-grid. Anand et al. [15] presented a decentralized droop

*Corresponding Author's Email: brezaie@nit.ac.ir (B. Rezaie)

controller by applying a low bandwidth communication to the conventional droop controllers, to improve voltage regulation in an isolated DC micro-grid. However, the dynamic behavior of controllers via a detailed model of the converter has not been considered in [14,15], while, in stand-alone micro-grids, the dynamic behavior of the converters considerably influences the voltage quality in small-signal and should be considered in the controller's design [16].

In [17] a droop control strategy has been proposed for voltage regulation in an islanded DC micro-grid based on energy stability analysis. However, the DGs in the DC micro-grid modeled simply as the ideal constant DC voltage sources equalized with transmission impedance. This simplification is presumed for nonlinear stability analysis and prediction of the qualitative behavior of the system as a function of model parameters. Moreover, the dynamic characteristics of the converters have been neglected in the model. Herrera et al. [18] considered the loads in the DC micro-grid as constant power loads due to high switching frequency, while the local stability analysis and controller design presented using the Lyapunov function. Liu et al. [19] represented small-signal modeling of an islanded DC micro-grid including a synchronous generator as the generation source of the micro-grid and an induction motor as the micro-grid load. In their developed model, the dynamic effects of the constant power load, and the filter design parameters on system stability, have been evaluated. However, the current and voltage control in the micro-grid have been performed exclusively via a synchronous generator connected to a rectifier, and the dynamic role of the power converters has been neglected.

In [20], a kind of linear mathematical modeling represented for state-space of all the converters in a DC micro-grid considering the currents, voltages and droop controllers, likewise, the dynamic stability analysis of the system and controllers has been performed. Furthermore, modeling the buck converters in [20] performed using the average model, where the duty-cycle of the converters was adjusted using the simple conventional PI controllers.

In [21] the authors employed the Lyapunov theorem for stabilization and optimized operation assessment in a stand-alone DC micro-grid using a nonlinear model, where the resources are battery storage devices. In this study, the two battery branches represent a fast charging branch and a slower charging one. The duty-cycles of the converters connected to the batteries have been controlled via a constant gain PI controller through a droop control method. Furthermore, a reduced-order model for DC/DC converters has been used that their performance differs from that of real samples and this issue affects the stability analysis. Although in [20,21], the researchers have considered stability, the PI controller as a linear operator could not provide acceptable accuracy in the range of the actual non-linear performance [22].

The topics related to stand-alone DC micro-grids have been the focus of research just in the last decade [23]. Hence, a lot of issues have remained intact or rarely focused on the simultaneous study on local control and stability analysis about the precise concept "stand-alone DC micro-grids". For instance, some studies have been privatized on specified energy resources models and the proposed control approaches have not been presented comprehensively for all kinds of resources [13,19,24]. Some studies have proposed model-independent approaches, but they have tested their proposed method on the resources with inherently stable dynamics such as constant DC supply, battery, or PV and the validity of these

methods has not considered for rotational electro-mechanical dynamics such as wind turbines, gas-micro-turbines and the like [17,21,25]. A lot of researches has simplified the modeling of micro-grids or converters or have used linear controllers to control a nonlinear system. These issues challenge the effectiveness of these methods in terms of actual performance, faced with nonlinearities, uncertainties, and disturbances [12,15,17,19-21]. In centralized control schemes, the control structure is reconstructed and updated to plug in additional resources. Moreover, the error in the central controller causes all units to malfunction. Besides, there is a pressing need for information and communication technologies [26,27]. Even in some distributed control schemes, despite the plug-and-play capability, there is complex bidirectional communication between the local controllers [28]. These issues increase the costs of establishing, maintaining, and reduce micro-grid reliability.

On the other hand, the converter is one of the controllable devices [23] that could potentially control and stabilize the output variables of the micro-grid as a general local platform regardless of the resource dynamics. In this case, the switching function of the converter could be considered as a non-physical control command. In addition to the challenges discussed above, in [29-32] and all the above-mentioned references, the effects of switching functions have not been examined on the dynamic behavior of converters.

In order to cover a significant portion of the recent challenges, the main objectives of our research are: (1) designing a generalized distributed local controller for RERs and any type of converter-based resources in stand-alone DC micro-grids; and (2) stabilizing the output voltage and currents of the stand-alone DC micro-grid through simply controlling the switching function of the converters regardless of resource dynamics.

The hypothesis of our study is so comprehensive that it covers various kinds of stand-alone DC micro-grids as follows:

- The stand-alone DC micro-grid consists of n resources.
- A battery unit represents all the ESSs in the micro-grid.
- The resources and the loads are connected to the common DC bus.
- All resources are connected to the bus via full-order DC/DC converters. (buck converter for DGs and bidirectional buck-boost converter for battery unit).

This paper represents a novel control strategy based on the direct Lyapunov method (DLM) to perform current and DC-bus voltage regulation considering the switching function control. In fact, the DC-bus voltage regulation is implemented via decreasing the effects of the energy oscillations. This approach determined a detailed and full-order dynamic model for the steady-state and dynamic operation of the converters connected to the DGs and the battery energy storage system (BESS). In fact, the proposed controller performs the voltage stabilizing by reducing the volatility of the generated currents. This is done by controlling the switching functions of the DC/DC converters. In this control plan, the steady-state and dynamic parts of the switching functions were calculated separately through a mathematical definition for variables errors. Then, the dynamic component of the switching function is computed using DLM in such a way the errors of the state-variables which are due to the system fluctuations are always damped. This simple and agile dynamic calculation acts as a closed-loop stabilizer-regulator controller.

The prominent features of this approach are its rapid and simple execution, fast transient-state response, low range dynamic oscillation, and its ability to generalize with all the stand-alone micro-grids comprising any type or number of RERs, ESSs, and the other DGs. Moreover, as can be seen in Figure 1, the controllers of the converters connected to the DGs are independent of each other and the only communication is conducted into the controller of the converter connected to the BESS. This feature facilitates the installation of new DGs in development plans.

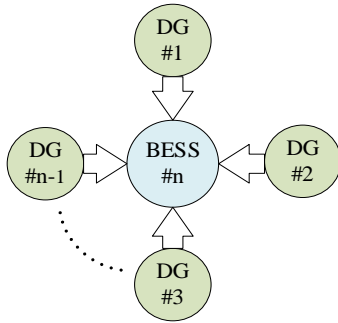


Figure 1. The communication topology of the proposed local controllers.

In summary, the main novelties and contributions of this work are as follows:

- The dynamic component of the switching function of the converters is extracted, regardless of resource dynamics, using the state-feedback through a mathematical method.
- This switching function is utilized as the control signal to stabilize the output voltage and currents of the stand-alone DC micro-grid.
- A generalized distributed local controller is proposed by presenting and proving a novel comprehensive stability theorem.
- This novel controller is applicable to all kinds and any number of converter-based energy resources in a stand-alone DC micro-grid.

The rest of this paper is organized as follows: In section 2, the precise model of the system is introduced. The methodological approach is explained through the steady-state analysis in section 3 and in section 4 through the energy analysis of the system by applying the DLM, the proper controller architecture is represented. Section 5 is devoted to the simulation of a stand-alone DC micro-grid consists of three DGs and a BESS controlled by the proposed controller, and evaluating two scenarios based on this system and the simulation results using MATLAB/SIMULINK[®] are discussed. The conclusion is drawn in the last section.

2. MULTI-SOURCE DC MICRO-GRID STRUCTURE

The general scheme of the proposed stand-alone DC micro-grid has been shown in Figure 2. This structure consists of n units, supplying the load so that, $n-1$ units are the DG units such as RERs or other energy resources connected to the BCs, and one unit is the BESS consists of a lithium-battery connected to a BBC. However, the proposed local control method is independent of the resource model. The BESS unit is employed to provide a constant DC-bus voltage with acceptable precision and agility for the stand-alone DC micro-grid in the steady-state operation or under dynamic changes

due to the load change. In this section, the detailed dynamic model of the converters is described.

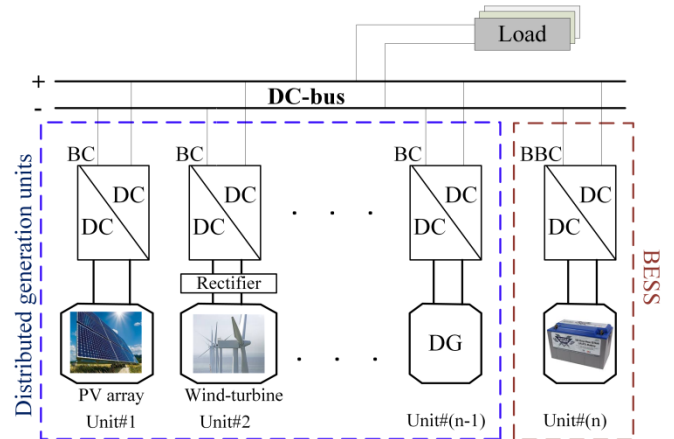


Figure 2. A typical stand-alone DC micro-grid configuration.

Considering the high initial cost of battery purchase, as well as the limited lifetime of the batteries with finite charging/discharging cycles, the BESS unit in this system is controlled only to regulate the DC-bus voltage, rather than supplying as an alternative resource. The controllers designed in this paper as the main contribution of this work are as follows:

- The controllers for the BCs connected to the DGs, to regulate the needed currents.
- A controller for the BBC connected to the BESS unit to regulate the desired DC voltage.

2.1. Buck DC/DC converters

As shown in Figure 3, the basic function of the BC is the current of an inductor controlled by switches. Therefore, the output current of the converter can be controlled by controlling the switching function. The switch (usually can be a power transistor) and diode have zero voltage drop and zero current in OFF and ON mode respectively. Input and output capacitors are considered respectively for smoothing the input and output currents of the BC. Since the injected power from the DGs to the DC micro-grid is accomplished by the BCs, a complete dynamic description of these converters is required. As shown in Figure 3, the dynamical scheme of a typical BC can be modeled as:

$$\begin{cases} \frac{dv_{ij}}{dt} = \frac{i_{ij}}{C_{ij}} - \frac{i_{Lj}u_j}{C_{ij}} \\ \frac{di_{Lj}}{dt} = \frac{v_{ij}u_j}{L_j} - \frac{v_{bus}}{L_j} \\ \frac{dv_{bus}}{dt} = \frac{i_{Lj}}{C_{oj}} - \frac{i_{oj}}{C_{oj}} \end{cases}, \quad j = 1, 2, 3 \quad (1)$$

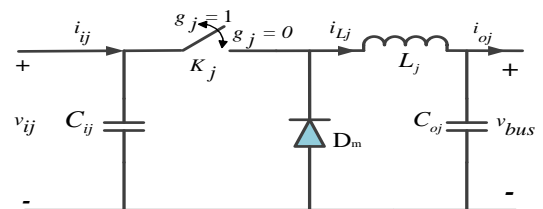


Figure 3. The detailed structure of a typical BC.

where C_{ij} , C_{oj} , L_j are respectively the input capacitor, output capacitor and the inductance of the BC, u_j , g_j , v_{ij} and i_{ij} are respectively the switching function, switching signal, input voltage and the input current of the BC. Moreover, i_{Lj} is the inductance current, v_{bus} the output voltage equals to the DC-bus voltage, and i_{oj} the output current of the BC that represents the contribution of each DG in the stand-alone DC micro-grid. In Equation (1), j represents the number of each of the DGs. K_j , represents an electrical switch that can be any kind of the typical controllable electrical switches. The switching signals (g_j) are generated by applying the switching function (u_j) to the Pulse Width Modulation (PWM), in the manner as shown in Figure 4. Finally, as shown in Figure 3, the signals g_j indicate the switches K_j be ON or OFF [33].

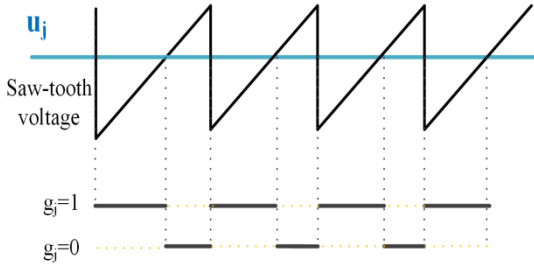


Figure 4. Switching signal generating by PWM.

2.2. Buck-boost DC/DC converter

The bidirectional BBC is the best choice for the operation of charging and discharging in a BESS unit. In Figure 5, a typical bidirectional BBC has been designed, and Equation (2) defines the function of the BBC in terms of the switching condition:

$$\begin{cases} \frac{di_{L_n}}{dt} = \frac{v_{in}}{L_n} - \frac{u_n v_{bus}}{L_n} \\ \frac{dv_{bus}}{dt} = \frac{u_n i_{L_n}}{C_{on}} - \frac{i_{on}}{C_{on}} \end{cases} \quad (2)$$

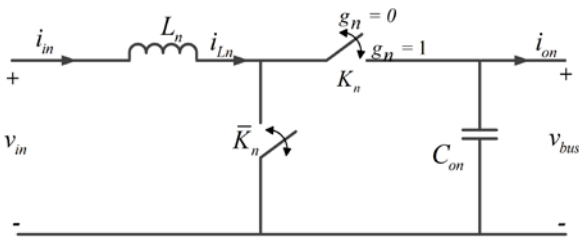


Figure 5. The detailed structure of a typical BBC.

where C_{on} , L_n , g_n and u_n are respectively the output capacitor, inductance, switching signal and the switching function of the BBC. Moreover, $i_{L_n} = i_{in}$ and v_{in} is respectively the input current and input voltage of the BBC, v_{bus} and i_{on} represents the output current of the BBC and the DC-bus voltage. In fact, the current i_{on} represents the contribution of the BESS in the DC micro-grid. During the

discharge mode, \bar{K}_n is open and the switching operation is performed on K_n . On the contrary, during the recharge mode, K_n is closed and the switching operation is performed on \bar{K}_n , also in this case, $(\bar{u}_n = 1 - u_n)$ replaced by u_n in the Equation (2). The dynamic Equation (1) and (2) are used for the aim of regulating the current and voltage of the DC-bus in the stand-alone DC micro-grid.

The overall scheme in this study concentrates on the dynamic part of the DC/DC converters. All fluctuations and disturbances caused by the mechanical and electrical parts of various kinds of the DGs will ultimately affect the input voltages and currents of the converters, and these effects have been examined in this study. However, the proposed design in this paper can be expanded to an implemental scheme, since different secondary controllers can be employed to control and manage various energy resources in the stand-alone DC micro-grids.

3. STEADY-STATE ANALYSIS

To control the DC-bus voltage in the steady-state operation, the switching functions of all BCs and BBC in the Equation (1) and (2) should be achieved by substituting the desired values of all state variables, marked by $*$ superscripts. According to Figure 3, considering the switching functions as a control signal, and through solving the Equation (1) and (2), the averaged switching functions u_j^* are obtained as follows:

$$u_j^* = \frac{i_{ij}^* - C_{ij} \dot{v}_{ij}^*}{2i_{Lj}^*} + \frac{L_j i_{Lj}^* + v_{bus}^*}{2v_{ij}^*}, \quad j = 1, 2, 3, \dots, (n-1) \quad (3)$$

$$u_n^* = \frac{v_{in}^* - L_n i_{L_n}^*}{2v_{bus}^*} + \frac{C_{on} \dot{v}_{bus}^* + i_{on}^*}{2i_{L_n}^*} \quad (4)$$

As can be seen, all the state variables are considered to achieve the averaged switching functions. Obviously, in this study to achieve the voltage stability and current regulation, the values of desired voltages and currents $v_{ij}^*, i_{Lj}^*, i_{L_n}^*, v_{bus}^*, i_{ij}^*$ are constant. Therefore, the steady-state references $\dot{v}_{ij}^*, i_{Lj}^*, i_{L_n}^*, v_{bus}^*$ are zero. Hence, according to Figure 3, where \dot{v}_{bus}^* is considered zero, the desired value of i_{Lj}^* represents i_{oj}^* . Consequently, the simplified results of the Equation (3) and (4) are respectively equal to $\frac{i_{ij}^*}{2i_{Lj}^*} + \frac{v_{bus}^*}{2v_{ij}^*}$ and $\frac{v_{in}^*}{2v_{bus}^*} + \frac{i_{on}^*}{2i_{L_n}^*}$. These

desired reference values are used for calculating the deviations of the variables from their desired steady-state values. For this purpose, v_{ij}^* and v_{bus}^* are respectively considered equal to the nominal voltages of the DGs, and the nominal voltage of the DC-bus. The output currents i_{oj}^* and i_{on}^* are issued by the outer layer controllers based on different methods of energy management and power-sharing in the micro-grids. Consequently, the input currents i_{ij}^* and $i_{L_n}^*$ can be calculated based on the equality of input/output power of the converters. To stabilize the DC-bus voltage, in this scheme, i_{on}^* is determined based on the difference between the generated and needed currents. Further details are provided in section 4.2.2.

4. ENERGY ANALYSIS AND DLM-BASED CONTROLLER DESIGN

The DLM analysis has been used to stabilize all the state variables in the proposed DC micro-grid, to reach their equilibrium points in a way that the micro-grid has a stable operation in steady and transient states. This method is based on the energy analysis of the state variables of the system [34].

4.1. Energy equations

First, the vectors of the state variables and their desired values are respectively defined as (5), (6):

$$\mathbf{X} = [\mathbf{v}_i \quad \mathbf{i}_L \quad i_{Ln} \quad v_{bus}]^T \quad (5)$$

$$\mathbf{X}^* = [\mathbf{v}_i^* \quad \mathbf{i}_L^* \quad i_{Ln}^* \quad v_{bus}^*]^T \quad (6)$$

where \mathbf{X} and \mathbf{X}^* represent the vectors of the state variables of all converters and their desired values, $(\mathbf{v}_i, \mathbf{i}_L)$, $(\mathbf{v}_i^*, \mathbf{i}_L^*)$ are respectively the vectors of the state variables of the BCs and their desired values, as described below:

$$\mathbf{v}_i = [v_{i1} \quad v_{i2} \quad \dots \quad v_{i(n-1)}] \quad (7)$$

$$\mathbf{v}_i^* = [v_{i1}^* \quad v_{i2}^* \quad \dots \quad v_{i(n-1)}^*] \quad (8)$$

$$\mathbf{i}_L = [i_{L1} \quad i_{L2} \quad \dots \quad i_{L(n-1)}] \quad (9)$$

$$\mathbf{i}_L^* = [i_{L1}^* \quad i_{L2}^* \quad \dots \quad i_{L(n-1)}^*] \quad (10)$$

So, the vector of the state variables errors can be written as:

$$\mathbf{E} = \mathbf{X} - \mathbf{X}^* = [\mathbf{e}_{v_i} \quad \mathbf{e}_{i_L} \quad e_{i_{Ln}} \quad e_{v_{bus}}]^T \quad (11)$$

where $\mathbf{e}_{v_i} = \mathbf{v}_i - \mathbf{v}_i^*$, $\mathbf{e}_{i_L} = \mathbf{i}_L - \mathbf{i}_L^*$, $e_{i_{Ln}} = i_{Ln} - i_{Ln}^*$, $e_{v_{bus}} = v_{bus} - v_{bus}^*$. In this way, the exact energy equation related to the errors of the state variables can be considered as the Lyapunov function, so that:

$$W_e(x) = \frac{1}{2} \text{tr}[\text{diag}(\mathbf{B}) \cdot \text{diag}(\mathbf{E})^2] \quad (12)$$

where, based on (1) and (2), and assuming the output filter capacitors $C_{o1} = C_{o2} = C_{o3} = \dots = C_{on} = C_o$, the vector \mathbf{B} and its arrays in (12) are extracted as follows:

$$\mathbf{B} = [\mathbf{C}_i \quad \mathbf{L} \quad L_n \quad nC_o]^T \quad (13)$$

$$\mathbf{C}_i = [C_{i1} \quad C_{i2} \quad \dots \quad C_{i(n-1)}] \quad (14)$$

$$\mathbf{L} = [L_1 \quad L_2 \quad \dots \quad L_{(n-1)}] \quad (15)$$

Subsequently, the derivative of the energy equation (12) is calculated as (16):

$$\dot{W}_e(x) = \text{tr}[\text{diag}(\mathbf{B}) \cdot \text{diag}(\mathbf{E}) \cdot \text{diag}(\dot{\mathbf{E}})] \quad (16)$$

By applying (11) and (13)-(15) to Equation (16) and after sorting out, all terms of (16) can be achieved as:

$$\dot{W}_e(x) = \sum_{j=1}^{n-1} C_{ij} e_{v_{ij}} \dot{e}_{v_{ij}} + \sum_{j=1}^{n-1} L_j e_{i_{Lj}} \dot{e}_{i_{Lj}} + \quad (17)$$

$$L_n e_{i_{Ln}} \dot{e}_{i_{Ln}} + nC_o e_{v_{bus}} \dot{e}_{v_{bus}}$$

In (17), the first two terms refer to the DG units, which are connected to the BCs, and the other terms refer to the BESS unit connected through BBC.

4.2. DLM-based controller and stability analysis

To design a proper controller to regulate the generated currents of the DG units, and with the aim of stabilizing the DC-bus voltage through regulating the current of the BESS unit, the switching functions of the BCs and BBC are separated into two components u_j^* and U_j , such that:

$$u_j = u_j^* - U_j \quad , \quad j = 1, 2, \dots, n \quad (18)$$

These components are respectively considered as the steady-state components and the dynamic components of the control signals. The steady-state components are the same as the averaged switching functions, have been defined previously in (3) and (4). In fact, U_j represents the dynamic effects of the state variables errors in each converter. Finally, the proper control signal is obtained by subtracting u_j^* and U_j . By applying (18) and (11) into (1) and (2), all terms of (17) can be rewritten as follows:

$$\sum_{j=1}^{n-1} C_{ij} e_{v_{ij}} \dot{e}_{v_{ij}} = \sum_{j=1}^{n-1} \underbrace{(i_{ij} - i_{ij}^*)}_{E_{ij}} e_{v_{ij}} - \sum_{j=1}^{n-1} \underbrace{u_j e_{i_{Lj}}}_{**} e_{v_{ij}} + \sum_{j=1}^{n-1} U_j i_{Lj}^* e_{v_{ij}} \quad (19)$$

$$\sum_{j=1}^{n-1} L_j e_{i_{Lj}} \dot{e}_{i_{Lj}} = \sum_{j=1}^{n-1} \underbrace{u_j e_{i_{Lj}}}_{*} e_{v_{ij}} - \sum_{j=1}^{n-1} U_j v_{ij}^* e_{i_{Lj}} - e_{v_{bus}} \sum_{j=1}^{n-1} \underbrace{e_{i_{Lj}}}_{**} \quad (20)$$

$$nC_o e_{v_{bus}} \dot{e}_{v_{bus}} = \underbrace{e_{v_{bus}} u_n}_{***} e_{i_{Ln}} - e_{v_{bus}} U_n i_{Ln}^* - \quad (21)$$

$$e_{v_{bus}} \sum_{j=1}^n \underbrace{(i_{oj} - i_{oj}^*)}_{E_{i_{Load}}} + e_{v_{bus}} \sum_{j=1}^{n-1} \underbrace{e_{i_{Lj}}}_{**}$$

$$L_n e_{i_{Ln}} \dot{e}_{i_{Ln}} = \underbrace{(v_{in} - v_{in}^*)}_{E_{v_{in}}} e_{i_{Ln}} - \underbrace{e_{v_{bus}} u_n}_{***} e_{i_{Ln}} + v_{bus}^* U_n e_{i_{Ln}} \quad (22)$$

where E_{ij} and $E_{v_{in}}$ are respectively the errors of the input currents of the BCs, and the error of the input voltage of the BBC connected to the BESS. Since, $i_{Load} = \sum_{j=1}^n i_{oj}$ and $i_{Load}^* = \sum_{j=1}^n i_{oj}^*$, therefore, $E_{i_{Load}}$ is the difference between the sum of the generated currents and their desired values, that it is equal to the difference between the injected currents and total load demand $(i_{Load} - i_{Load}^*)$. As can be seen, in the Equations (19)-(22), each pair of the terms identified by ‘*’, ‘**’ and ‘***’, are respectively symmetric, so the final simplified equation by replacing (19)-(22) into (17), can be rewritten as:

$$\dot{W}_e(x) = \sum_{j=1}^{n-1} e_{v_{ij}} E_{i_{ij}} + \sum_{j=1}^{n-1} U_j (i_{Lj}^* e_{v_{ij}} - v_{ij}^* e_{i_{Lj}}) + \quad (23)$$

$$U_n (v_{bus}^* e_{i_{Ln}} - i_{Ln}^* e_{v_{bus}}) + E_{v_{in}} e_{i_{Ln}} - e_{v_{bus}} E_{i_{Load}}$$

According to DLM, to reach the global asymptotical stability, if the total system energy is positive, therefore its derivative must be definitely negative [34]. On this basis, to calculate the dynamic part of the switching functions as a component of the control signal, we can state the following theorem:

Theorem 1. In a DC micro-grid with the energy equation of the state variables errors defined by (12), and the derivative of the energy equation defined by (23), there are $(U_{j,j=1,2,\dots,n})$ equal to (24) and (25) making the system globally asymptotically stable according to the Lyapunov definition, such that:

$$U_j = \frac{\alpha_j (i_{Lj}^* e_{v_{ij}} - v_{ij}^* e_{i_{Lj}})^2 - e_{v_{ij}} E_{i_{ij}}}{i_{Lj}^* e_{v_{ij}} - v_{ij}^* e_{i_{Lj}}}, \forall \alpha_j < 0, j=1,2,\dots,(n-1) \quad (24)$$

$$U_n = \frac{\alpha_n (v_{bus}^* e_{i_{Ln}} - i_{Ln}^* e_{v_{bus}})^2 + e_{v_{bus}} E_{i_{Load}} - E_{v_{in}} e_{i_{Ln}}}{v_{bus}^* e_{i_{Ln}} - i_{Ln}^* e_{v_{bus}}}, \forall \alpha_n < 0 \quad (25)$$

Proof. At first, we consider the Lyapunov stability conditions [34]:

$$\begin{cases} W_e(0) = 0 \\ W_e(x) > 0, & \forall x \neq 0 \\ W_e(x) \rightarrow \infty, & \text{as } \|x\| \rightarrow \infty \\ \dot{W}_e(x) < 0, & \forall x \neq 0 \end{cases} \quad (26)$$

According to (12), it is obvious that $W(0) = 0$, $W(x) > 0$ for all $x \neq 0$ and $W(x) \rightarrow \infty$ as $\|x\| \rightarrow \infty$. To establish all constraints of the Lyapunov stability theory, we assume that (23) is negative. A rigorous approach is that the energy equation of each unit is negative. This procedure helps to prove the stability of the micro-grid in the various situation of mono-source to multi-source generation, even regardless of the participation of the BESS unit. As a result, the distributed performance of the controllers is also guaranteed. In this approach, (23) can be divided into two general parts. One part contains the first two terms, referring to the DG units connected to the BCs, and the other part contains remained terms, referring to the BESS unit connected to the BBC, supposing both terms are negative. As described above, we have:

$$e_{v_{ij}} E_{i_{ij}} + U_j (i_{Lj}^* e_{v_{ij}} - v_{ij}^* e_{i_{Lj}}) < 0 \quad (27)$$

After replacing (24) into (27):

$$e_{v_{ij}} E_{i_{ij}} + \left(\frac{\alpha_j (i_{Lj}^* e_{v_{ij}} - v_{ij}^* e_{i_{Lj}})^2 - e_{v_{ij}} E_{i_{ij}}}{i_{Lj}^* e_{v_{ij}} - v_{ij}^* e_{i_{Lj}}} \right) (i_{Lj}^* e_{v_{ij}} - v_{ij}^* e_{i_{Lj}}) < 0 \quad (28)$$

$$\Rightarrow \alpha_j (i_{Lj}^* e_{v_{ij}} - v_{ij}^* e_{i_{Lj}})^2 < 0 \Rightarrow \alpha_j < 0 \quad (29)$$

Therefore, it is concluded that Equation (29) is always true for $\alpha_j < 0$. Similarly, for the other parts of (23), we assume:

$$U_n (v_{bus}^* e_{i_{Ln}} - i_{Ln}^* e_{v_{bus}}) + E_{v_{in}} e_{i_{Ln}} - e_{v_{bus}} E_{i_{Load}} < 0 \quad (30)$$

After replacing (25) into (30):

$$\left(\frac{\alpha_n (v_{bus}^* e_{i_{Ln}} - i_{Ln}^* e_{v_{bus}})^2 + e_{v_{bus}} E_{i_{Load}} - E_{v_{in}} e_{i_{Ln}}}{v_{bus}^* e_{i_{Ln}} - i_{Ln}^* e_{v_{bus}}} \right) \times \quad (31)$$

$$(v_{bus}^* e_{i_{Ln}} - i_{Ln}^* e_{v_{bus}}) + E_{v_{in}} e_{i_{Ln}} - e_{v_{bus}} E_{i_{Load}} < 0 \\ \Rightarrow \alpha_n (v_{bus}^* e_{i_{Ln}} - i_{Ln}^* e_{v_{bus}})^2 < 0 \Rightarrow \alpha_n < 0 \quad (32)$$

It is concluded that (32) is always true for $\alpha_n < 0$.

Consequently, by applying (24) and (25), the derivative of the energy equation of the system will always be negative, therefore all conditions of the Lyapunov stability theory are satisfied, and the system is globally asymptotically stable according to the Lyapunov definition, so the theorem is proved.

After clearing the effects of the dynamic errors of the state variables from the average switching function u_j^* , the revised switching functions $u_j = u_j^* - U_j$ are applied to the PWM signal generator as a control command and consequently, the switching signals g_j are generated and applied to the converters.

4.2.1. Current regulating

As we can see in Equation (24), all errors of the state variables, input variables, and their desired values are involved in (24) that affect the output currents of the DGs. According to this equation, it is obvious that choosing the proper Lyapunov function leads to the accuracy and agility of the controller in eliminating the deviations. The signals $U_{j,j=1,2,\dots,(n-1)}$ are the dynamic components of the BC switching functions and related to the deviations of the variables on output currents. The current control design is based on Equations (3), (18), and (24). According to Theorem 1, calculating $U_{j,j=1,2,\dots,(n-1)}$ through Equation (24) will lead to system stability. Therefore, the controller calculates $U_{j,j=1,2,\dots,(n-1)}$ at each step based on the state-feedback according to Figure 6. Since the switching function is placed in the energy equations equal to (18), by subtracting U_j from u_j^* , the modified switching functions are obtained dynamically and applied to the converter. The alpha presence of all the variables affecting the output currents in the equation. As a result, this increases the coefficients weigh the effects of the errors. Although for any negative values of α_j , the stability of the output currents and damping the oscillation are guaranteed, but the proper adjustment of α_j will reduce the steady-state error and increase the response rapidity as can be seen in section 5. According to Figure 6, the BC controller calculates u_j^* and U_j based on the desired reference current $i_{oj^*,j=1,2,\dots,(n-1)}$ and applies the modified switching signal u_j as a control signal to the PWM subsequently. Finally, based on Figure 4, the proper switching signals are generated and applied to the BC as described in section 2.1.

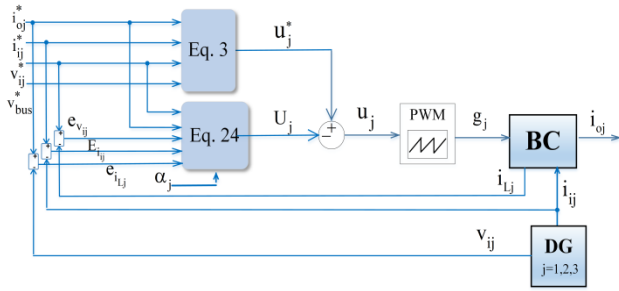


Figure 6. The detailed structure of the proposed BC controller.

4.2.2. Voltage stabilizing

The voltage control design is based on Equations (4), (18), and (25). According to Theorem 1, calculating U_n through Equation (25) will lead to system stability. Therefore, the controller calculates U_n at each step based on the state-feedback according to Figure 7. Since the switching function is placed in the energy equations equal to (18), by subtracting U_n from u_n^* , the modified switching functions are obtained dynamically and applied to the BBC.

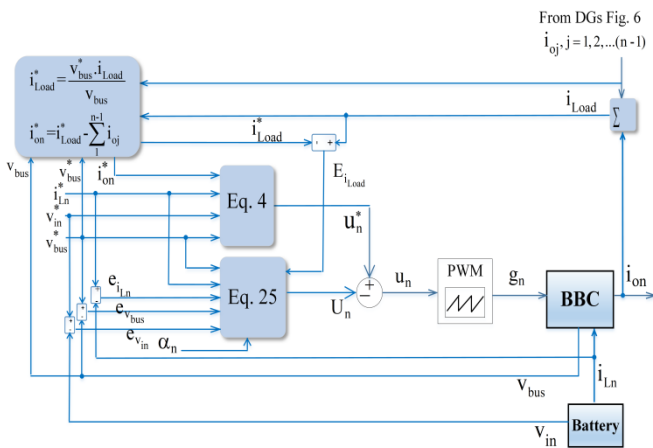


Figure 7. The detailed structure of the proposed BBC controller.

As can be seen in Equation (25), the effective variables and errors in the stabilization of the DC-bus voltage are involved in the calculation of the switching function. To adjust the DC-bus voltage to the desired value (v_{bus}^*), the deviation effects of the variables from their desired values are eliminated from the switching function by weighting α_n and consequently, according to Figure 7 the modified switching function is applied to the PWM. Based on the Equation (25), the factors such as the load variations, the inability of DG units to provide the needed power ($E_{i_{Load}}$), DC-bus voltage fluctuations ($e_{v_{bus}}$), and the deviations of the input voltage of the converter relative to its nominal value ($E_{v_{in}}$), affect the dynamical component of the switching function.

Based on Figure 7, to stabilize the DC-bus voltage and supply the load, the required load demand (i_{Load}^*) is subtracted from the total actual generated current of the DG units ($\sum_{j=1}^{n-1} i_{oj}$) and the result is considered as the desired reference current of the BESS unit (i_{on}^*). Obviously, when the total output power of the DG units exceeds the load demand,

the (i_{on}) will be negative and the battery will be charged.

Choosing the proper and accurate Lyapunov function has resulted in the participation of all effective errors on the DC-bus voltage stabilization in Equation (25). As can be seen in Figure 7, the BESS unit controller, in addition to stabilizing the fluctuations of the DC-bus voltage, compensates the needed current. Thus, in this scheme, the proper performance of the proposed BC controllers is its ability to reduce the contribution of the BESS unit to the transient and steady-state operation and consequently the proper performance of the BBC controller connected to the BESS unit, is its ability to inject needed currents, stabilize the DC-bus voltage through eliminating the fluctuations in transient and steady-state operation. As can be seen from Figures 6 and 7, the communication needs between the controllers are at their minimum level due to the independent operation of the BC controllers. Based on Figure 1, the only one-way communication is conducted via the BBC controller connected to the BESS.

5. SIMULATION AND RESULTS

In this section, to validate the performance of the proposed controller, a simulation has been performed in the MATLAB/SIMULINK[®] software. In this simulation, a stand-alone DC micro-grid consisting of two RERs, one fossil fuel energy resource, and one BESS that are a photovoltaic array, a wind-turbine unit, a gas-micro-turbine unit, and a lithium battery, respectively. The structure of the simulated micro-grid is shown in Figure 8. This micro-grid feeds a variable resistive load and the equations of ($v_{ij}, i_{ij}, j=1,2,3,4$) correspond to the [29, 35]. The DGs, BESS unit and the electrical load are connected to a common DC-bus. Further details about the parameters of the micro-grid have been listed in Table 1. To evaluate the performance of the controllers, several events are compiled in the form of two scenarios in sections 5.1 and 5.2 respectively. These considered events including the step changes in the reference values of the output currents (i_{oj}^*), the load changes, the simultaneous changes in generation level, the imbalance between generation and consumption, and the sudden disconnecting of a resource. As can be seen from the results, the proposed controller has a proper operation and is able to supply the load with desirable values of current and voltage, stability, and acceptable rapidity and accuracy. In Section 5.3, the performance of the proposed controller is investigated using multiple α_j . Finally, in section 5.4, to validate the proposed controller, its performance is compared with a conventional PI controller applied to the PWM.

Table 1. The details of the simulated DC micro-grid.

Parameter	Value	Parameter	Value
DC-bus voltage	950 (V)	Battery capacity	10 (Ah)
BC & BBC output capacitance	2.1 (mF)	Battery nominal voltage	1340 (V)
BC input capacitance	1 (mF)	BC & BBC inductance	5 (mH)
Switching frequency	5 (kHz)	BC & BBC input voltage	1400 (V)
Resistive load	19.95-31.35 (kW)	Number of DGs	3
		Number of BESS	1

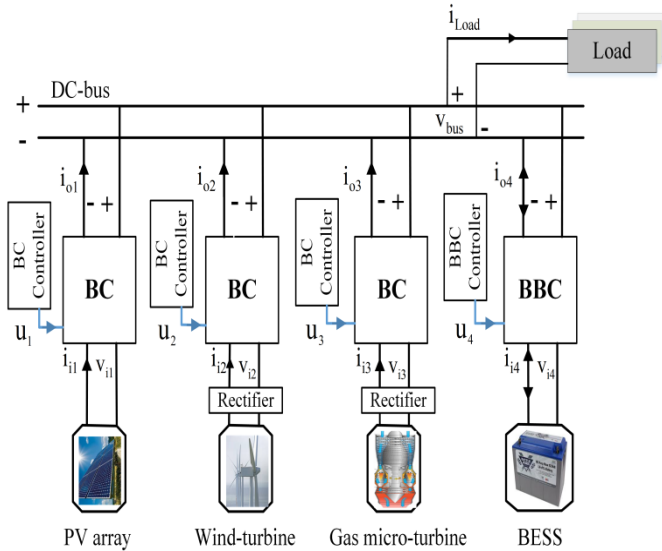


Figure 8. The structure of the simulated stand-alone DC micro-grid.

5.1. Scenario I: The changes in the load side

In this scenario, at first, the contribution rate of all DG units is assumed constant and the primary load demand is equal to 24(A). In two steps, the load increment at $t=1$ s and $t=2$ s, as well as in the next step, the load decrement at $t=3$ s are applied. These changes of load demand are respectively equal to +3(A), +6(A), and -12(A). The output current of each converter ($i_{oj}, j=1,2,3,4$), is shown in Figure 9. Moreover Figure 10 shows the total generated current, load demand (i_{Load}, i_{Load}^*), and the DC-bus voltage (v_{bus}). In Figure 9 the currents are displayed with more precise scale for greater clarity. Based on this figure, the load change has slight effects on the output currents of the BCs, with maximum oscillation range around 1.5 %. These oscillations are well removed. It means that the BC controllers have proper performance in the tracking of their set points ($i_{oj}, j=1,2,3$), because the BBC controller and BESS quickly compensate for the voltage drop caused by the increased load (Figure 10). Moreover, the BBC controller connected to the BESS unit performed well between $t=1-3$ s through regulating the current (i_{o4}) to meet the increment of the load requirement and in this way, the DC-bus voltage has been kept constant properly. In each event, new reference values are reflected along with the errors caused by the transient-states through Equations (24) and (25) in U_j . The new U_j is then deducted from u_j^* , thereby reducing the reflection of these fluctuations in the output current. The very slight saw-tooth fluctuations observed in the steady-state currents are related to the switching effect of the converters and are inevitable.

According to Figure 10, the DC-bus voltage has slight variations during the load changes, with quickly transient states. Moreover, to balance the needed and generated power, the BBC controller puts the BESS unit in the charge mode at $t=3$ s. After each event, the partial oscillations of the transient state in the output currents of the BCs are due to changes in the DC-bus voltage caused by sudden changes of the load. Changing the load causes a change in the equivalent impedance of the system. As can be seen in Figure 9, when the load increases (resistance decreases), the duration of the transient-state is longer than the load reduction state (increase

in resistance). However, these fluctuations are damped by a very slight range. Moreover, the BESS unit compensates for the DC-bus voltage with minimal fluctuations.

Theoretically, in this scenario, the effects of the DC-bus voltage errors are reflected by Equation (25) through considering $e_{v_{bus}}$ in the modified switching function of the BBC controller which results in the rapid elimination of fluctuations from the DC-bus voltage. Moreover, $\dot{W}(x)$ is calculated using equation (16) and shown in Figure 11. As can be seen in this figure, during Scenario I, $\dot{W}(x)$ is negative. Since $W_e(x) > 0$, based on (26), this result validates the stability of the system introduced by Theorem 1.

More details about the events and their results related to each scenario are listed in Table 2. In this table, i_{Load} is the steady-state current of the load, v_{bus} the steady-state voltage of the DC-bus that is equal to the load voltage. The error $e_{v_{bus}} \%$ is the steady-state error of the DC-bus voltage, expressed as a percentage.

5.2. Scenario II: The changes in the generation side

In this scenario, the load is assumed constant while the desired set points of the output currents ($i_{oj}^*, j=1,2,3$) are changed as modeling of changes in the generation level of the resources. The reference currents are respectively reduced equal to 5(A), 4(A), and 2(A) in three stages, between $t=4-6$ s. According to Figure 12, it is observed that the transient-states caused by this change, rapidly disappear in the output currents of each BCs. Also, the amplitude of the oscillations is negligible. Since the generated currents are less than the load demand, the BBC controller puts the BESS unit in the discharging mode through reversing the current (i_{on}). The BESS unit quickly discharges and prevents the DC-bus voltage from decreasing. Based on Figure 13 the proposed controller has acceptable performance in voltage stabilization. In this scenario, the desired reference currents ($i_{oj}^*, j=1,2,3,4$) and ($i_{ij}^*, j=1,2,3,4$) are changed.

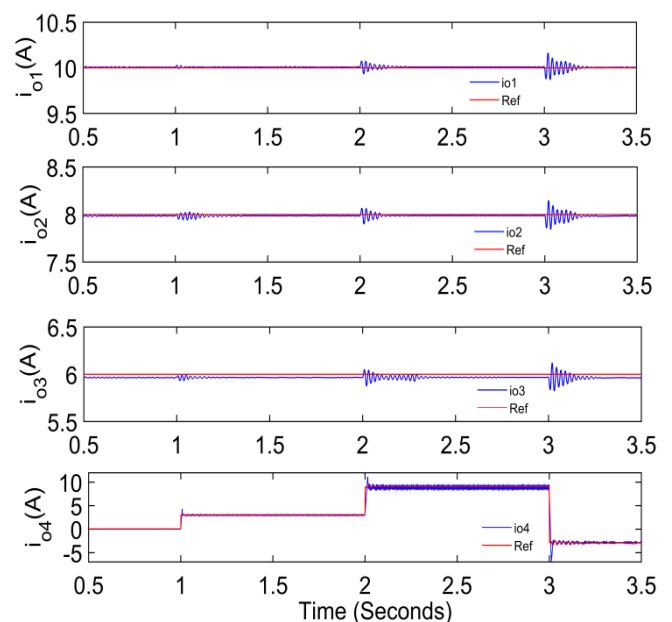


Figure 9. The output currents of DGs ($i_{oj}, j=1,2,3$) and BESS unit (i_{o4}) under load change during Scenario I.

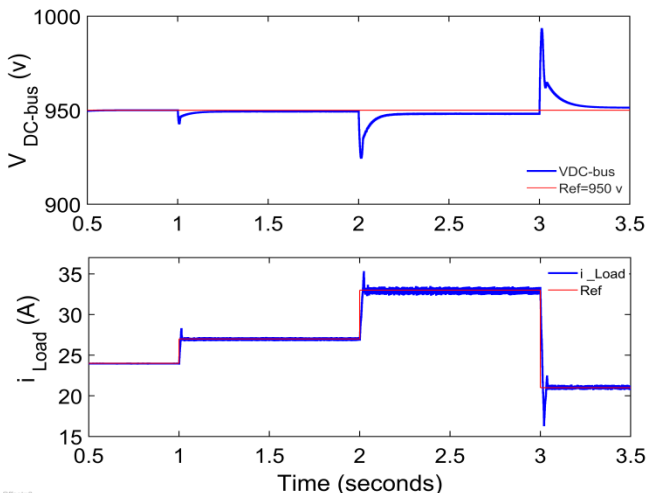


Figure 10. The total load current and DC-bus voltage under load change during Scenario I.

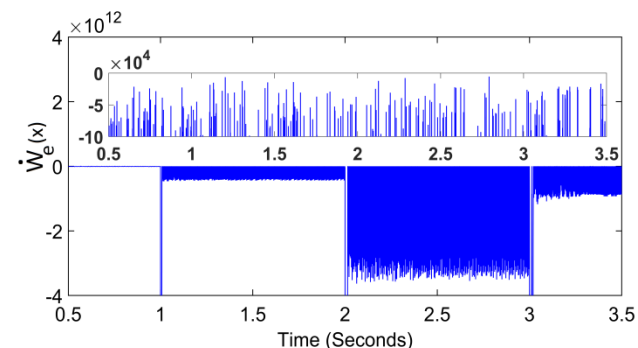


Figure 11. Calculating the derivative of energy function according to Equation (16) during Scenario I.

As mentioned in section 3, ($i_{oj}^* = i_{Lj}^*, j=1,2,3$) and ($i_{in}^* = i_{Ln}^*$). Therefore, based on Equations (24) and (25), these new reference values are included in the calculation along with their error values ($E_{i_{Load}}, E_{i_{ij}}, e_{i_{Lj}}, e_{i_{Ln}}$), and in this way, they are reflected in the modified switching functions (u_j). Consequently, in addition to generating new output currents (i_{oj}), the effects of their fluctuations are compensated properly. Moreover, in a harsh condition at $t=7$ s the desired output currents of DGs are increased simultaneously equal to 7(A) for each one, which is a serious stress for the system. As the output current exceeds the load demand, the BBC controller puts the BESS unit in the charging mode again. According to Figure 12, the transient-state caused by this change disappears rapidly in the output currents, and the amplitude of the oscillations is negligible. The BC controllers quickly attenuate the fluctuations caused by these changes by applying the error effects through Equation (24). Moreover, the output currents follow their set-points properly in the steady-state with acceptable accuracy. In addition, the BESS unit compensates the oscillations of the transient-state instantly. The DC-bus voltage is depicted in Figure 13. Based on this figure, in the steady-state, the BESS unit prevents the DC-bus voltage from increasing, and the proposed controller has proper performance against the changes of the generation set points. Based on section 4.2.2 i_{o4}^* is set equal to $i_{o4}^* = i_{Load}^* - \sum_{j=1}^3 i_{oj}^*$. Hence, according to Figure 12, i_{o4}^* may be

inherently oscillating. So, it does not interfere with stability. For instance, at $t=7-8$ s after a sudden step change in generation equal to +21(A), the fluctuation of i_{o4}^* are equal to the sum of the switching effects of the four converters and ($i_{o4} - i_{o4}^*$) is damping. The proposed controller is able to damp the oscillations well and ensure stability.

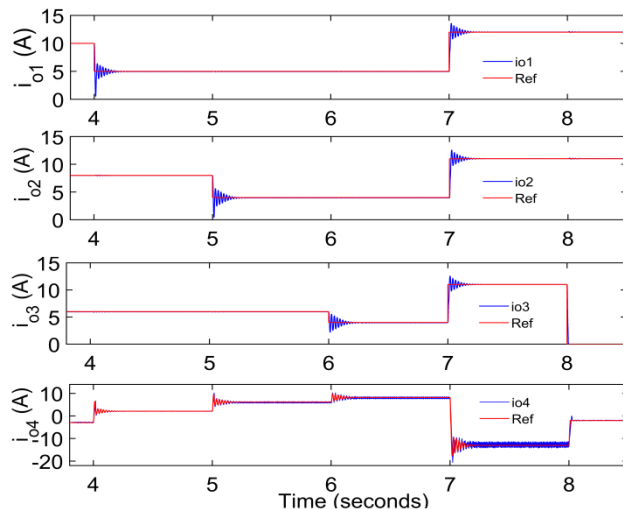


Figure 12. The output currents of DGs ($i_{oj}, j=1,2,3$) and BESS unit (i_{o4}) during Scenario II.

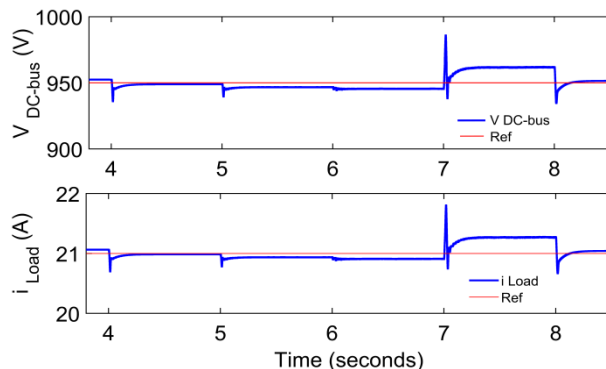


Figure 13. The total load current and DC-bus voltage during Scenario II.

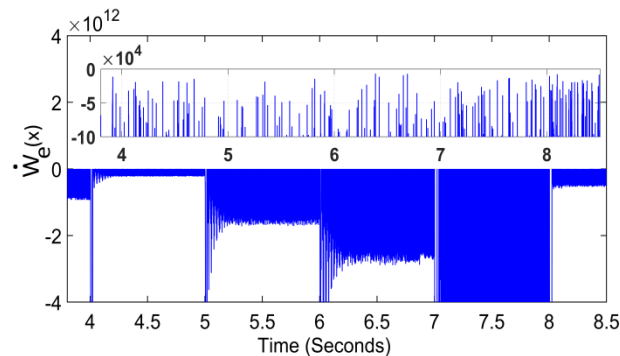


Figure 14. Calculating the derivative of energy function according to Equation (16) during Scenario II.

The steady-state error of the DC-bus voltage is equal to 1.26 %, which is still acceptable. In the following, at $t=8$ s, DG3 is abruptly disconnected from the micro-grid thus losing a significant portion of the generations, equal to 11(A). As a

result, based on Figure 13, the voltage drop occurs in DC-BUS. The BBC controller quickly alleviates this voltage drop through changing the contribution of BESS unit. As can be seen from Figure 12, DG1 and DG2 follow their set-points after a very slight and rapid transition. Moreover, $\dot{W}_e(x)$ is

calculated and shown in Figure 14 during this scenario. As can be seen in this figure, during the events, $\dot{W}_e(x)$ is negative and based on (26), validates the stability of the system introduced by Theorem 1. Further details of the simulation results are given in Table 2.

Table 2. The summary of the events and their results.

	Time (s)	Events	i_{Load}^* (A)	i_{Load} (A)	V_{bus} (V)	$E_{i_{Load}}^{(\%)}$	$e_{V_{bus}}^{(\%)}$
Scenario I	$t < 1$	Load=cte	24	23.95	950.01	-0.21	+0.001
	1	Load \uparrow	27	26.95	948.80	-0.17	-0.120
	2	Load \uparrow	33	32.90	946.60	-0.30	-0.350
	3	Load \downarrow	21	21.15	952.50	+0.71	+0.260
Scenario II	4	DG1 \downarrow	21	20.96	948.88	-0.19	-0.120
	5	DG2 \downarrow	21	20.78	946.70	-1.05	-0.350
	6	DG3 \downarrow	21	20.70	945.50	-1.43	-0.470
	7	DG1,2,3 \uparrow	21	21.31	962.00	+1.47	+1.260
	8	DG3:off	21	21.08	951.75	+0.38	+0.180

5.3. The effects of the proposed controller on transient-state, accuracy, and stability

In this section, in order to investigate the effect of the proposed controller on the performance of DGs, the generated current of one of the DGs (i_{o1}) is simulated with different coefficients of the controller (α_1). According to Theorem 1, the system error for $\alpha_1 < 0$ will be dampened. Three allowed values are assigned to α_1 . The considered events are according to Table 1 at $t=3$ s, 4 s. As can be seen in Figure 15, changing the α_1 leads to a change in the speed and accuracy of the controller. According to Equation (24), changing the α_1 changes the weight of the error term $(i_{Lj}^* e_{v_{ij}} - v_{ij}^* e_{i_{Lj}})^2$ on closed-loop. For this reason, ($\alpha_1 = -0.001$) causes lower undershoot and higher steady-state error, ($\alpha_1 = -0.8$) causes higher undershoot and higher steady-state accuracy. Also, ($\alpha_1 = -0.005$) causes a moderate mode. This feature makes the controller flexible in various applications based on exploitation policy. It should be noted that theoretically, the curves related to ($\alpha_1 = -0.001$) and ($\alpha_1 = -0.005$) also move towards the reference with a very slight slope, in this case, a secondary controller can quickly reduce the steady-state error. However, it occurs much faster by applying ($\alpha_1 = -0.8$), and if necessary, the proper filters can be used to compensate for the transient-state fluctuations. Moreover, as can be seen in Figure 16 and based on Equations (23) and (24), applying a positive coefficient ($\alpha_1 = 1$) causes system instability. In this case, the values of U_1 will cause the $\dot{W}_e(x)$ to be positive and the errors will be incremental.

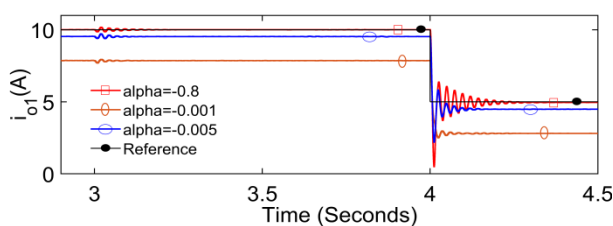


Figure 15. Comparing the generated current (i_{o1}) with various negative coefficients ($\alpha_1 = -0.001, -0.005, -0.8$).

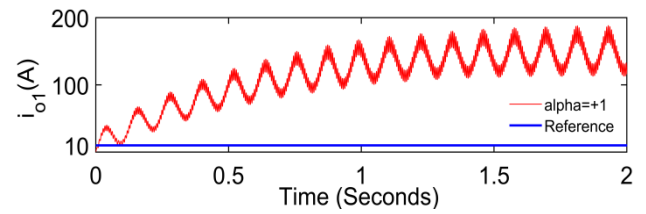


Figure 16. The generated current (i_{o1}) with positive coefficient ($\alpha_1 = +1$).

5.4. Comparison of the proposed controller with conventional PI controller

In this section, the performance of the proposed controller is compared with the conventional PI controller [20, 21]. As mentioned, the application of linear controllers on non-linear systems is sensitive to changes in reference values [22]. In this comparison, the values of α_j have been set equal to 0.25 for all units. The PI controller issues the switching functions (u_j) by comparing (i_{oj}, i_{oj}^*). The PI controller is set so that both controllers perform the same function before changing the reference values ($i_{o1}^* = 2$, $i_{o2}^* = 8$, $i_{o3}^* = 6$ (A)). Then, at $t=1$ s, i_{o1}^* changes equal to +13(A) and at $t=2$ s, i_{o2}^* and i_{o3}^* change respectively equal to -7(A) and +10(A). Figure 17 shows i_{oj} considering both control methods. Based on this figure, at $t=1$ s and $t=2$ s, a significant transient-states and steady-state fluctuations related to i_{o1} and i_{o3} , are observed in the performance of the PI controller compared to the proposed controller. Because in the PI controller, only the output current error is considered and u_j will fluctuate in proportion to current oscillation, which will cause more oscillation. However, in the proposed control method, the average of the switching function u_j^* is always constant and U_j dynamically corrects the switching functions ($u_j = u_j^* - U_j$) based on Equations (24) and (25) and considering the errors of all state-variables. This feature reduces the amplitude and duration of transient-state oscillations. At $t=2$ s, after a sharp decrease, i_{o2} has been cut-off using the PI controller due to the presence of

a rectifier according to Figure 8 which prevents reverse current. However, this causes destructive tensions in the converter. Also, according to Figure 17, severe fluctuations of i_{oj} have led to significant battery participation using PI controller that will reduce battery life-span.

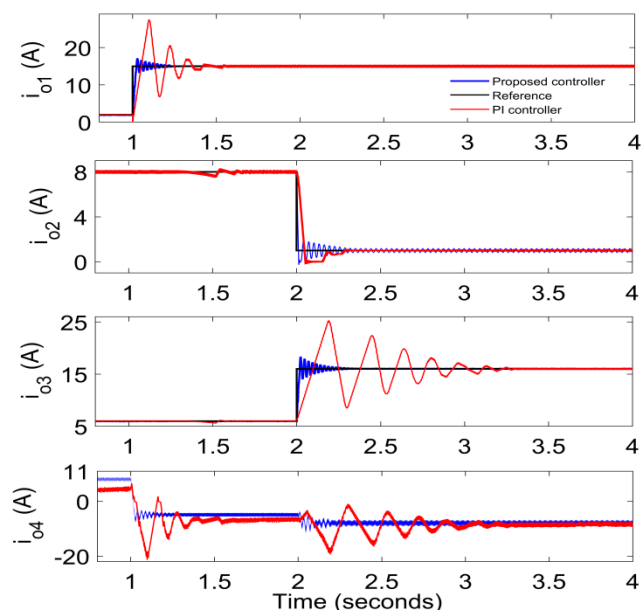


Figure 17. Comparison of the proposed controller with conventional PI control.

6. CONCLUSIONS

In this paper, a novel local controller for a multi-resource converter-based stand-alone DC micro-grid has been proposed based on DLM. A comprehensive dynamic micro-grid model associated with the converter-based ESS, RERs and gas-micro-turbine has been considered. In this proposed method, the steady-state and dynamic components of the switching functions have been separately investigated in the dynamic model to decrease the fluctuations due to the load alterations and performance of the DGs. Thereby, the controller ensures the fluctuation damping of the output and system stability. Besides, the proposed method ensures stable performance regardless of the dynamic equations of the resources and the number of DGs. Moreover, the independence of the DG controllers, simplicity, and easy execution are the other advantages of this method. The desired DC-bus voltage, accurate current generation, and fast response have been achieved by simulation in the MATLAB/SIMULINK[®] environment for various operating conditions. The simulation results show that the DGs are controlled individually with the negligible effects on each other. Moreover, the controllers exhibited good performance compared to conventional PI controllers in eliminating the oscillations caused by sudden changes in the generation, and are flexible in various applications based on exploitation policy. It can be predicted for example the combining an outer layer fuzzy or neural controller with the proposed method to adjust the alpha coefficients can be considered as future works.

7. ACKNOWLEDGEMENT

The authors acknowledge the support of Babol Noshirvani University of Technology through Grant program No. BNUT/925120010/2020.

REFERENCES

1. Rezagholizadeh, M., Aghaei, M. and Dehghan, O., "Foreign direct investment, stock market development, and renewable energy consumption: Case study of Iran", *Journal of Renewable Energy and Environment (JREE)*, Vol. 7, No. 2, (2020), 8-18.
2. Carrasco, J.M., Franquelo, L., Bialasiewicz, J., Galvan, E., Portillo, R., Prats, M.M., Leon, J. and Moreno-Alfonso, N., "Power-electronic systems for the grid integration of renewable energy sources", *Industrial Electronics, IEEE Transactions A: Survey*, Vol. 53, (2006), 1002-1016. (DOI: 10.1109/TIE.2006.878356).
3. Justo, J.J., Mwasilu, F., Lee, J. and Jung, J.W., "AC-micro-grids versus DC-micro-grids with distributed energy resources", *Renewable and Sustainable Energy Reviews A: Review*, Vol. 24, (2013), 387-405. (DOI: 10.1016/j.rser.2013.03.067).
4. Elsayed, A.T., Mohamed, A.A. and Mohammed, O.A., "DC micro-grids and distribution systems", *Electric Power Systems Research A: Overview*, Vol. 119, (2015), 407-417. (DOI: 10.1016/j.epr.2014.10.017).
5. Azizi, N. and Moradi CheshmehBeigi, H., "Reactive and active power control of grid WECS based on DFIG and energy storage system under both balanced and unbalanced grid conditions", *Journal of Renewable Energy and Environment (JREE)*, Vol. 4, No. 4, (2017), 31-38.
6. Rahmani, M., Faghihi, F., Moradi CheshmehBeigi, H. and Hosseini, S., "Frequency control of islanded microgrids based on fuzzy cooperative and influence of STATCOM on frequency of microgrids", *Journal of Renewable Energy and Environment (JREE)*, Vol. 5, No. 4, (2019), 27-33.
7. Joung, K.W., Kim, T. and Park, J.W., "Decoupled frequency and voltage control for stand-alone microgrid with high renewable penetration", *IEEE Transactions on Industry Applications*, Vol. 55, No. 1, (2018), 122-133. (DOI: 10.1109/tia.2018.2866262).
8. Kim, J.Y., Jeon, J.H., Kim, S.K., Cho, C., Park, J.H., Kim, H.M. and Nam, K.Y., "Cooperative control strategy of energy storage system and micro sources for stabilizing the micro-grid during islanded operation", *IEEE Transactions on Power Electronics*, Vol. 25, No. 12, (2010), 3037-3048. (DOI: 10.1109/TPEL.2010.2073488).
9. Dastgeer, F. and Gelani, H.E., "A comparative analysis of system efficiency for AC and DC residential power distribution paradigms", *Energy and Buildings*, Vol. 138, (2017), 648-654. (DOI: 10.1016/j.enbuild.2016.12.077).
10. Xu, L. and Chen, D., "Control and operation of a DC micro-grid with variable generation and energy storage", *IEEE Transactions on Power Delivery*, Vol. 26, No. 4, (2011), 2513-2522. (DOI: 10.1109/TPWRD.2011.2158456).
11. Fallah, S., Deo, R., Shojafar, M., Conti, M. and Shamshirband, S., "Computational intelligence approaches for energy load forecasting in smart energy management grids", *State of the Art, Future Challenges, and Research Directions Energies*, Vol. 11, No. 3, (2018), 596. (DOI: 10.3390/en11030596).
12. Chen, D., Xu, L. and Yao, L., "DC voltage variation based autonomous control of DC micro-grids", *IEEE Transactions on Power Delivery*, Vol. 28, No. 2, (2013), 637-648. (DOI: 10.1109/TPWRD.2013.2241083).
13. Augustine, S., Mishra, M.K. and Lakshminarasamma, N., "Adaptive droop control strategy for load sharing and circulating current minimization in low-voltage stand-alone DC micro-grid", *IEEE Transactions on Sustainable Energy*, Vol. 6, No. 1, (2015), 132-141. (DOI: 10.1109/TSTE.2014.2360628).
14. Dizqah, A.M., Maheri, A., Busawon, K. and Kamjoo, A., "A multivariable optimal energy management strategy for stand-alone dc micro-grids", *IEEE Transactions on Power Systems*, Vol. 30, No. 5, (2015), 2278-2287. (DOI: 10.1109/TPWRS.2014.2360434).
15. Anand, S., Fernandes, B.G. and Guerrero, J.M., "Distributed control to ensure proportional load sharing and improve voltage regulation in low voltage DC micro-grids", *Fuel*, Vol. 3, No. 4, (2013). (DOI: 10.1109/TPEL.2012.2215055).
16. Kordkheili, H., Banejad, M., Kalat, A., Pouresmaeil, E. and Catalão, J., "Direct-lyapunov-based control scheme for voltage regulation in a three-phase islanded microgrid with renewable energy sources", *Energies*, Vol. 11, No. 5, (2018), 1161. (DOI: 10.3390/en11051161).
17. Tahim, A.P.N., Pagano, D.J., Lenz, E. and Stramosk, V., "Modeling and stability analysis of islanded DC microgrids under droop control", *IEEE*

- Transactions on Power Electronics*, Vol. 30, No. 8, (2014), 4597-4607. (DOI: 10.1109/TPEL.2014.2360171).
18. Herrera, L., Zhang, W. and Wang, J., "Stability analysis and controller design of DC microgrids with constant power loads", *IEEE Transactions on Smart Grid*, Vol. 8, No. 2, (2015), 881-888. (DOI: 10.1109/TSG.2015.2457909).
 19. Liu, S., Zhu, W., Cheng, Y. and Xing, B., "Modeling and small-signal stability analysis of an islanded DC microgrid with dynamic loads", *Proceedings of 15th International Conference on Environment and Electrical Engineering*, (2015), 866-871. (DOI: 10.1109/EEEIC.2015.7165277).
 20. Ghanbari, N., Bhattacharya, S. and Mobarrez, M., "Modeling and stability analysis of a dc microgrid employing distributed control algorithm", *Proceedings of 9th IEEE International Symposium on Power Electronics for Distributed Generation Systems*, (2018), 1-7. (DOI: 10.1109/PEDG.2018.8447707).
 21. Makrygiorgou, D. and Alexandridis, A., "Stability analysis of dc distribution systems with droop-based charge sharing on energy storage devices", *Energies*, Vol. 10, No. 4, (2017), 433. (DOI: 10.3390/en10040433).
 22. Perez, F. and Damm, G., DC microgrids, In *Microgrids design and implementation*, (2019), 472-473. (DOI: 10.1007/978-3-319-98687-6_16).
 23. Fei, G.A.O., Ren, K.A.N.G., Jun, C.A.O. and Tao, Y.A.N.G., "Primary and secondary control in DC microgrids", *Journal of Modern Power Systems and Clean Energy A: Review*, Vol. 7, No. 2, (2019), 227-242. (DOI: 10.1007/s40565-018-0466-5).
 24. Sitbon, M., Aharon, I., Averbukh, M., Baimel, D. and Sassonker, M., "Disturbance observer based robust voltage control of photovoltaic generator interfaced by current mode buck converter", *Energy Conversion and Management*, Vol. 209, (2020). (DOI:10.1016/j.enconman.2020.112622).
 25. Amiri, H., Markadeh, G.A., Dehkordi, N.M. and Blaabjerg, F., "Fully decentralized robust backstepping voltage control of photovoltaic systems for DC islanded microgrids based on disturbance observer method", *ISA Transactions*, (2020). (DOI: 10.1016/j.isatra.2020.02.006).
 26. Kumar, J., Agarwal, A. and Agarwal, V., "A review on overall control of DC microgrids", *Journal of Energy Storage*, Vol. 21, (2019), 113-138. (DOI: 10.1016/j.est.2018.11.013).
 27. Mehdi, M., Jamali, S.Z., Khan, M.O., Baloch, S. and Kim, C.H., "Robust control of a DC microgrid under parametric uncertainty and disturbances", *Electric Power Systems Research*, Vol. 179, (2020). (DOI: 10.1016/j.epsr.2019.106074).
 28. Nahata, P., Soloperto, R., Tucci, M., Martinelli, A. and Ferrari-Trecate, G., "A passivity-based approach to voltage stabilization in DC microgrids with ZIP loads", *Automatica*, Vol. 113, (2020). (DOI: 10.1016/j.automatica.2019.108770).
 29. Tani, A., Camara, M.B. and Dakyo, B., "Energy management in the decentralized generation systems based on renewable energy-Ultracapacitors and battery to compensate the wind/load power fluctuations", *IEEE Transactions on Industry Applications*, Vol. 51, No. 2, (2015), 1817-1827. (DOI: 10.1109/TIA.2014.2354737).
 30. Kumar, M., Srivastava, S.C., Singh, S.N. and Ramamoorthy, M., "Development of a new control strategy based on two revolving field theory for single-phase VCVSI integrated to DC micro-grid", *International Journal of Electrical Power & Energy Systems*, Vol. 98, (2018), 290-306. (DOI: 10.1016/j.ijepes.2017.11.042).
 31. Camara, M.B., Dakyo, B. and Gualous, H., "Polynomial control method of DC/DC converters for DC-bus voltage and currents management-Battery and supercapacitors", *IEEE Transactions on Power Electronics*, Vol. 27, No. 3, (2012), 1455-1467. (DOI: 10.1109/TPEL.2011.2164581).
 32. Gavagsaz-Ghoachani, R., Phattanasak, M., Martin, J.P., Nahid-Mobarakeh, B., Pierfederici, S. and Riedinger, P., "Observer and lyapunov-based control for switching power converters with LC input filter", *IEEE Transactions on Power Electronics*, Vol. 34, No. 7, (2019), 7053-7066. (DOI: 10.1109/tpe.2018.2877180).
 33. Muhammad, H.R., *Power electronics handbook*, Prentice Hall, (2001), 64-66.
 34. Slotine, J.J.E. and Li, W., *Applied nonlinear control*, Englewood Cliffs, NJ: Prentice Hall, (1991), 65-66.
 35. Guda, S.R., Wang, C. and Nehrir, M.H., "Modeling of microturbine power generation systems", *Electric Power Components and Systems*, Vol. 34, No. 9, (2006), 1027-1041. (DOI: 10.1080/15325000600596767).

ABSTRACTS

Evaporation Characteristics of Diesel and Biodiesel Fuel Droplets on Hot Surfaces

Mehdi Zare^a, Barat Ghobadian^{a*}, Seyed Reza Hassan-Beygi^b, Gholamhasan Najafi^a

^a Department of Biosystems Engineering, Tarbiat Modares University (TMU), Tehran, Iran.

^b Department of Agrotechnology, College of Abouraihan, University of Tehran, Tehran, Iran.

PAPER INFO

Paper history:

Received 15 October 2019

Accepted in revised form 03 March 2020

Keywords:

Critical Surface Temperature

Evaporation Time

ANOVA

CI Engine

Transesterification

ABSTRACT

In CI engines, the evaporation rate of fuel on various hot surfaces, including the combustion chamber, has a significant effect on deposit formation and accumulation, the exhaust emissions of PM and NO_x, and their efficiency. Therefore, the evaporation of liquid fuel droplets impinging on hot surfaces has become an important subject of interest to engine designers, manufacturers, and researchers. The aim of this study is to investigate the evaporation characteristics based on droplet lifetime and critical surface temperature (the maximum heat transfer rate) of diesel and biodiesel fuel droplets on hot surfaces. In order to determine the effects of diesel fuel, canola oil biodiesel, and castor oil biodiesel, the droplets impinging on the hot surfaces of aluminum alloy (7075) and steel alloy (1.5920) and the evaporation lifetime of diesel and biodiesel fuels were measured. Statistical analysis (ANOVA and Duncan's multiple-range test) was carried out using SAS software. The results showed the maximum critical surface temperature of 450 °C for the castor oil biodiesel on steel 1.5920 surface and the minimum one for diesel fuel (350 °C). In this case, both surfaces had the same droplet lifetimes of approximately 2 s. The results of ANOVA showed the significant effect of the surface material and fuel type on the evaporation lifetime of fuel droplet at 1 % probability.

چکیده

در موتورهای اشتعال تراکمی نرخ تبخیر سوخت روی سطوح داغ موجود در محفظه احتراق تأثیر بسزایی روی تشکیل و تجمع رسوب روی این سطوح دارد. علاوه بر این نرخ تبخیر سوخت بر تولید آلاینده های PM و NO_x توسط موتور و بازده آن تأثیر دارد. به دلایل مذکور، بررسی تبخیر قطره سوخت ریخته شده روی سطح داغ برای طراحان موتور، سازندگان و پژوهشگران همواره مورد توجه قرار گرفته است. هدف پژوهش حاضر، بررسی عمر قطره و دمای بحرانی صفحه داغ (بیشینه نرخ انتقال حرارت) قطرات سوخت دیزل و بیودیزل روی صفحه داغ است. سوخت‌های مورد استفاده در پژوهش، سوخت دیزل، سوخت بیودیزل روغن کلزا و نیز سوخت بیودیزل روغن کرچک است. جنس صفحه داغ مورد استفاده در پژوهش نیز آلومینیوم آلیاژی ۷۰۷۵ و فولاد شماره ۱/۵۹۲۰ است. نتایج حاصل نشان داد که بیشینه دمای صفحه بحرانی مربوط به قطره سوخت بیودیزل روغن کرچک ریخته شده روی صفحه فولادی و برابر ۴۵۰ درجه سلسیوس بوده و کمینه دمای صفحه بحرانی مربوط به قطره سوخت دیزل و برابر ۳۵۰ درجه سلسیوس بوده و در هر دو حالت عمر قطره سوخت حدوداً ۲ ثانیه اندازه گیری شد. برای بررسی تأثیر نوع سوخت و جنس صفحه، آنالیز آماری به کمک نرم افزار SAS انجام شد. نتایج تجزیه واریانس نشان داد که جنس صفحه و نوع سوخت در سطح ۱ درصد تأثیر معناداری بر عمر قطره سوخت ریخته شده روی سطح داغ دارند.

Foreign Direct Investment, Stock Market Development, and Renewable Energy Consumption: Case Study of Iran

Mahdieh Rezagholizadeh^{a*}, Majid Aghaei^a, Omid Dehghan^b

^a Department of Economics and Administrative Sciences, University of Mazandaran, Babolsar, Iran.

^b Department of Energy Economics, Petroleum University of Technology, Tehran, Iran.

PAPER INFO

Paper history:

Received 28 November 2019

Accepted in revised form 11 April 2020

Keywords:

Foreign Direct Investment

Stock Market

Renewable Energy

GDP

ARDL Test

A B S T R A C T

Concerning environmental pollution issues derived from fossil energy consumption, the application of renewable energies plays an important role in countries, especially in their energy sector policymaking. Since determining the relationship between different variables and renewable energy not only has significant policy applications in energy sector but also is necessary in achieving sustainable development goals, this study assesses the impact of effective factors on the development of renewable energy consumption in Iran with emphasis on the role of foreign direct investment (FDI) and financial sector development (especially stock market development). This study applies Auto-Regressive Distributed Lag (ARDL) bounding test method over the period of 1978-2016. The research findings show that there is a causal relationship between foreign direct investment and the stock market and renewable energy consumption in Iran such that the increase of foreign direct investment and stock market development will increase the consumption of renewable energies in Iran. On the other hand, a growth in renewable energies consumption will significantly reduce CO₂ emission in the long run. Besides, increasing FDI and stock market development will raise the economic growth of a country and, in return, increase CO₂ emission.

چکیده

با توجه به مسائل مربوط به آلودگی‌های زیست‌محیطی ناشی از مصرف انرژی، طی سال‌های اخیر استفاده از انرژی‌های تجدیدپذیر در کشورها جایگاه ویژه‌ای داشته و در سیاست‌گذاری بخش انرژی آن‌ها نقش مهمی ایفا می‌کند. نظر به اینکه تعیین رابطه بین متغیرهای مختلف با انرژی تجدیدپذیر، نه تنها کاربردهای سیاستی قابل ملاحظه‌ای در عرصه انرژی دارد، بلکه برای رسیدن به اهداف توسعه پایدار نیز ضروری می‌باشد، مطالعه حاضر به ارزیابی تأثیر عوامل مؤثر بر مصرف انرژی تجدیدپذیر در ایران از کانال سرمایه‌گذاری مستقیم خارجی و توسعه بخش مالی (با تأکید بر توسعه بازار سهام) با استفاده از تکنیک آزمون کرانه‌ای خودرگرسیون برداری با وقفه‌های توزیعی، طی دوره زمانی ۱۳۹۴-۱۳۵۶ می‌پردازد. یافته‌های تحقیق بیانگر این است که رابطه علیت از سرمایه‌گذاری مستقیم خارجی و بازار سهام به مصرف انرژی تجدیدپذیر در ایران وجود دارد، به گونه‌ای که افزایش در سرمایه‌گذاری خارجی و توسعه بازار سهام منجر به افزایش مصرف این نوع انرژی در کشور می‌شود. از سوی دیگر افزایش مصرف انرژی‌های تجدیدپذیر در بلندمدت، به طور معنی‌داری منجر به کاهش میزان انتشار دی‌اکسید کربن می‌شود. همچنین افزایش میزان سرمایه‌گذاری مستقیم خارجی و توسعه بازار سهام، رشد اقتصادی کشور را بیشتر نموده و در مقابل، میزان انتشار دی‌اکسید کربن را نیز افزایش می‌دهد.

Application of Artificial Neural Networks to the Simulation of Climate Elements, Drought Forecast by Two Indicators of SPI and PNPI, and Mapping of Drought Intensity; Case Study of Khorasan Razavi

Mohammad Hossein Jahangir*, Mahnaz Abolghasemi, Seyedeh Mahsa Mousavi Reineh

Department of Renewable Energies and Environment, Faculty of New Sciences and Technologies, University of Tehran, Tehran, Iran.

PAPER INFO

Paper history:

Received 01 January 2020

Accepted in revised form 25 April 2020

Keywords:

Forecasting of Drought Intensity

Artificial Neural Network

Simulation

Multi-Layer Perceptron

Levenberg-Marquardt

Razavi Khorasan

ABSTRACT

Drought is considered as a destructive disaster that can have irreversible effects on different aspects of life. In this study, artificial neural network was used as a powerful means of modeling nonlinear and indefinite processes in order to simulate drought intensities at 7 synoptic stations of Khorasan Razavi from more than 35 years ago up to the year 2014. Input data were the calculations of the two indicators of PNPI and SPI by DIC software, and the output layer (drought intensity) was taken to the Matlab software and employed as the teaching data (from 25 years), experiment (from 5 years), and validation (from another 5 years). The 3-9-1 structure of the network of layers had the maximum accuracy with the error rate of less than 2 % and high correlation (more than 90 %). After trial and error for each station through sigmoid stimulation function in the Perceptron network, it was observed that the stations of Mashhad and Quchan had the minimum error and the maximum error was related to the station of Neyshabur. The results of comparisons and observations showed that the artificial neural network had high efficiency in simulation of the data. The obtained correlation amount of 0.999 for the base station represented the small error of the model in prediction. Drought forecasting was performed in this study by the trained algorithm in the artificial neural network without using the observation data. The results showed that rainfall, temperature, and speed models had a positive role in forecasting the provinces that would experience drought. Due to its lower amount of error, SPI indicator was selected for mapping, the findings of which showed that the highest drought intensity belonged to the near normal to normal wet lands.

چکیده

خشکسالی به عنوان یک فاجعه مخرب در نظر گرفته می‌شود که می‌تواند تأثیرات جبران ناپذیری بر جنبه‌های مختلف زندگی داشته باشد. در این مطالعه از شبکه عصبی مصنوعی به عنوان ابزاری قدرتمند برای مدل‌سازی فرآیندهای غیرخطی و نامشخص به منظور شبیه‌سازی شدت خشکسالی در ۷ ایستگاه سینوپتیک خراسان رضوی برای بیش از ۳۵ سال تا سال ۲۰۱۴ استفاده شده است. داده‌های ورودی محاسبات دو شاخص SPI و PNPI توسط نرم افزار DIC و لایه خروجی (شدت خشکسالی) به نرم افزار Matlab برده شد و به عنوان داده‌های آموزش (از ۲۵ سال)، آزمایش (از ۵ سال) و اعتبار سنجی (از ۵ سال دیگر) استفاده شد. ساختار ۳-۹-۱ از شبکه لایه‌ها دارای حداکثر دقت با میزان خطای کمتر از ۲٪ و همبستگی زیاد (بیش از ۹۰٪) بودند. پس از آزمایش و خطا برای هر ایستگاه از طریق عملکرد تحریک سیگموئید در شبکه پرسپترون، مشاهده شد که ایستگاه‌های مشهد و قوچان دارای حداقل خطا و بیشترین خطا مربوط به ایستگاه نیشابور است. نتایج مقایسه‌ها و مشاهدات نشان داد که شبکه عصبی مصنوعی در شبیه‌سازی داده‌ها از راندمان بالایی برخوردار است. مقدار همبستگی به دست آمده ۰/۹۹۹ برای ایستگاه پایه، نشانگر خطای کوچک مدل در پیش‌بینی است. پیش‌بینی خشکسالی در این مطالعه توسط الگوریتم آموزش دیده در شبکه عصبی مصنوعی و بدون استفاده از داده‌های مشاهده‌ای انجام شد. نتایج نشان داد که مدل‌های بارندگی، دما و سرعت نقش مثبتی در پیش‌بینی نقاطی که خشکسالی را تجربه می‌کنند، دارند. شاخص SPI با توجه به خطای کمتری که داشت، برای نقشه‌برداری انتخاب شد که یافته‌های آن نشان داد که بیشترین شدت خشکسالی متعلق به اراضی مرطوب نزدیک به نرمال است.

A Review of Application of Experimental Design Techniques Related to Dark Fermentative Hydrogen Production

Fatemeh Boshagh^a, Khosrow Rostami^{b*}

^a Department of Chemical Technologies, Iranian Research Organization for Science and Technology (IROST), P. O. Box: 3353-5111, Tehran, Iran.

^b Department of Biotechnology, Iranian Research Organization for Science and Technology (IROST), P. O. Box: 3353-5111, Tehran, Iran.

PAPER INFO

Paper history:

Received 12 December 2019

Accepted in revised form 26 April 2020

Keywords:

Biohydrogen Production

Dark Fermentation

Experimental Design

Optimization

ABSTRACT

The current review purpose is to present a general overview of different experimental design methods that are applied to investigate the effect of key factors on dark fermentation and are efficient in predicting the experimental data for biological hydrogen production. The methods of two levels full and fractional factorials, Plackett–Burman, and Taguchi were employed for screening the most important factors in dark fermentation. The techniques of central composite, Box–Behnken, Taguchi, and one factor at a time for optimization of the dark fermentation were extensively used. Papers on the three levels full and fractional factorials, artificial neural network coupled with genetic algorithm, simplex, and D-optimal for the optimization of the dark fermentation are limited, and no paper on the Dohrlert design has been reported to date. The artificial neural network coupled with genetic algorithm is a more suitable method than the RSM technique for the optimization of dark fermentation. Literature shows that the optimization of critical factors plays a significant role in dark fermentation and is useful to improve the hydrogen production rate and hydrogen yield.

چکیده

هدف این مقاله، مروری بر روشهای طراحی آزمایش است که برای مطالعه اثر فاکتورهای کلیدی در تولید هیدروژن به روش تخمیر در تاریکی استفاده شده‌اند. روش‌های فاکتوریل کامل و جزئی در دو سطح، پلاکت-بورمن و تاگوچی برای غربالگری فاکتورهای مؤثر در تولید هیدروژن به روش تخمیر در تاریکی بکار رفته‌اند. روش‌های ترکیب مرکزی، باکس-بنکن، تاگوچی و یک فاکتور در یک زمان برای بهینه‌سازی تولید هیدروژن به روش تخمیر در تاریکی بطور گسترده‌ای استفاده شده‌اند. مقالات درباره روش‌های فاکتوریل کامل و جزئی در سه سطح، شبکه عصبی، شبکه عصبی همراه با الگوریتم ژنتیک، طراحی مختلط و دی اپتیمال برای بهینه‌سازی تولید هیدروژن به روش تخمیر در تاریکی محدود هستند و تاکنون هیچ مقاله‌ای درباره روش طراحی دوهرلرت گزارش نشده است. شبکه عصبی و شبکه عصبی توأم با الگوریتم ژنتیک در مقایسه با روش‌های پاسخ سطح برای بهینه‌سازی تخمیر در تاریکی مناسب‌ترند. مرور مقالات نشان می‌دهد بهینه‌سازی فاکتورهای کلیدی نقش مهمی در تولید هیدروژن به روش تخمیر در تاریکی ایفا می‌کند و سبب افزایش بازده و آهنگ تولید هیدروژن می‌شود.

Energy Modeling and Techno-Economic Analysis of a Biomass Gasification-CHAT-ST Power Cycle for Sustainable Approaches in Modern Electricity Grids

Saeed Hosseinpour^a, Seyed Alireza Haji Seyed Mirza Hosseini^{a*}, Ramin Mehdipour^b, Amir Hooman Hemmasi^a, Hassan Ali Ozgoli^c

^a Department of Energy Engineering, Faculty of Natural Resources and Environment, Science and Research Branch, Islamic Azad University, Tehran, Iran.

^b Department of Mechanical Engineering, Tafresh University, Tafresh, Iran.

^c Department of Mechanical Engineering, Iranian Research Organization for Science and Technology (IROST), Tehran, Iran.

PAPER INFO

Paper history:

Received 03 February 2020

Accepted in revised form 26 April 2020

Keywords:

Biomass Gasifier

Cascaded Humidified Advanced Turbine

Steam Turbine

Combined Cycle

Economic Analysis

ABSTRACT

In this study, an advanced combined power generation cycle was evaluated to obtain sustainable energy with high power and efficiency. This combined cycle includes biomass gasification, the Cascaded Humidified Advanced Turbine (CHAT), and the steam turbine. The fuel consumed by the system is derived from the gas produced in the biomass gasification process. The biomass consumed in this study is wood because of its reasonable supply and availability. The economic analysis conducted in the present research has produced significant gains. The proposed cycle with current prices intended to sell electricity in Iran has a positive Net Present Value (NPV). Therefore, the presented cycle in terms of energy supply has good economic value. Due to the significantly higher purchase/sale price of electricity from renewable power plants in developed countries in Europe or the United States, the power generation cycle proposed in this study may be more economically feasible in other regions than Iran. Of course, with a slight price increase in electricity sales in Iran ($3 \text{ US}\$ \text{ kWh}^{-1}$), the proposed system will have acceptable NPV. Because of the complicated equipment used in high-pressure and low-pressure turbines and compressors sets, the equipment used in this cycle requires a higher initial investment cost than conventional power generation systems. The results showed that the investment cost per unit of energy was approximately 909 USD kW^{-1} .

چکیده

در این مطالعه، یک سیکل ترکیبی پیشرفته تولید توان به منظور حصول انرژی پایدار دارای قدرت و راندمان بالا مورد ارزیابی قرار گرفته شد. این سیکل ترکیبی شامل گازی ساز زیست‌توده، سیکل توربین پیشرفته مرطوب آبشاری (CHAT) و توربین بخار می‌باشد. سوخت مصرفی این سیستم از گاز تولیدشده در فرآیند گازی سازی زیست‌توده تأمین شده است. زیست‌توده مصرفی در این پژوهش به دلیل قیمت تهیه مناسب و در دسترس بودن، چوب می‌باشد. تحلیل اقتصادی انجام شده در پژوهش حاضر، منجر به دستاوردهای قابل توجهی شده است. سیکل حاضر با قیمت‌های کنونی در نظر گرفته شده برای فروش الکتریسیته در ایران دارای مقدار ارزش کنونی خالص (NPV) مثبت می‌باشد. از اینرو، سیکل ارائه شده در شرایط پیش روی تأمین انرژی، دارای مطلوبیت اقتصادی مناسبی است. به دلیل بیشتر بودن قابل ملاحظه قیمت خرید/فروش الکتریسیته نیروگاه‌های برق تجدیدپذیر در کشورهای توسعه یافته اروپا یا ایالات متحده، سیکل تولید توان پیشنهادی در این مطالعه، می‌تواند شرایط مناسب‌تری از دیدگاه اقتصادی در سایر مناطق بررسی شده در مقایسه با ایران داشته باشد. البته با افزایش قیمت فروش الکتریسیته در ایران به میزان اندکی، سیستم ارائه شده دارای NPV مناسبی خواهد بود ($3 \text{ US}\$ \text{ kWh}^{-1}$). به دلیل بهره‌گیری از تجهیزات پیشرفته و پیچیده به کار رفته در مجموعه توربین و کمپرسورهای فشار بالا و فشار پایین، تجهیزات مورد استفاده در این سیکل، نیازمند هزینه سرمایه‌گذاری اولیه بالاتری در مقایسه با سیستم‌های رایج تولید توان می‌باشند. نتایج نشان داد که هزینه سرمایه‌گذاری به ازای هر واحد انرژی تقریباً برابر 909 USD kW^{-1} می‌باشد.

A Novel Local Control Technique for Converter-Based Renewable Energy Resources in the Stand-Alone DC Micro-Grids

Arash Abedi, Behrooz Rezaie*, Alireza Khosravi, Majid Shahabi

Department of Control, Faculty of Electrical and Computer Engineering, Babol Noshirvani University of Technology, Babol, Iran.

PAPER INFO

Paper history:

Received 12 February 2020

Accepted in revised form 12 May 2020

Keywords:

DC/DC Converter

Stability Analysis

Stand-Alone DC Micro-Grid

Switching Function

ABSTRACT

This paper presents a novel local control method for the converter-based renewable energy resources in a stand-alone DC micro-grid based on energy analysis. The studied DC micro-grid comprises the renewable energy resources, back-up generation unit, and battery-based energy storage system, which are connected to the common DC-bus through the buck and bidirectional buck-boost converters. The proposed control method satisfies the stability of the micro-grid output variables, along with current control and voltage regulation by controlling the switching functions of the converters, regardless of the energy resource dynamics. The dynamic component of the switching function is extracted as a control signal using the state-feedback through a mathematical method. The control inputs are designed based on Lyapunov stability theorem to guarantee the stability of output variables (DC-bus voltage and generated currents) in a stand-alone DC micro-grid through an energy analysis. The proposed distributed controller can be easily generalized as a platform with all kinds of the stand-alone DC micro-grids comprising any type or number of distributed generations such as renewable energy resources, fossil-fuel-based generations, and energy storage units. Other features of this local control method are simplicity, celerity, comprehensiveness, and independence of the distributed generations. The dynamic performance assessment of the proposed controller is verified through a simulation in MATLAB/SIMULINK® environment. The results validate the accuracy and stability of the proposed control strategy in various operating conditions.

چکیده

این مقاله یک روش کنترل محلی جدید را برای منابع انرژی تجدیدپذیر مبتنی بر مبدل در یک ریزشبه DC مستقل، بر اساس تجزیه و تحلیل انرژی ارائه می‌نماید. ریزشبه DC مورد مطالعه شامل منابع انرژی تجدیدپذیر، واحد تولیدی پشتیبان و سیستم ذخیره انرژی مبتنی بر باتری است که از طریق مبدل‌های کاهنده و کاهنده-افزاینده دو طرفه به یک باس DC مشترک متصل می‌شوند. روش کنترلی پیشنهادی، بدون در نظر گرفتن دینامیک منبع انرژی، پایداری متغیرهای خروجی ریزشبه را به همراه کنترل جریان و تنظیم ولتاژ، از طریق کنترل توابع سوئیچینگ مبدل‌ها برآورده می‌کند. مؤلفه دینامیکی تابع سوئیچینگ به عنوان یک سیگنال کنترلی از طریق یک روش ریاضی با استفاده از فیدبک حالت، استخراج می‌شود. ورودی‌های کنترلی براساس قضیه پایداری لیاپانف برای تضمین پایداری متغیرهای خروجی (ولتاژ شین DC و جریان‌های تولیدی) در یک ریزشبه مستقل DC و از طریق تجزیه و تحلیل انرژی، طراحی می‌شود. کنترل‌کننده توزیع‌شده پیشنهادی، به راحتی می‌تواند به عنوان یک طرح کلی جهت کاربرد در انواع ریزشبه‌های مستقل DC، متشکل از هر نوع یا هر تعداد از منابع تولید پراکنده نظیر منابع انرژی تجدیدپذیر، تولیدکننده‌های مبتنی بر سوخت‌های فسیلی و واحدهای ذخیره انرژی تعمیم یابد. از دیگر ویژگی‌های این روش کنترل محلی، سادگی، سرعت عمل، جامعیت و استقلال واحدهای تولید پراکنده می‌باشد. عملکرد دینامیکی کنترل‌کننده پیشنهادی از طریق شبیه‌سازی در محیط سیمولینک نرم افزار متلب مورد ارزیابی قرار گرفته است و نتایج به‌دست آمده، پایداری و درستی عملکرد استراتژی کنترلی پیشنهادی را در شرایط مختلف تأیید می‌کند.

CONTENTS

Mehdi Zare Barat Ghobadian Seyed Reza Hassan-Beygi Gholamhasan Najafi	Evaporation Characteristics of Diesel and Biodiesel Fuel Droplets on Hot Surfaces	1-7
Mahdieh Rezagholizadeh Majid Aghaei Omid Dehghan	Foreign Direct Investment, Stock Market Development, and Renewable Energy Consumption: Case Study of Iran	8-18
Mohammad Hossein Jahangir Mahnaz Abolghasemi Seyedeh Mahsa Mousavi Reineh	Application of Artificial Neural Networks to the Simulation of Climate Elements, Drought Forecast by Two Indicators of SPI and PNPI, and Mapping of Drought Intensity; Case Study of Khorasan Razavi	19-26
Fatemeh Boshagh Khosrow Rostami	A Review of Application of Experimental Design Techniques Related to Dark Fermentative Hydrogen Production	27-42
Saeed Hosseinpour Seyed Alireza Haji Seyed Mirza Hosseini Ramin Mehdipour Amir Hooman Hemmasi Hassan Ali Ozgoli	Energy Modeling and Techno-Economic Analysis of a Biomass Gasification-CHAT-ST Power Cycle for Sustainable Approaches in Modern Electricity Grids	43-51
Arash Abedi Behrooz Rezaie Alireza Khosravi Majid Shahabi	A Novel Local Control Technique for Converter-Based Renewable Energy Resources in the Stand-Alone DC Micro-Grids	52-63

